AD-A149 828 BASIC STUDIES OF GASES FOR FAST SWITCHES(U) OAK RIDGE 1/1
NATIONAL LAB TN L G CHRISTOPHOROU ET AL. JAN 85
N00014-82-F-0123

UNCLASSIFIED F/G 20/9 NL

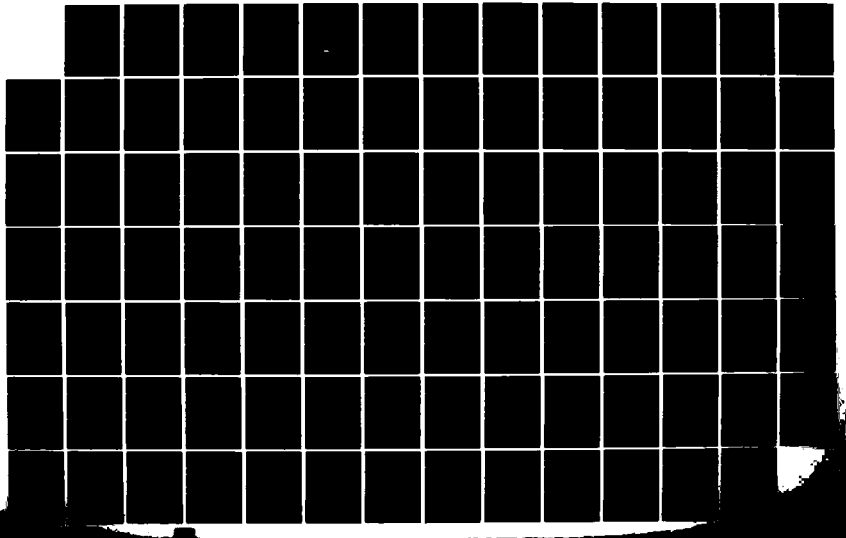

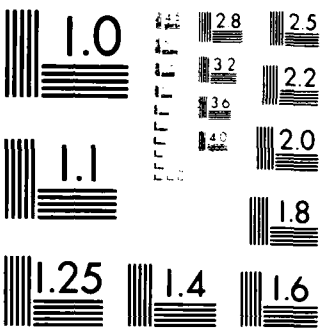

UNCLASSIFIED

SECURITY CLASSIFICATION OF THIS PAGE (When Data Entered)

(12)

REPORT DOCUMENTATION PAGE

READ INSTRUCTIONS BEFORE COMPLETING FORM

1 REPORT NUMBER: N00014-82-F-0123	2 GOVT ACCESSION NO.
3 RECIPIENT'S CATALOG NUMBER	
4 TITLE (and Subtitle): Basic Studies of Gases for Fast Switches, Annual Summary Report, October 1, 1983 to September 30, 1984	5 TYPE OF REPORT & PERIOD COVERED: Annual Summary Report Oct. 1, 1983 to Sept. 30,1984
	6 PERFORMING ORG. REPORT NUMBER
7 AUTHOR(s): L. G. Christophorou and S. R. Hunter	8 CONTRACT OR GRANT NUMBER(s): DOE 42 01 24 60 2
9 PERFORMING ORGANIZATION NAME AND ADDRESS: Oak Ridge National Laboratory, P. O. Box X, Oak Ridge, Tennessee 37831	10 PROGRAM ELEMENT, PROJECT, TASK AREA & WORK UNIT NUMBERS
11 CONTROLLING OFFICE NAME AND ADDRESS: Physics Division, Code 421, Office of Naval Research, Arlington, Virginia 22217	12 REPORT DATE: January 1984
	13 NUMBER OF PAGES: 99
14 MONITORING AGENCY NAME & ADDRESS (if different from Controlling Office)	15 SECURITY CLASS. (of this report)
	15a DECLASSIFICATION DOWNGRADING SCHEDULE

16 DISTRIBUTION STATEMENT (of this Report)

Approved for public release: distribution unlimited.

17 DISTRIBUTION STATEMENT (of the abstract entered in Block 20, if different from Report)

18 SUPPLEMENTARY NOTES

19 KEY WORDS (Continue on reverse side if necessary and identify by block number)

Diffuse discharge switches, electron drift velocity, attachment rate constants, high voltage breakdown, gas mixtures, electron transport, perfluorocarbons.

20 ABSTRACT (Continue on reverse side if necessary and identify by block number)

Desirable electron attachment and electron drift characteristics of gases for possible use in diffuse discharge switches are indicated. Gas mixtures for possible use in externally sustained (e-beam) diffuse discharge switches are suggested on the basis of electron attachment rate constants and electron drift velocities measured as a function of the density-normalized electric field E/N. Of particular promise are mixtures of Ar and C_3F_8.

DD FORM 1 JAN 73 1473 EDITION OF 1 NOV 65 IS OBSOLETE

S/N 0102-LF-014-6601

SECURITY CLASSIFICATION OF THIS PAGE (When Data Entered)

Interagency Agreement DOE No. 40-1246-82
Navy No. N00014-82-F-0123

Office of Naval Research
Physics Division
Arlington, Virginia 22217

BASIC STUDIES OF GASES FOR FAST SWITCHES

Annual Summary Report
October 1, 1983 to September 30, 1984

by

L. G. Christophorou and S. R. Hunter
Health and Safety Research Division

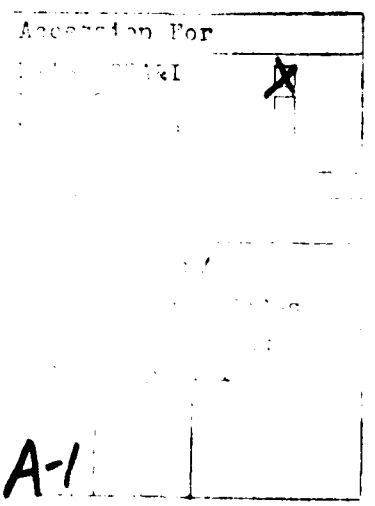

Oak Ridge National Laboratory
P. O. Box X
Oak Ridge, Tennessee 37831

January 1985

BASIC STUDIES OF GASES FOR FAST SWITCHES

L. G. Christophorou and S. R. Hunter

Oak Ridge National Laboratory
Oak Ridge, Tennessee 37831

I. INTRODUCTION

There has been increasing interest in recent years in the possibility of using inductive energy storage devices as a means of storing and transferring energy in numerous repetitive, pulsed power applications. The major advantages to be realized using this technology are that the intrinsic energy density of these devices is of the order of 10^2 to 10^3 times those for capacitive systems[1] and that this energy can be transferred to the load on the very short time scale of a few nanoseconds. The major technological problem to be faced when using this type of energy storage system is in the design of a repetitive opening switch. A leading contender for this switching concept is an externally sustained diffuse gas discharge operating at gas pressures of one to several atmospheres. Two possible electron sources have been proposed for the external control of the discharge current. They operate by means of gas ionization by pulsed electron beams (e-beams)[2] or by resonant ionization processes of the gaseous medium using a pulsed high power laser.[3] A number of operating parameters may be defined for these types of switches, which are common to both switching concepts. These parameters can then form a basis for tailoring specific gases and gas mixtures to optimize these operating conditions as nearly as possible.

The operating principle of the diffuse switch in the energy storage cycle is given in Fig. 1 (Ref. 1). In the *conducting* stage, the switch S_2 is open, and the switch S_1 is conducting by means of a diffuse discharge,

which is sustained by ionization of the gas mixture using either an e-beam or a laser. In the opening stage, the external ionization source is removed, thus opening S_1, and the switch S_2 is closed to allow the energy stored in the inductor, L_s, to be transferred to the load, Z_L. It is known, however, that in an inductive system where one attempts to rapidly open the conducting switch, a very large voltage is induced across the switch due to the term $V_i = -L\ di/dt$ (L is the inductance of L_s in Fig. 1, and i is the current). This induced voltage tends to maintain a conducting arc between the electrodes of the switch S_1 and to quote Kristiansen et al.,[1] "How to interrupt the conduction process against a high-driving voltage is the essence of an opening switch."

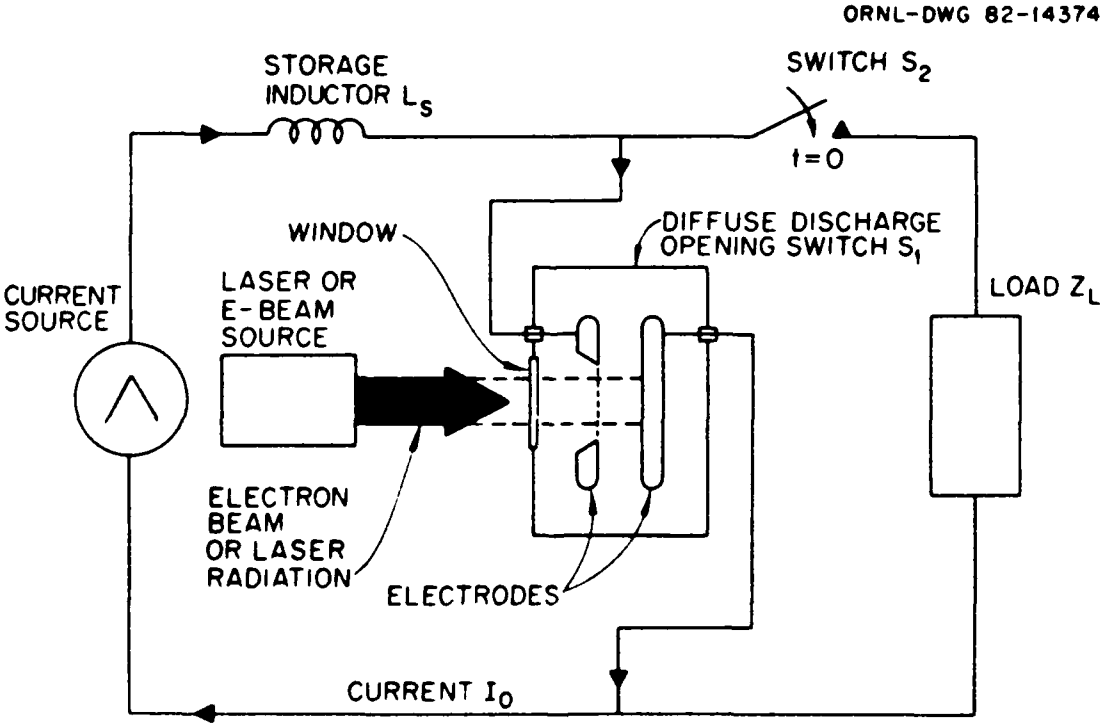

Fig. 1. Inductive energy discharge circuit (from Ref. 1).

The circuit equation governing the electron number density, n_e, in the diffuse discharge switch, S_1, which is driven by an external electron beam flux, J_b, at a given E/N, is

$$\frac{dn_e}{dt} = \langle d\varepsilon/dx \rangle J_b W^{-1} - k_a n_e N_a - k_{R_1} n_e n_+ , \quad (1)$$

where $\langle d\varepsilon/dx \rangle$ is the mean energy loss in the direction of the beam, W is the average energy required to produce an ion pair,[4] k_a is the electron attachment rate constant, N_a is the attaching gas number density, k_{R_1} is the two-body recombination rate constant, and n_+ is the positive ion number density. A similar expression may be written when the current in the switch is sustained by resonance (laser) photoionization of the gas mixtures. The current density in the switch J_s is given by Ohm's law, i.e.,

$$J_s = e n_e w , \quad (2)$$

where w is the electron drift velocity.

In the conducting stage, the electron current density in the switch must be as large as possible for a given e-beam current. In order for the switch to be as effective as possible, the electron loss terms in Eq. (1) must be minimized. Along with the minimization of the electron attachment rate constant k_a, the electron ionization rate constant k_i resulting from the applied electric field must be small,[2] otherwise the switch opening time will be increased considerably. This source of ionization can be ignored provided that $k_i \ll k_a$ during the conducting *and* opening stages of the switch.

Conversely, the electron gain term $\langle d\varepsilon/dx \rangle J_b W^{-1}$ must be maximized so as to enhance the current gain in the discharge by minimizing the

nonionizing inelastic processes in the gas constituents, while attempting to maximize their ionization cross sections. To maximize the efficiency of ion pair production, and hence the current in the switch, W must be minimized for a given gas mixture. A further criterion for enhancing the switch current, J_s, from Eq. (2) is to maximize the electron drift velocity (or mobility) at the given electric field strength during the conduction stage. The desirable characteristics of the gaseous medium during the conduction stage may thus be summarized as follows: (1) maximum electron drift velocity, w; (2) minimum e-beam ionization energy, W; (3) minimum electron loss terms k_a and k_{R_1}; and (4) $k_i \ll k_a$.

In the *opening* stage, the voltage across the switch increases rapidly due to the induced voltage across the inductor, causing an accompanying increase in E/N across the discharge gap. This basic difference between the conducting stage, where the applied conduction voltage is comparatively small ($E/N \simeq 3 \times 10^{-17}$ V cm^2),[3] and the opening stage, where the E/N across the gap may increase to values of $\gtrsim 120 \times 10^{-17}$ V cm^2, is the key to tailoring gas mixtures with the desired operating characteristics.

In the opening stage, the external electron source is ceased, and the largest rate of decrease in the current of switch S_1 occurs when k_a is as large as possible. Similarly, the response time of the switch is improved from Eq. (2) by choosing a gas mixture in which the electron drift velocity decreases when the E/N across the discharge gap increases. The gas mixture must also be able to withstand a high breakdown field ($\gtrsim 120 \times 10^{-17}$ V cm^2) for successful operation of the switch at very short opening times.

A further desirable characteristic of the gas mixture which becomes important when it is proposed to operate the switch at high repetition frequencies and a closed gas system is that the gas mixture be "self-healing". That is, the composition of the gas mixture is unaffected by the repetitive operation of the switch.[3] This characteristic is unobtainable when using a gas which attaches electrons dissociatively to form negative ion and neutral fragments. Repetitive operation of the switch will eventually alter the composition of the gas, and a possible degradation in performance will result unless one employs a flowing rather than a closed gas system. It is desirable in these circumstances that electron attachment proceeds via stabilization of the parent negative ion. This attachment mechanism does not lead to molecular fragmentation and thus increases the operating life of the gas mixture in the switch.

The desirable characteristics of the gaseous medium during the opening stage may now be summarized:

1. Minimum electron mobility, μ;
2. Maximum electron attachment rate, k_a;
3. High breakdown strength ($E/N_{\ell im} > 120 \times 10^{-17}$ V cm^2);
4. Self-healing gas mixtures for static gas-filled switches.

The desirable characteristics of the gas mixture in terms of the electron drift velocity $w(E/N)$ and $k_a(E/N)$ are shown in Fig. 2. The drift velocity must be large at the E/N values indicated by the shaded region characteristic of the conduction stage, and k_a must be as small as possible in this E/N range. In the opening stage, w must be as small as possible and k_a as high as possible at the E/N values (indicated by the shaded region in Fig. 2) characteristic of this stage.

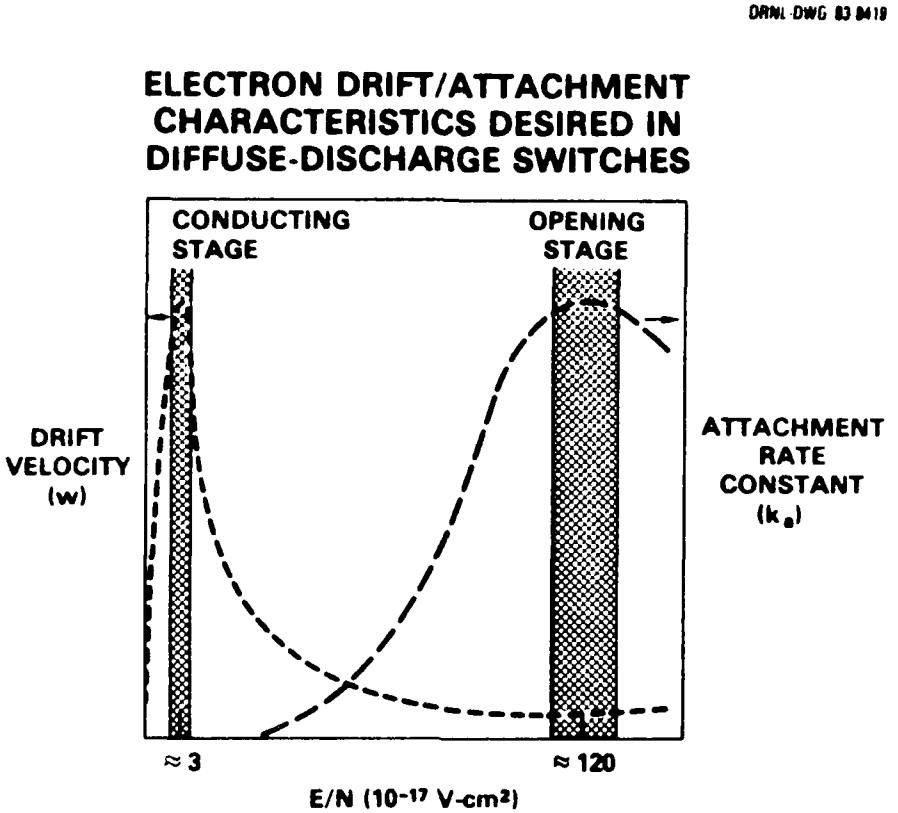

Fig. 2. Schematic illustration of the desirable characteristics of the w(E/N) and k_a(E/N) functions of the gaseous medium in an externally (e-beam-sustained) diffuse discharge switch. Indicated in the figure are rough estimates of the E/N values for the conducting and opening stages of the switch.

II. TECHNIQUES

We have used experimental techniques that have been developed in this laboratory during the past 10 years or so to identify gases and gas mixtures which have the desirable characteristics outlined in Section I when used in diffuse discharge opening switches. These measurements have allowed us to tailor gas mixtures which can optimize the characteristics required in a given switching configuration.

Measurements of w in pure gases and gas mixtures have been made in the apparatus described by Christophorou et al.[5,6,7] This apparatus has been used to measure w in gas mixtures for use in high speed proportional

counters and to study the density dependence of w in dense polar gases. Electron attachment rate constant, k_a, measurements were obtained as a function of mean electron energy, $\langle\varepsilon\rangle$, in a high pressure electron attachment apparatus which has been described previously.[4,8] This apparatus has been used to screen highly electron attaching gases for possible use as gaseous dielectrics in high voltage transmission equipment.[9] These measurements have enabled us to identify several gases with desirable electron attaching properties for use in diffuse discharge opening switches.[10-13]

We have designed and built a new experiment during the past financial year to measure the W values [Eq. (1)] of selected gases and gas mixtures which have been identified as possessing the desirable electron drift velocity and attachment characteristics described above.[10-13] The information is not only useful in modeling the electron conduction characteristics in these switching mixtures but also can be used to optimize the electron production efficiency by the electron beam by adding small percentages of an appropriate impurity to the gas mixture. The experimental technique is outlined in Appendix A, and the measurements are given in Section III.B.

III. TECHNICAL PROGRESS

The measurements that have been performed during this reporting period have allowed us to continue our studies on identifying attaching gas/buffer gas mixtures which have very desirable electron attaching and drift velocity characteristics for possible use in diffuse discharge opening switches. Our measurements of the electron attachment rate constants and negative ion production cross sections for several electronegative gases with the desirable electron attaching properties have now been published.[8,14,15]

A. New Experimental Techniques

1. An apparatus has been designed and constructed to enable us to measure the average energy required to produce an electron-positive ion pair, W, in the energy decay of high energy α particles (E ~ 5.6 MeV). This information is important in modeling the efficiency of e-beam switched gas discharges, where the high energy e-beam is required to produce multiple electron-positive ion pairs in the diffuse discharge. At high enough energies (i.e., initial energies $\gtrsim 3 \times 10^4$ eV), the ionizing efficiencies of electrons and α particles of the same velocity are almost identical and do not depend on the initial energy of the ionizing particle,[4] thus allowing data derived from α-particle energy decay studies to be used in high energy electron decay studies. The experimental technique and schematic diagram of the experimental apparatus are given in Appendix A.

2. A new high temperature electron attachment chamber has been designed and constructed to replace the original apparatus. We found that the insulators used in the original chamber lost their electrical insulating properties at temperatures in excess of 300°C, effectively shorting the electrodes of the drift assembly to ground. After unsuccessfully trying different types of insulating material in order to increase the electrical impedance at high temperatures, a different chamber configuration was designed and built. In this chamber, the insulating support rods are connected to the vacuum vessel at the top and bottom of the chamber where the temperature is kept close to room temperature. A temperature gradient is maintained across the vessel, such that only the central portion of the chamber containing the drift assembly electrodes is maintained at high gas temperatures. This

modification has allowed us to perform measurements up to 500°C with good electrical insulation characteristics. Operation of the apparatus at higher gas temperatures is possible but is not achievable at present due to corona problems at the highest temperatures.

B. Basic Data

We have measured the electron attachment and ionization coefficients and electron drift velocities in O_2, CF_4, C_2F_6, C_3F_8, and $n\text{-}C_4F_{10}$ gases using a new method of data analysis. The pressure dependence of the electron attachment coefficient in O_2, C_3F_8, and $n\text{-}C_4F_{10}$ has also been analyzed. A paper describing this technique and the measurements in these gases is in preparation.

Measurements of α/N and η/N in C_2F_6/Ar and C_2F_6/CH_4 gas mixtures have been obtained over the concentration range of from 0.1 to 100% which can be used in modeling studies of diffuse discharge switches. These measurements and their significance have been discussed in a paper which was presented at the Fourth International Symposium on Gaseous Dielectrics in May 1984 (see Part C of this section).

High pressure electron attachment rate constant measurements ($k_a = \eta w/N$) have been obtained in N_2 and Ar buffer gases for the perfluoroethers $(CF_3)_2O$ and $(CF_3)_2S$ from thermal energy (~0.04 eV) to ~4.8 eV. Both $(CF_3)_2S$ and $(CF_3)_2O$ have very desirable electron attaching properties for use in diffuse discharge switches. Knowledge of the electron energy distribution functions for N_2 and Ar buffer gases has enabled us to obtain the electron attachment cross sections (σ_a) for these electronegative gases from such measurements. Single collision negative ion production studies have been performed for these gases which have identified the initial negative ion and neutral fragments which will be produced

during the operation of the switching gas discharge. These measurements have recently been published (see Part C of this section).

Measurements of the electron attachment rate constant, k_a, have been made as a function of the mean electron energy, $\langle\varepsilon\rangle$, at gas temperatures up to 700 K in $CC\ell F_3$ and up to 750 K in C_2F_6. A substantial increase in the rate of electron attachment with gas temperature has been observed in both of these molecules, which is interpreted as electron attachment to higher vibrational levels of the ground state of these molecules. A paper describing these measurements has been accepted for publication (see Part C).

Electron drift velocity measurements have been made in many gas mixtures, including CF_4/Ar, CF_4/CH_4, C_2F_6/Ar, C_2F_6/CH_4, C_3F_8/Ar, C_3F_8/CH_4, CF_3OCF_3/Ar, CF_3OCF_3/CH_4, C_2F_6/N_2, CF_4/C_2F_6, and Ar/CH_4 over a concentration range of 0.1-100% of the attaching gas in the buffer gas. The majority of these measurements have been reported at the Fourth International Symposium on Gaseous Dielectrics.[13] All these mixtures, except the C_2F_6/N_2 mixture, exhibit a pronounced negative differential conductivity region over a wide range of fractional concentrations of the attaching gas in the buffer gas, and the position of the maximum in the drift velocity is greatly affected by the concentration of the attaching gas.[13] The ability to tailor the gas mixture to obtain the desired mobility enhancement over the appropriate E/N range is essential in order to optimize the operating conditions of the diffuse discharge in the switch.

Measurements of the ratio of the transverse diffusion coefficient to the electron mobility, D_T/μ, have been made in the attaching gases CF_4 and C_2F_6 each in the buffer gases CH_4 and Ar, using the D_T/μ apparatus

at the Australian National University. Preliminary data analysis has been made on the measurements in the C_2F_6/CH_4 gas mixtures, and the results were presented at the Fourth International Symposium on Gaseous Dielectrics.[13]

An extensive series of measurements of the W value have been made in several binary and ternary gas mixtures containing C_2F_6. The apparent W value of pure C_2F_6 has been found to be very dependent on the total gas pressure and applied voltage (Fig. 3) due to the large negative ion-positive ion recombination coefficient in this gas. The true W value of C_2F_6 has been found to be 34.7 eV/ion pair from an extrapolation of these measurements to infinite applied voltages (Fig. 3). W values have also been obtained in the binary gas mixtures C_2F_6/Ar, C_2F_6/C_2H_2, $C_2F_6/2\text{-}C_4H_8$, C_2H_2/Ar, and $2\text{-}C_4H_8$/Ar. Penning ionization processes have been found to significantly decrease the W value in the latter two gas mixtures and appear to be absent in the first three mixtures. Measurements of W have also been made in the ternary gas mixtures $C_2F_6/Ar/2\text{-}C_4H_8$ and $C_2F_6/Ar/C_2H_2$. The measurements in the $C_2F_6/Ar/2\text{-}C_4H_8$ gas mixtures are given in Fig. 4 and indicate that gas mixtures containing Ar and C_2F_6 and a small percentage of low ionization potential impurity (such as C_2H_2 or $2\text{-}C_4H_8$) can be tailored so as to minimize the W value of the gas mixture and hence to optimize the efficiency of electron production in an e-beam-controlled diffuse discharge switch. A paper is being written in which these measurements and their theoretical analysis are described in detail.

C. Publications

The preponderance of the results from the experiments outlined above have been described in several papers which have either been

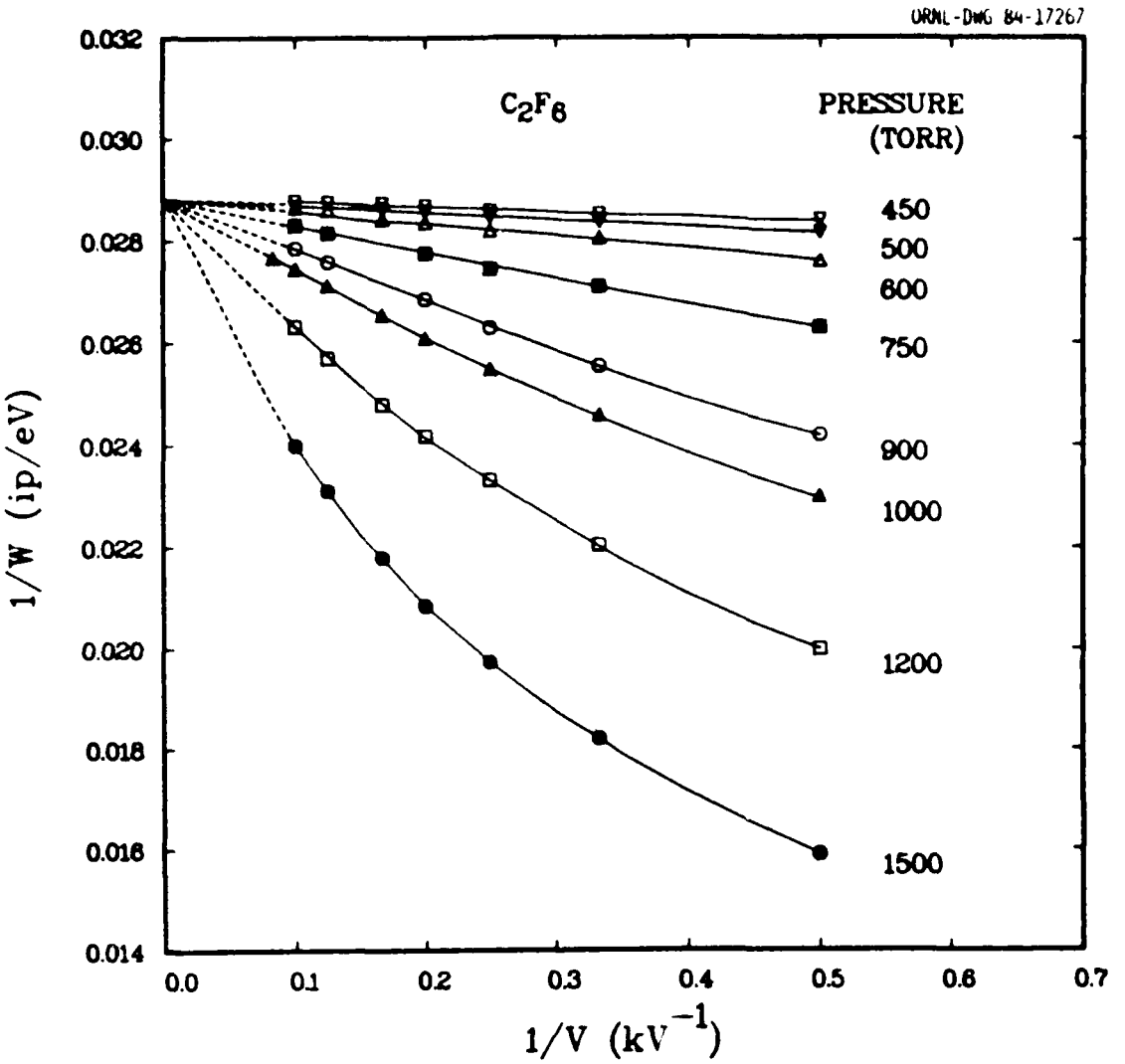

Fig. 3. 1/W versus 1/V for C_2F_6 at various gas pressures.

published or accepted for publication. The electron drift velocity, attachment, and ionization measurements have been presented at the Fourth International Symposium on Gaseous Dielectrics held in Knoxville, Tennessee, April 29-May 3, 1984, and published in *Gaseous Dielectrics IV* (L. G. Christophorou, ed.)[13] (see Appendix B). The material in this paper is being prepared for an open literature publication. Our measurements of the electron attachment rate constants and negative ion production cross sections for the fluoroethers and fluorosulfides have recently

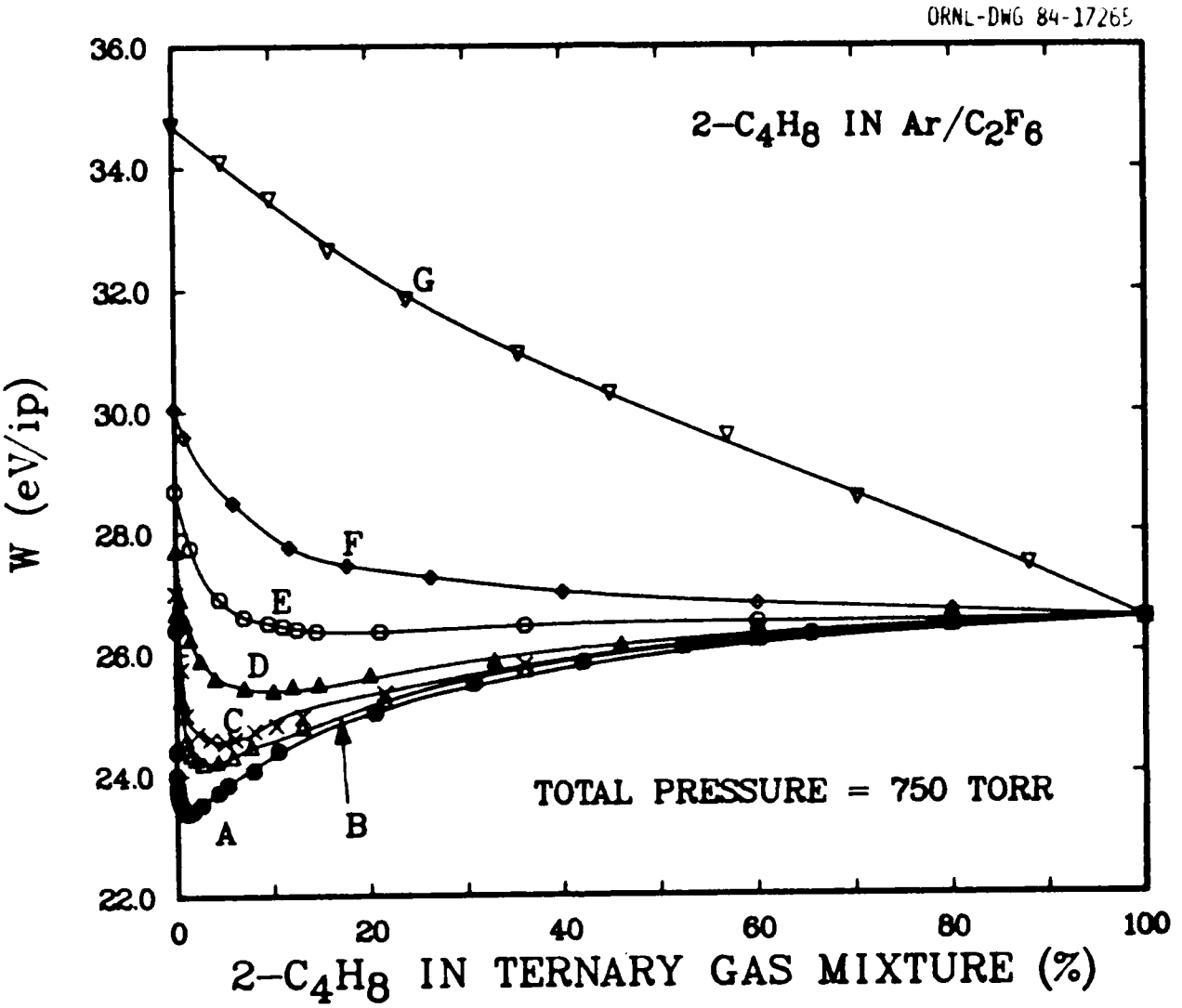

Fig. 4. W for the ternary gas mixtures 2-C_4H_8/Ar/C_2F_6 as a function of the percentage of 2-C_4H_8 in Ar/C_2F_6 for the following Ar/C_2F_6 compositions: A = 100% Ar/0% C_2F_6; B = 99% Ar/1% C_2F_6; C = 98% Ar/2% C_2F_6; D = 95% Ar/5% C_2F_6; E = 90% Ar/10% C_2F_6; F = 80% Ar/20% C_2F_6; F = 80% Ar/20% C_2F_6; G = 0% Ar/100% C_2F_6.

been published (see Appendix C). The molecules CF_3SCF_3 and CF_3OCF_3 have very desirable electron attachment properties for use in diffuse discharge switching applications. Our high temperature electron attachment rate constant measurements to C_2F_6 and $CC\ell F_3$ have been accepted for publication and will be published shortly (see Appendix D). The electron attachment

rate constant for C_2F_6 has been found to increase with increasing gas temperature. This enhanced electron attachment at elevated gas temperatures may, in fact, be beneficial to the operation of the switch at these temperatures.

A complete listing of publications and presentations which have been partially or totally sponsored by the Office of Naval Research is given in the accompanying Publications Report.

IV. REFERENCES

1. M. Kristiansen and K. M. Schoenbach, Final Report on Workshop on Repetitive Opening Switches, April 21, 1981, Department of Electrical Engineering, Texas Technological University, Lubbock, Texas.
2. R. F. Fernsler, D. Conte, and I. M. Vitkovitsky, IEEE Trans. Plasma Sci. PS-8, 176 (1980).
3. K. H. Schoenbach, G. Schaefer, E. E. Kunhardt, M. Kristiansen, L. L. Hatfield, and A. H. Guenther, Proc. 3rd IEEE Int. Pulsed Power Conf., Albuquerque, New Mexico, June 1-3, 1981, p. 142.
4. L. G. Christophorou, Atomic and Molecular Radiation Physics, Wiley-Interscience, New York, 1971.
5. L. G. Christophorou, D. L. McCorkle, D. V. Maxey, and J. G. Carter, Nucl. Instr. Meth. 163, 141 (1979).
6. L. G. Christophorou, D. V. Maxey, D. L. McCorkle, and J. G. Carter, Nucl. Instr. Meth. 171, 491 (1979).
7. L. G. Christophorou, J. G. Carter, and D. V. Maxey, J. Chem. Phys. 76, 2653 (1982).
8. S. R. Hunter and L. G. Christophorou, J. Chem. Phys. 80, 6150 (1984).

9. L. G. Christophorou, in Electron and Ion Swarms (L. G. Christophorou, ed.), Pergamon Press, New York, 1981, p. 261.

10. L. G. Christophorou, S. R. Hunter, J. G. Carter, and R. A. Mathis, Appl. Phys. Lett. 41, 147 (1982).

11. L. G. Christophorou, S. R. Hunter, J. G. Carter, S. M. Spyrou, and V. K. Lakdawala, in Proc. 4th IEEE Int. Pulsed Power Conf. (M. F. Rose and T. H. Martin, eds.), The Texas Tech Press, Lubbock, Texas, 1983, p. 702.

12. J. G. Carter, S. R. Hunter, L. G. Christophorou, and V. K. Lakdawala, in Proc. 3rd Int. Swarm Seminar (W. Lindinger, H. Villinger, and W. Federer, eds.), Innsbruck, Austria, 1983, p. 30.

13. S. R. Hunter, J. G. Carter, L. G. Christophorou, and V. K. Lakdawala, in Gaseous Dielectrics IV (L. G. Christophorou and M. O. Pace, eds.), Pergamon Press, New York, 1984, p. 224.

14. S. M. Spyrou, I. Sauers, and L. G. Christophorou, J. Chem. Phys. 78, 7200 (1983).

15. S. M. Spyrou, S. R. Hunter, and L. G. Christophorou, J. Chem. Phys. 81, 4481 (1984).

APPENDIX A

The experimental technique for determining the gas ionizing efficiency, W, in gases and gas mixtures for use in diffuse discharge switching applications.

ALPHA PARTICLE IONIZATION EFFICIENCIES OF GAS MIXTURES FOR USE IN DIFFUSE DISCHARGE OPENING SWITCHES

Experimental Technique

To perform an experiment, open the grounding switch, S, at time $t_1 = 0$.

Current will flow into high quality (low loss) capacitor C from charge generated in chamber by α-particle decay in the gas.

The voltage will then rise across the capacitor and is measured by a very high impedance voltmeter, V_1--current drain through voltmeter should be negligible in comparison with current in the circuit (i.e., $R \sim 10^{14}\ \Omega$).

To keep the E/N constant across the drift gap, the voltage rise must be compensated for by applying an equal voltage to the other side of the capacitor. This is done by connecting a 5 V power supply and linear resistor to the earthing side of C and adjusting the potentiometer to increase the voltage to keep the voltage in the circuit $\sim$0 as measured by V_1. The voltage in the compensating circuit is monitored with the voltmeter, V_2, and when the voltage has risen to a given value, say V_x, the experiment is stopped and the time to reach the voltage--$t_2 = t$ is recorded. The grounding switch is closed, and all potentials returned to zero and the procedure repeated at a different gas presure, applied voltage, or gas composition and different values of t_2 are recorded.

Data Analysis

The energy required to produce one electron-ion pair, W, is derived as follows:

The charge on the capacitor is

$$Q = CV ,$$

and the rate of change of charge on C is

$$\frac{dQ}{dt} = C \frac{dV}{dt} .$$

The number of electron-positive ion pairs formed is given by

$$\frac{\text{Total change in charge across C}}{\text{electron charge}} = \frac{C}{e} \frac{dV}{dt} .$$

The total energy deposited in the gas/minute by the α source is = NE - no. of αs per minute $\times$ energy of each α.

$$\text{Thus } W = \frac{\text{energy deposited/minute}}{\text{no. of electron-ion pairs formed/minute}} = \frac{NE\ e}{C\ dV/dt} ,$$

knowing N, E, and C and measuring ΔV and Δt we can find W.

In practice, if W for argon is known, then an unknown W for a mixture can be found from

$$\frac{W_{Ar}}{\Delta T_{Ar}} = \frac{W_{unknown}}{\Delta T_{unknown}} .$$

By measuring the ΔT for argon and the "unknown" gas mixture [i.e., the time required to charge C to a given (aribtrary) voltage], W of the mixture can be found.

The accuracy of the technique can be found by measuring ΔT in argon and nitrogen and by measuring the ratio

$$\frac{\Delta T_{Ar}}{\Delta T_{N_2}} = \frac{W_{Ar}}{W_{N_2}} .$$

We have found the ratio to be within ~0.2% of the generally accepted ratio of W_{Ar} and W_{N_2}.

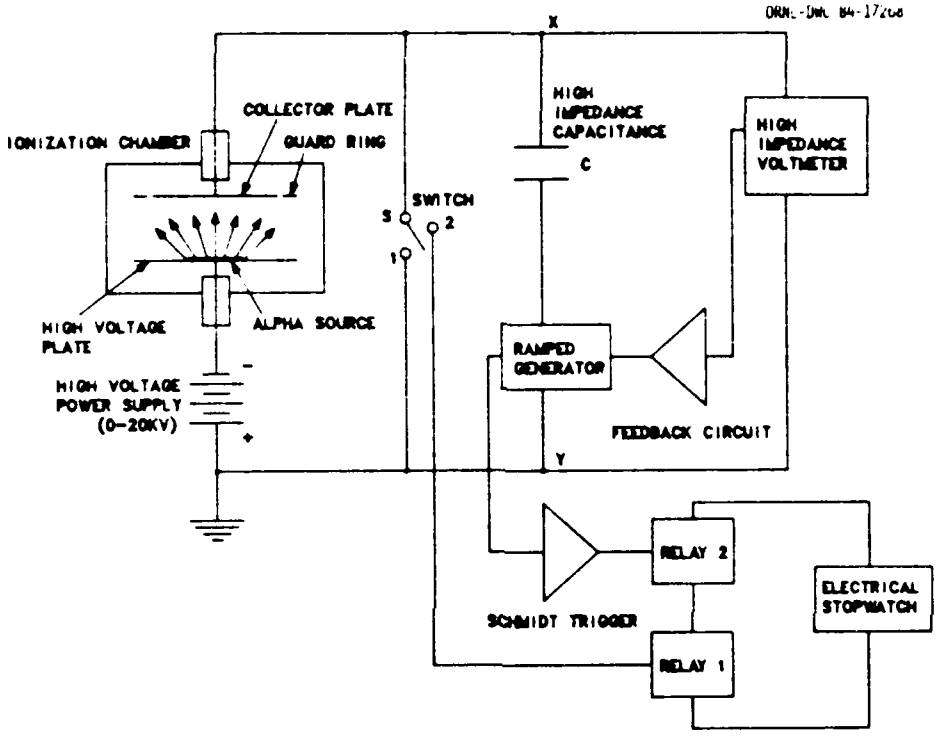

APPENDIX B

TRANSPORT PROPERTIES AND DIELECTRIC STRENGTHS OF GAS MIXTURES FOR USE IN DIFFUSE DISCHARGE OPENING SWITCHES

S. R. Hunter,* J. G. Carter, L. G. Christophorou,* and V. K. Lakdawala†

Atomic, Molecular and High Voltage Physics Group
Health and Safety Research Division
Oak Ridge National Laboratory
Oak Ridge, Tennessee 37831

*Also, The University of Tennessee, Knoxville, Tennessee 37996

†Present address: Department of Electrical Engineering, Old Dominion University, Norfolk, Virginia 23508

ABSTRACT

Gas mixtures for possible use in diffuse discharge switching applications require both high dielectric strength and specific transport properties in the conducting and the opening stages of the operation of the switch. In the conducting stage, the electron drift velocity must be large, and the electron loss processes (e.g., due to electron attachment and recombination) must be low so as to maximize the efficiency of the current gain in the discharge while maintaining low discharge impedance. In the opening stage, strong electron attachment along with high dielectric strength is required of the gas mixtures in order to extinguish the discharge as quickly as possible (and thus achieve a fast opening time) to prevent arcing occurring between the switch electrodes due to the high voltages induced across the switch in the opening phase. In this paper, we will present measurements of the electron drift velocity, attachment, diffusion and ionization coefficients, and high voltage dielectric strengths of several gas mixtures proposed as candidates for use in diffuse discharge switching applications. These include C_3F_8/Ar, C_3F_8/CH_4, C_2F_6/Ar, C_2F_6/CH_4, CF_4/Ar, CF_4/CH_4, CF_3OCF_3/Ar, and CF_3OCF_3/CH_4. For some of these mixtures, the above transport and dielectric strength measurements have been performed over the concentration range from 0 to 100% of the attaching gas in the nonattaching buffer gas.

KEYWORDS

Electron drift velocity; diffusion; ionization, attachment coefficients; diffuse discharge switches; pulsed power; negative differential conductivity

INTRODUCTION

There has been considerable interest in recent years in the possibility of using inductive energy storage devices as a means of storing and rapidly transferring electrical energy in numerous pulsed power applications. The primary advantage to be gained from the use of these energy storage devices is that they have potential energy storage densities 100 to 1000 times that of comparable capacitive storage systems (Burton and co-workers, 1979, Kristiansen and Schoenbach, 1981). One of

the major problems to be faced with this technology before it can be introduced in a number of applications is that these inductive energy systems require a switching device that can repetitively switch (repetition rates > 10 pps and more than 10^5 shots) high currents (e.g., 100 kA for inertial fusion confinement) with opening times of the order of a few nanoseconds and being capable of withstanding high voltages (>100 kV) during the opening stage without breakdown. (Kristiansen and Schoenbach, 1981, 1982).

One of the most promising contenders for fast repetitive switching is an externally sustained diffuse gas discharge operating at gas pressures of one to several atmospheres. Two different types of external electron sources have been proposed for the control of the discharge current. They are by means of volume gas ionization by pulsed high energy electron beams ("e-beam controlled", e.g. Hunter, 1976; Fernsler and co-workers, 1980) or by resonant ionization of the gaseous medium using a pulsed high power laser ("optically controlled", e.g. Schoenbach and co-workers, 1982)

DIFFUSE DISCHARGE SWITCH OPERATING PARAMETERS

The motion of the charge carriers in the diffuse discharge driven by an external electron beam of flux J_B at a given E/N is governed by the following continuity equation.

$$\frac{dn_e}{dt} = \left(\frac{dE}{dx}\right) J_B W^{-1} + k_1 n_e N_T - k_a n_e N_a - k_R n_e n_+ \quad , \tag{1}$$

where $\langle dE/dx \rangle$ is the average energy deposited in the gas by the electrons from the e-beam in traveling a distance dx, W is the average energy required to produce an ion pair (and includes a contribution to the volume ionization by excited state ionization of a lower ionization potential gas additive in the case of Penning gas mixtures), k_1 is the electron ionization rate constant, k_a is the electron attachment rate constant, k_R is the two-body electron-ion recombination rate constant (in highly attaching gas mixtures recombination due to negative ion-positive ion neutralization will also be a significant process), n_e, n_+, N_a, and N_T are, respectively, the electron, positive ion, attaching gas, and total gas number densities. Similar equations may be written for the positive and negative ions produced in the discharge.

The electron current density J_e in the discharge is given by

$$J_e(r,x) = e\left[n_e w - D_L \frac{\partial n_e}{\partial x} - D_T \frac{\partial n_e}{\partial r}\right], \tag{2}$$

and is dependent on the electron drift velocity w, the longitudinal D_L and transverse D_T diffusion coefficients, and where r is the radial direction perpendicular to the applied field. At the gas pressures proposed for most switching applications ($P_T \geq 1$ atm), the diffusion terms in Eq. (2) are negligibly small in comparison with the electron drift velocity, W. The positive and negative ion current densities ($J_+ = en_+w_+$ and $J_- = en_-w_-$, respectively) do not play a significant role in the transient stages (e.g., in the opening stage) of the switching action of the discharge. However, the positive and negative ion fluxes in the discharge do cause significant space-charge distortion, such that the electric field within the

discharge is spatially dependent, and Poisson's equation must be solved in order to determine the field, i.e.,

$$\frac{\partial^2 V}{\partial x^2} = -\frac{e}{\varepsilon_\ell}(n_+ - n_- - n_e) \text{ and } E = -\frac{\partial V}{\partial x} \quad , \tag{3}$$

where ε_ℓ is the permittivity of the gaseous medium.

With the aid of Eqs. (1) and (2), it is possible to establish several requirements of a gas mixture in the diffuse discharge which will optimize the performance of the switch. The conductivity of the discharge must be maximized while the switch is conducting (i.e., the voltage drop, and hence the E/N, across the discharge should be low ($E/N \lesssim 3 \times 10^{-17}$ V cm^2, Schoenbach and co-workers, 1982) to minimize power losses and, consequently, gas heating effects in the switch). The opening time of the switch must be as short as possible (i.e., largest rate of decrease in the discharge current, once the e-beam has been switched off in order to maximize the voltage developed across the inductive energy storage device (i.e., $V = -L\,di/dt$, where L is the inductance). Consequently, the electron conductivity in the discharge must be minimized during the opening stage, and the gas mixture must be able to withstand high transient voltage levels ($E/N > 10^{-15}$ V cm^2) while the switch is opening.

These operating conditions allow us to define several desirable characteristics of the gaseous medium in the conducting (low E/N) and opening (high E/N) stages of the switching action. In the conducting stage, the requirements are as follows:

1. Maximum electron drift velocity w - the larger w is, the higher the conductivity of the discharge and the greater the current density in the diffuse discharge.

2. Minimum e-beam "ionization energy" W - the smaller W is, the greater the current gain in the discharge with a consequent increase in the efficiency of the coupling of the e-beam to the discharge and a greater control of the resultant discharge current.

3. Minimum electron loss terms k_a and k_p - the conductivity of the discharge drastically decreases and space-charge problems increase when the highly mobile electrons are converted into relatively immobile negative ions. Similarly, conductivity will decrease if electron and negative ion-positive ion recombination in the discharge is large due to the loss of the charge carriers. A further problem that results from large recombination coefficients is that the current gain in the switch will decrease, and the energy released in the recombination process will result in increased gas kinetic energy causing heating problems in the gas under repetitive operation.

4. Minimum ionization rate constant k_i - the conductivity of the gas is required to be completely controlled by the external ionization source otherwise the opening time of the switch will be considerably increased due to additional gas ionization when the e-beam is switched off (Fernsler and co-workers, 1980).

In the opening stage the requirements of the gas mixture are as follows:

1. Minimum electron drift velocity w - i.e., reduced electron mobility and hence lower electron conductivity in the gas mixture.

2. Maximum electron attachment rate constant k_a - i.e., lower gas conductivity by converting highly mobile electrons into relatively immobile negative ions and by removing free electrons from the discharge, reducing the current density due to additional ionization processes as the E/N increases.

3. High breakdown strength $E/N_{f,H}$ (defined as the E/N at which $k_i = k_a$) $> 10^{-15}$ V cm^2 - the higher the value of $E/N_{f,H}$, the faster the permissible rate of decrease in the electron conductivity in the discharge, and hence the shorter the opening time of the switch.

4. Self-healing gas mixtures - for closed cycle operation without a time dependent degradation in the performance of the switch, it is required that the gas mixture composition not change with time. The gases in the switch can be fragmented either by collisions with high energy electrons from the e-beam or by neutral dissociation and dissociative attachment processes occurring during the diffuse discharge, particularly during the opening phase where the E/N quickly rises to very large values ($E/N \geq 10^{-15}$ V cm^2). This problem can be reduced by using gases that attach electrons nondissociatively and also have low neutral dissociation cross sections and large neutral-neutral and negative ion-positive ion recombination coefficients at high E/N value.

5. In photoexcited and photoionized gas discharges (required for laser-controlled discharges) it is desirable to have an electron attaching gas in which electron attachment can be increased (or decreased) from photoabsorption of the laser radiation (Schoenbach and co-workers, 1982).

The desirable characteristics for the E/N dependence of ν and k_a for the gas mixture in the diffuse discharge are shown in Fig. 1 (Christophorou and co-workers 1982a, 1983).

EXPERIMENTAL MEASUREMENTS

In this section we outline some of our recent measurements of the electron attachment, diffusion, and ionization coefficients, electron drift velocities and breakdown field strengths of several gas mixtures which we propose as candidates in diffuse discharge switch applications. Some of these data have been reported by us elsewhere (Christophorou and co-workers, 1979, 1982a, 1983, Carter and co-workers, 1983).

Electron Attachment and Ionization

High pressure (P_g > 1 atm) electron attachment studies of the perfluoroalkanes (Hunter and Christophorou, 1984) and several fluorinated ethers (Spyrou and co-workers, 1984) have shown that several of these molecules possess electron attachment rate constants which have desirable energy dependences for diffuse discharge switching applications (i.e., they attach electrons efficiently at high energies and have much reduced electron attachment rate constants at near-thermal energies). These measurements are summarized in Fig. 2 and have been obtained using the high-pressure swarm technique outlined by Christophorou (1971) and Hunter and Christophorou (1984). The molecule C_3F_8 is particularly noteworthy in that electron attachment to this molecule at atmospheric pressures is predominantly by parent negative ion stabilization, and thus this molecule could possibly be used in closed-cycle switches.

In order to better characterize the transport parameters of the electrons in gas mixtures of practical significance, we have measured the electron attachment coefficient η/N_g in pure C_3F_8 (Fig. 3) as well as the effective ionization

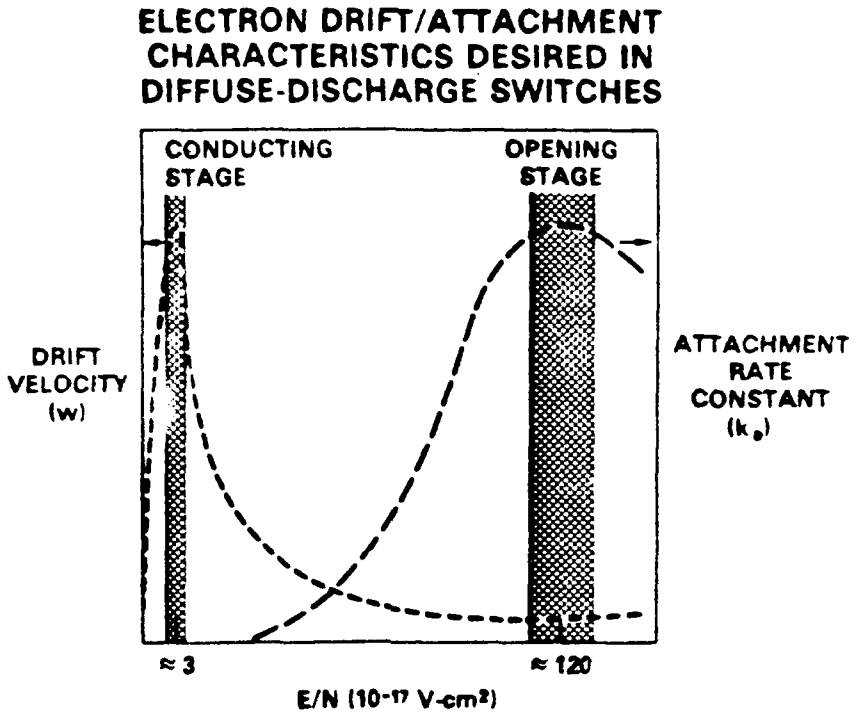

Fig. 1. Schematic illustration of the desirable characteristics of the w(E/N) and k_a(E/N) functions of the gaseous medium in an externally (e-beam) sustained diffuse discharge switch. Approximate values of the E/N for the discharge in the conducting and opening stages of the switch are shown in the figure (Christophorou and co-workers, 1982a).

coefficient $(\alpha_T + \eta)/p\lambda_T$ (where α_T is the unnormalized Townsend ionization coefficient, and p is the fractional concentration of the attaching gas in the buffer gas) in C_2F_6/Ar (Fig. 4a) and C_2F_6/CH_4 (Fig. 4b) gas mixtures. The attachment coefficient measurements in C_3F_8 are pressure dependent (Fig. 3) as has been found in electron attachment studies to C_3F_8 in a high-pressure Ar buffer gas (Hunter and Christophorou, 1984).* With our present technique (Hunter and co-workers, 1984) we are unable to separate α_T/λ_T and η/λ_a in gases where η/λ_a is dependent on the gas pressure. Consequently, we present the η/λ_a values in C_3F_8 up to only 16[illegible] $\times 10^{-17}$ V cm^2 beyond which ionization processes are expected to be

---

*Using this technique, mean electron energies $\langle\varepsilon\rangle$ up to ~4.5 eV are obtainable at comparatively low E/N values ($\leq 5 \times 10^{-17}$ V cm^2) as the electron energy gain and loss processes in the experiment are dominated by the elastic electron scattering cross section of the Ar buffer gas. In contrast, the $\langle\varepsilon\rangle$ of pure C_3F_8 even at E/N values as high as 1.5×10^{-15} V cm^2 is only ~2.5 eV, and thus the two experiments are probing the same mean energy range and, correspondingly, the same electron attachment processes.

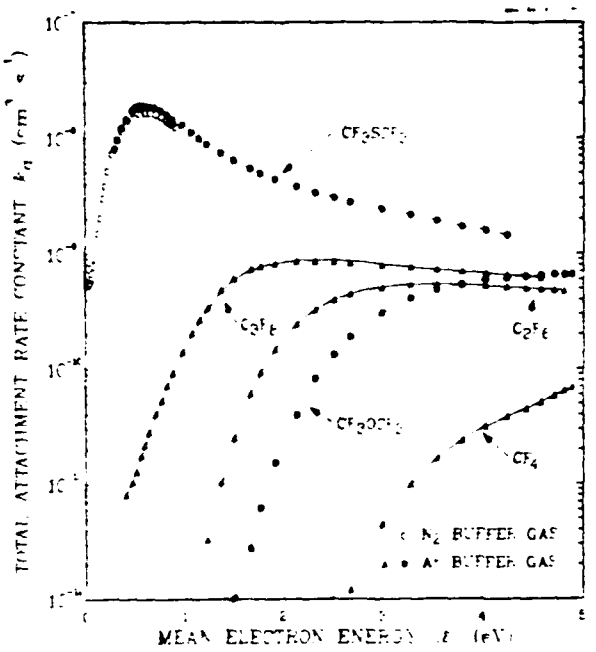

Fig 2. Total electron attachment rate constants as a function of the mean electron energy $\langle\varepsilon\rangle$ for CF_4, C_2F_6, C_3F_8, CF_3SCF_3, and CF_3OCF_3 (Hunter and Christophorou 1984, Spyrou and co-workers, 1984).

significant (Naidu and Prasad, 1972). The measurements in the C_2F_6 gas mixtures indicate that the peak in the electron attachment in these mixtures can be positioned at appropriate E/N values by either varying the attaching gas-buffer gas combination, or by varying the percentage of the attaching gas in the buffer gas, such as to maximize the rate of decrease in the conductivity of the discharge and thus minimize the opening time of the switch.

Electron Drift Velocity

Measurements of w in gas mixtures comprised of CF_4, C_2F_6, C_3F_8, and CF_3OCF_3 in buffer gases of Ar and CH_4 are given in Figs. 5-8. These measurements were obtained using the technique outlined by Christophorou and co-workers (1982b) and were made over a concentration range of 0.1-100% of the attaching gas in the buffer gas. All of these gas mixtures exhibit a pronounced negative differential conductivity (NDC) region over a wide range of fractional concentrations of the attaching gas in the buffer gas (i.e., a region over which the electron drift velocity decreases with increasing E/N in contrast to the more usual behavior where w increases with E/N). Petrović and co-workers (1984) and Robson (1984) have recently quantified the conditions under which NDC can occur. For NDC to be exhibited by a gas mixture it is essential that the gas, or one of the constituents of the gas mixture, possess inelastic processes with either a rapidly increasing threshold scattering cross section, or a cross section with a rapidly decreasing high-energy tail. Negative differential conductivity is also enhanced in the gas mixture when the elastic scattering cross section increases rapidly with energy along with the inelastic cross section. Further enhancement occurs when the inelastic process has a threshold at relatively large electron energies. The use of gas mixtures in which one gas possesses predominantly elastic scattering at low electron energies and a deep Ramsauer-Townsend minimum in the elastic scattering cross section with a rapidly increasing momentum transfer cross section Q_m at higher electron energies (e.g., the heavier rare gases), and the other gas is a

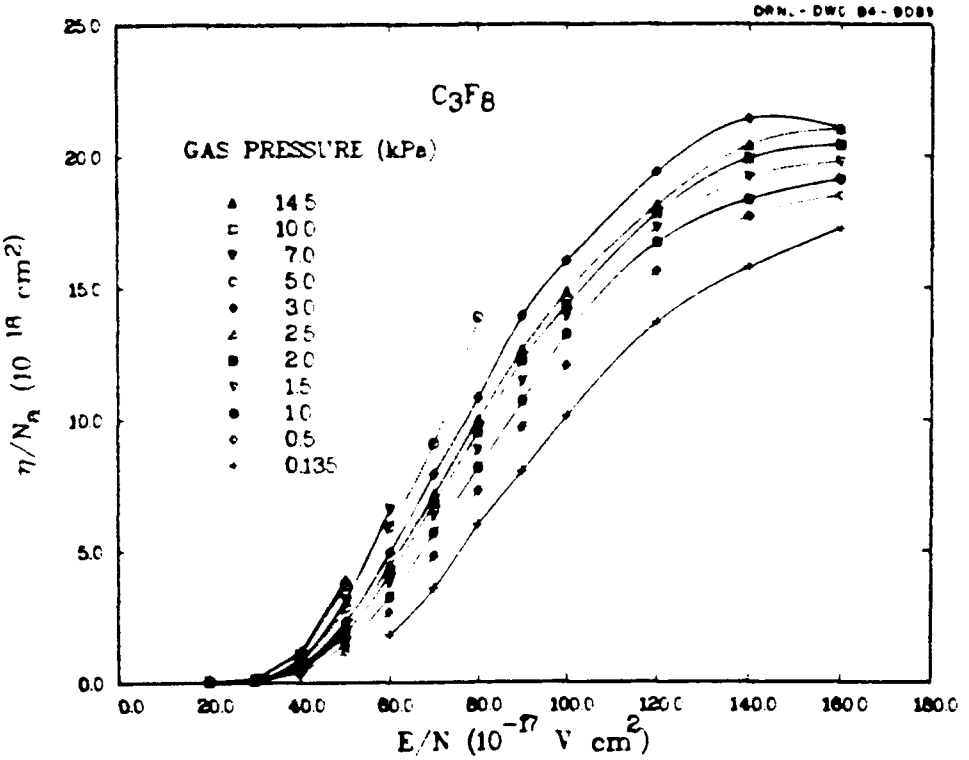

Fig 3. Electron attachment coefficient η/N_a as a function of E/N for C_3F_8 at the gas pressures indicated in the figure.

molecular gas possessing large resonant inelastic vibrational scattering processes at electron energies in the range 1-4 eV, allows one to change the degree of the NDC effect and the E/N range over which it is observed (Christophorou and coworkers, 1979). This ability to tailor the gas mixture to obtain the desired effect over the appropriate E/N range is essential in order to optimize the operating conditions of the diffuse discharge in the switch.

The peak values of w and the E/N values at which they occur are plotted in Figs. 9a and 9b, respectively, as a function of the percentage of the attaching gases CF_4, C_2F_6, and C_3F_8 in the buffer gases Ar and CH_4. It is apparent from these figures (and Figs. 5-8) that gas mixtures comprised of $\geq$15% of any of these attaching gases in Ar possess peak w values of $\geq 10^7$ cm s^{-1}, while at all concentrations of the attaching gas in CH_4, the peak value of w is 10^7 cm s^{-1} or greater. Further, it is evident from these findings that by varying the concentration of the attaching gas in the buffer gas, the w(E/N) functions can be chosen to have maximum values in the E/N range of 1-10 x 10^{-17} V cm^2, which is roughly the range characteristic of the conduction stage of the switch. It is seen from Figs. 4-9 that the maximum of both η/N_a(E/N) and w(E/N) shifts to higher E/N values as the concentration of the attaching gas is increased. The value of the mean electron energy $\langle\varepsilon\rangle$ in the mixture decreases with increasing attaching gas concentration, and as a consequence, the value of E/N which corresponds to the mean energy for

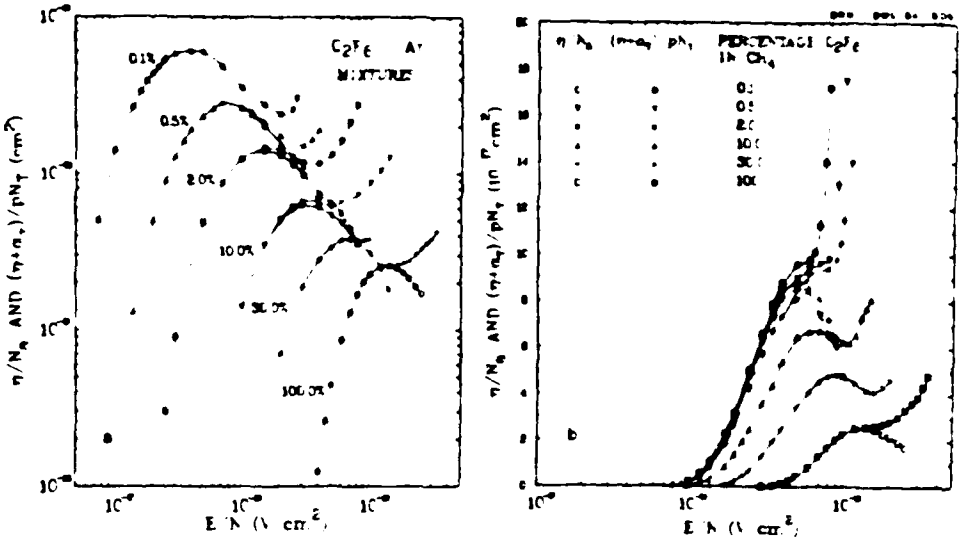

Fig 4 The electron attachment coefficient η/N_e for C_2F_6 and the effective ionization coefficient $(\alpha_T + \eta)/pN_T$ (where α_T is the unnormalized Townsend ionization coefficient and p is the fractional concentration of C_2F_6 in the buffer gas) for the gas mixtures (a) C_2F_6/Ar and (b) C_2F_6/CH_4. The actual parameter measured in the electron attachment experiment is $(\alpha_T + \eta)$ (in units of cm^{-1}). This measurement can be either normalized to the attaching gas number density N_e when $\alpha_T = 0$ to obtain the *normalized attachment coefficient* of attaching gas constituent of the mixture, or it can be normalized to the total gas number density N_T to find the effective ionization coefficient of the mixture as a whole

which w or η/N_e maximize increases. This ability to tailor the gas mixture to position the maximum in w or η/N_e at given E/N values allows considerable freedom in designing the operating parameters of the diffuse discharge switches.

D_T/μ Measurements

Measurements of D_T/μ in CF_4 and C_2F_6 in buffer gases of CH_4 and Ar have been made using the D_T/μ apparatus at the Australian National University (Crompton and Jory 1962). Preliminary analysis of the measurements in C_2F_6/CH_4 gas mixtures has been made; the D_T/μ data are given in Fig 10. These data along with those on η/N_e and $(\alpha_T + \alpha_T)/pN_T$ in Figs 3 and 4, will be used in a Boltzmann equation analysis of the electron motion in these gas mixtures to obtain information on the electron scattering processes and the electron energy distribution function as a function of E/N and gas composition.

Breakdown Field Strength Measurements

The high voltage dc uniform field breakdown strength, $(E/N)_{flw}$, has been measured in mixtures of the attaching gases C_2F_6 and C_3F_8 in buffer gases of Ar and CH_4 (Christophorou and co-workers, 1983). These measurements are given in Fig 11 and indicate that gas mixtures composed of $\gtrsim$20% of C_2F_6 or C_3F_8 in Ar have $(E/N)_{flw}$ values in excess of 10^{-15} V cm^2 and can thus withstand the voltage levels characteristic of the opening stage of the switch. The C_2F_6/CH_4 and C_3F_8/CH_4 mixtures possess high breakdown strengths over a wider (and lower) range of concentrations

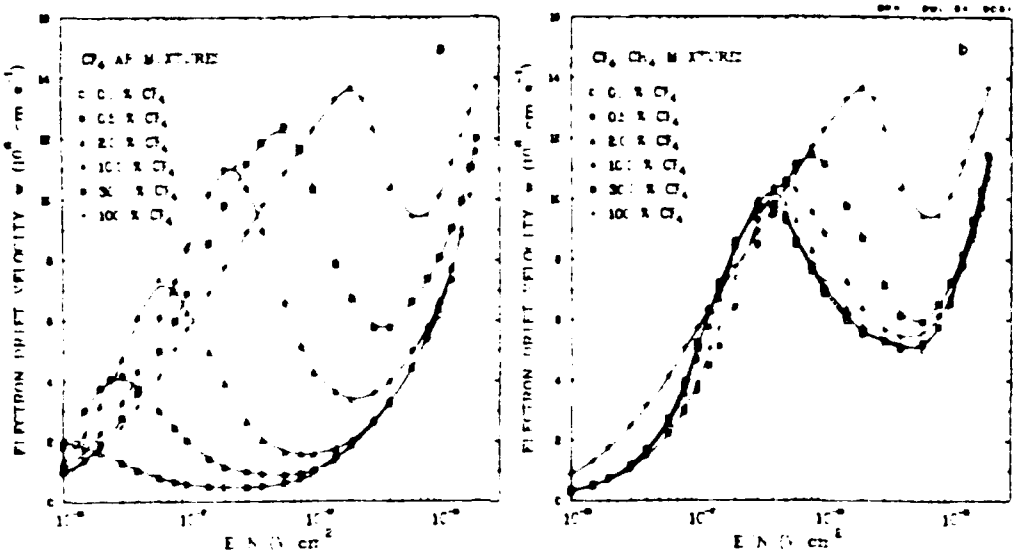

Fig 5 Electron drift velocity w versus E/N for several (a CF_4/Ar and (b CF_4/CH_4 gas mixtures

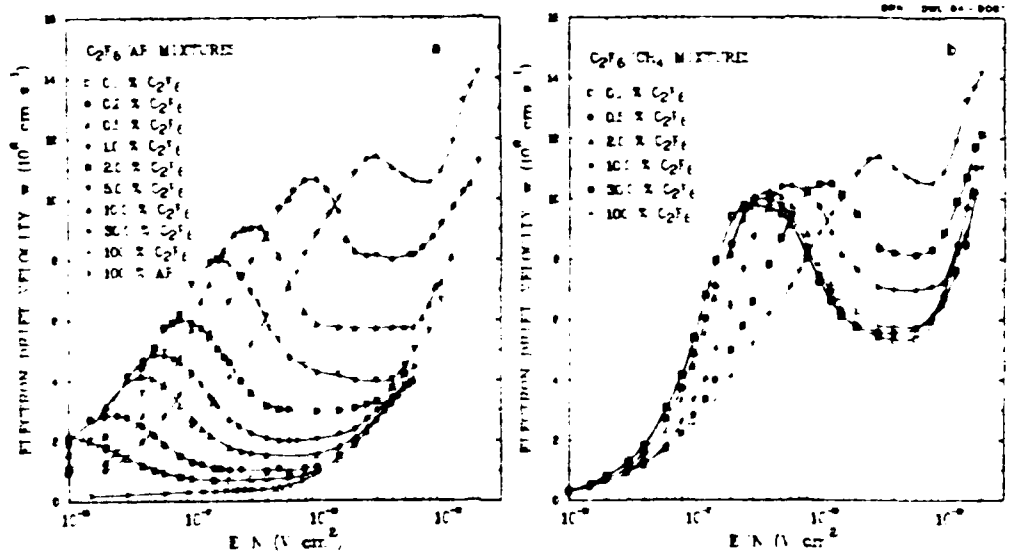

Fig 6 Electron drift velocity w versus E/N for several (a) C_2F_6/Ar and (b) C_2F_6/CH_4 gas mixtures

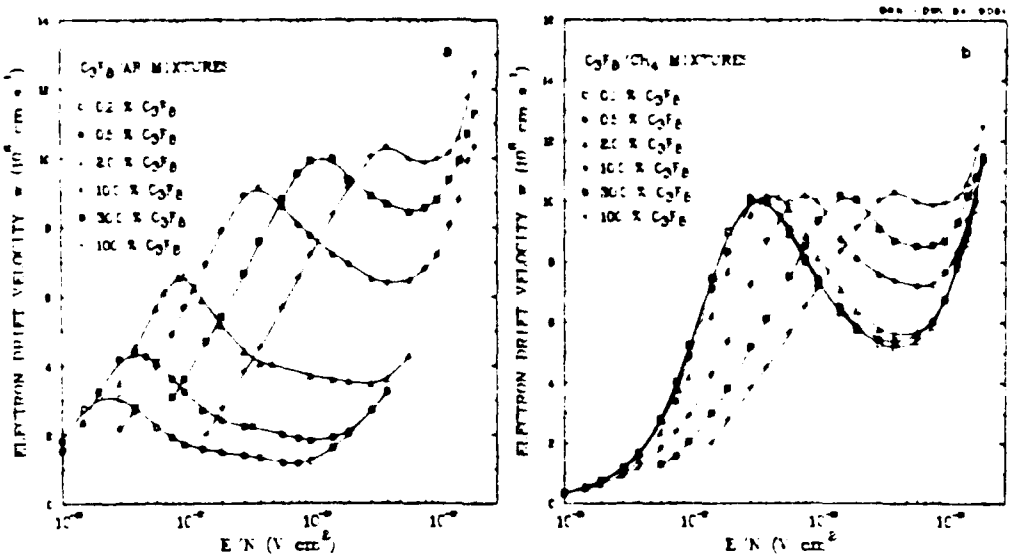

Fig. 7. Electron drift velocity w versus E/N for several (a) C_3F_8/Ar and (b) C_3F_8/CH_4 gas mixtures

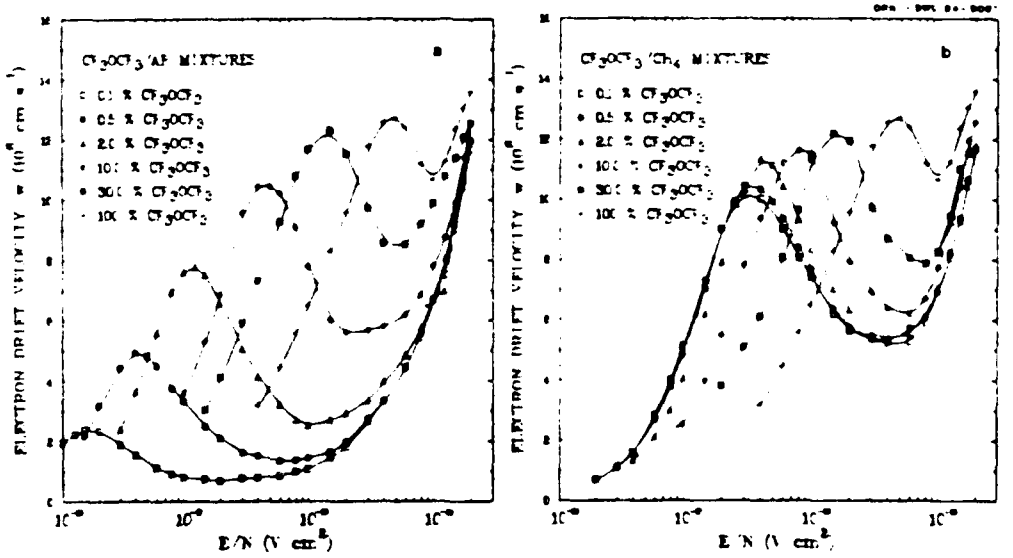

Fig. 8. Electron drift velocity w versus E/N for several (a) CF_3OCF_3/Ar and (b) CF_3OCF_3/CH_4 gas mixtures

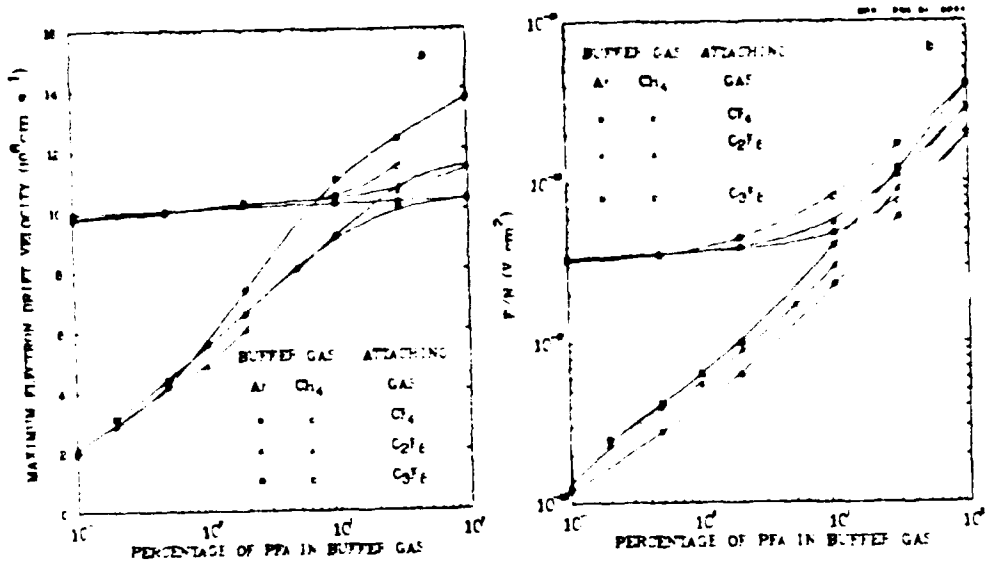

Fig 9. Plot of (a) the maximum value of the drift velocity and (b) the E/N value at the maximum value of v as a function of the percentage concentration of CF_4, C_2F_6 and C_3F_8 in Ar and CH_4.

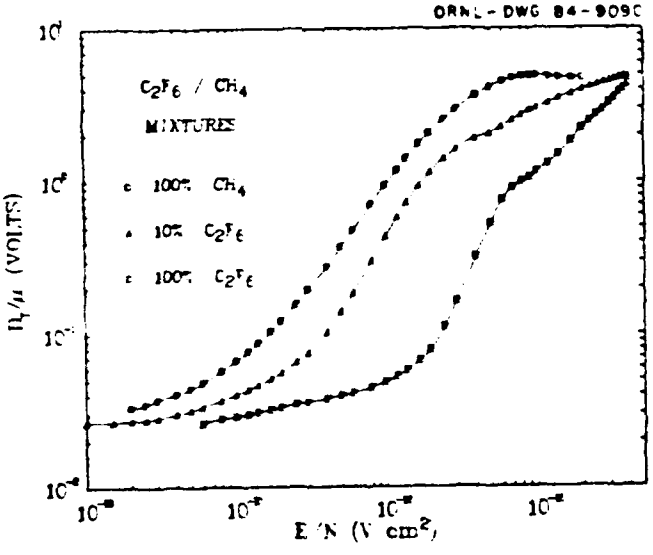

Fig 10. Preliminary values of D_T/μ for the pure gases CH_4 and C_2F_6 and the 10% C_2F_6/90% CH_4 gas mixture plotted as a function of E/N.

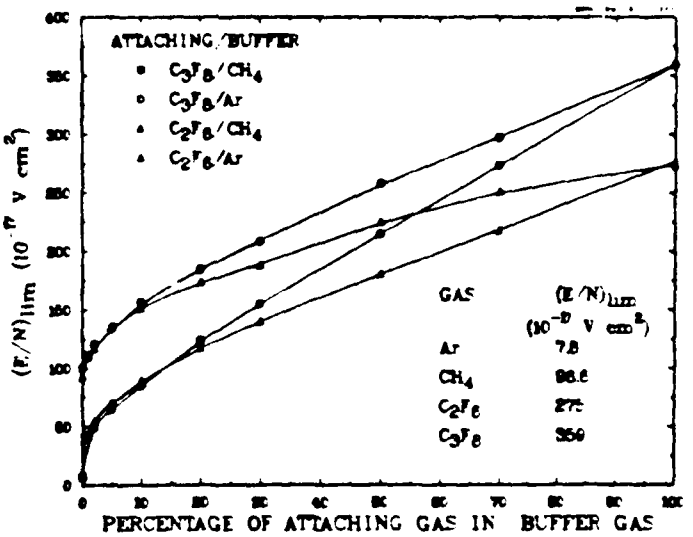

Fig 11. $(E/N)_{lim}$ versus percentage of C_2F_6 or C_3F_8 in the buffer gases Ar or CH_4. The total gas pressure was 108.7 kPa at a temperature of 295 K. No ultraviolet (UV) irradiation of the electrode gap was made except for the C_2F_6/CH_4 mixtures; as a result the $(E/N)_{lim}$ values for C_2F_6/CH_4 mixtures are ~5% lower than they would have been without UV irradiation (Christophorou and co-workers, 1983).

of the attaching gas in CH_4 enabling a wider choice of gas mixtures to be made while still maintaining high breakdown field strengths.

DISCUSSION

All the gas mixtures discussed in this paper are considered to be good candidates for diffuse discharge switching applications. This conclusion is supported by the recent findings and interest (e.g. Bletzinger, 1983a,b; Byszewski and co-workers, 1984; Runhardt, 1984; Scherrer and co-workers, 1984; Schoenbach and co-workers, 1984) in using the mixtures in actual e-beam switching devices. Bletzinger (1983a,b) has shown that the current decay in the diffuse discharge is dominated by recombination processes at early times and that the decay can be considerably enhanced at later times by the addition of small amounts of the perfluoroalkanes CF_4, C_2F_6, and C_3F_8 to the discharge. Knowledge of the nature and magnitude of the recombination processes in the discharge, along with the gas ionizing efficiency of the e-beam (which is a measure of W--the average energy required to produce a positive ion-electron pair in the discharge) would be of considerable value in modeling the temporal behavior of the electron conductivity in the discharge. Measurements of these parameters and the decomposition of the gas by the external electron beam are currently in progress at the authors' laboratory. The effects of gas heating on the electron transport and breakdown properties in the discharge are also required and are also presently under investigation.

The studies outlined in this paper and the continuing investigations will allow accurate modeling of the often complex and interrelated phenomena that occur within the diffuse discharge. This in turn will allow the overall performance of these switching devices to be predicted accurately and as a consequence, the tailoring of the gaseous constituents and operating parameters of the discharge to achieve optimum performance.

ACKNOWLEDGMENTS

One of us (S. R. H.) wishes to gratefully acknowledge Dr. R. W. Crompton and his colleagues in the Ion Diffusion Unit at the Australian National University for allowing him to use their research facilities for the D_T/μ measurements and for providing such kind hospitality during his stay.

Research sponsored in part by the Office of Naval Research under contract DOE No. 40-1244-82, in part by the Naval Surface Weapons Center under contract DOE No. 40-1271-82, and in part by the Division of Electric Energy Systems, U.S. Department of Energy, under contract DE-AC05-84OR21400 with Martin Marietta Energy Systems, Inc.

REFERENCES

Bletzinger, P. (1983a). Scaling of electron beam switches. Proceedings of the 4th IEEE International Pulsed Power Conference, Albuquerque, New Mexico, June 6-8 (in press).

Bletzinger, P. (1983b). Characteristics of electron beam ionized discharges with added attaching gases. Proceedings of the XVI International Conference on Phenomena in Ionized Gases, Vol. 2, Düsseldorf, August 29-September 2, pp. 218-219.

Burton, J. K., D. Conte, R. D. Ford, W. H. Lupton, V. E. Scherrer, and I. M. Vitkovitsky (1979). Inductive storage--prospects for high power generation. Proceedings of the 2nd IEEE International Pulsed Power Conference, Lubbock, Texas, June 11-14, pp. 284-286.

Byszewski, W. W., M. J. Enright, and J. M. Proud (1984). Transient gas discharges in perfluorocarbon-argon mixtures. In L. G. Christophorou and M. O. Pace (Eds.), Gaseous Dielectrics IV, Pergamon Press, New York, pp. 255-260.

Carter, J. G., S. R. Hunter, L. G. Christophorou, and V. K. Lakdawala (1983). Electron drift velocity and ionization and attachment coefficients in gases/mixtures for diffuse-discharge opening switches. Proceedings of the 3rd International Swarm Seminar, Innsbruck, Austria, August 3-5, pp. 30-36.

Christophorou, L. G. (1971). Atomic and Molecular Radiation Physics, Wiley-Interscience, London.

Christophorou, L. G., D. L. McCorkle, D. V. Maxey, and J. G. Carter (1979). Fast gas mixtures for gas-filled particle detectors. Nucl. Instr. Meth., 163, 141-149.

Christophorou, L. G., S. R. Hunter, J. G. Carter, and R. A. Mathis (1982a). Gases for possible use in diffuse-discharge switches. Appl. Phys. Lett., 41, 147-149.

Christophorou, L. G., J. G. Carter, and D. V. Maxey (1982b). Electron motion in high pressure polar gases. NH$_3$. J. Chem. Phys., 76, 2653-2661.

Christophorou, L. G., S. R. Hunter, J. G. Carter, S. M. Spyrou, and V. K. Lakdawala (1983). Basic studies of gases for diffuse-discharge switching applications. In T. H. Martin and M. F. Rose (Eds.), Proceedings of the 4th IEEE International Pulsed Power Conference, The Texas Tech. Press, Lubbock, Texas, pp. 702-708.

Crompton, R. W. and R. L. Jory (1962). On the swarm method for determining the ratio of electron drift velocity to diffusion coefficient. Aust. J. Phys., 15, 451-469.

Fernsler, R. F., D. Conte, and I. M. Vitkovitsky (1980). Repetitive electron-beam controlled switching. IEEE Trans. Plasma Sci., PS-8, 176-180.

Hunter, R. C. (1976). Electron beam controlled switching. Proceedings of the IEEE International Pulsed Power Conference, Lubbock, Texas, November, pp. 1C6-1--1C6-6.

Hunter, S. R. and L. G. Christophorou (1984). Electron attachment to the perfluoroalkanes $n\text{-}C_NF_{2N+2}$ (N = 1-6) using high pressure swarm techniques. J. Chem. Phys. (in press).

Hunter, S. R., J. G. Carter, and L. G. Christophorou (1984). Electron attachment and ionization coefficients in the perfluoroalkanes (in preparation).

Kristiansen, M. and R. H. Schoenbach (1981). Executive summary. Final Report on Workshop on Repetitive Opening Switches, Tamarron, Colorado, January 28-30.

Kristiansen, M. and R. H. Schoenbach (1982). Final Report on Workshop on Diffuse Discharge Opening Switches, Tamarron, Colorado, January 13-15.

Kunhardt, E. E. (1984). Basic topics of current interest in switching for pulsed power applications. In L. G. Christophorou and M. C. Pace (Eds.), Gaseous Dielectrics IV, Pergamon Press, New York, pp. 213-222.

Naidu, M. S. and A. N. Prasad (1972). Mobility, diffusion and attachment of electrons in perfluoroalkanes. J. Phys. D 5, 983-993.

Petrovic, Z., R. W. Crompton, and G. N. Haddad (1984). Model calculations of negative differential conductivity in gases. Aust. J. Phys. (in press).

Robson, R. E. (1984). Generalized Einstein relation and negative differential conductivity in gases. Aust. J. Phys. (in press).

Scherrer, V. E., R. J. Commisso, R. F. Fernsler, and I. M. Vitkovitsky (1984). Study of gas mixtures for e-beam controlled switches. In L. G. Christophorou and M. C. Pace (Eds.), Gaseous Dielectrics IV, Pergamon Press, New York, pp. 238-245.

Schoenbach, K. H., G. Schaefer, M. Kristiansen, L. L. Hatfield, and A. H. Guenther (1982). Concepts for optical control of diffuse discharge opening switches. IEEE Trans. Plasma Sci., PS-10, 246-251.

Schoenbach, K. H., G. Schaefer, M. Kristiansen, H. Krompholz, H. Harjes, and D. Skaggs (1984). Investigations of e-beam controlled diffuse discharges. In L. G. Christophorou and M. O. Pace (Eds.), Gaseous Dielectrics IV, Pergamon Press, New York, pp. 248-254.

Spyrou, S. M., S. R. Hunter, and L. G. Christophorou (1984). Fragmentation and electron attachment of fluoroethers and fluorosulfides under low-energy (<10 eV) electron impact (in preparation).

GASEOUS DIELECTRICS IV

Proceedings of the
Fourth International Symposium on
Gaseous Dielectrics
Knoxville, Tennessee, U.S.A.
April 29 - May 3, 1984

Edited by
Loucas G. Christophorou
and
Marshall O. Pace

Pergamon Press

New York • Oxford • Toronto • Sydney • Paris • Frankfurt

APPENDIX C

Studies of negative ion formation in fluoroethers and fluorosulphides using low-energy (≤ 10 eV) electron beam and electron swarm techniques[a]

S. M. Spyrou[b] S. R. Hunter,[b] and L. G. Christophorou[b]
Atomic, Molecular, and High Voltage Physics Group, Health and Safety Research Division, Oak Ridge National Laboratory, Oak Ridge, Tennessee 37831

(Received 13 June 1984, accepted 12 July 1984)

The attachment of low-energy (≤ 10 eV) electrons to four fluoroethers (CF_3OCF_3, CF_3OCF_2H, CF_2HOCF_2H and CF_3OCH_3) and two fluorosulphides (CF_3SCF_3 and CF_3SCH_3) has been studied using a time-of-flight mass spectrometer (TOFMS) and a high pressure electron swarm technique. The relative cross sections as a function of incident electron energy for all observed anions were measured by employing the former, and the total absolute electron attachment rate constants were measured by employing the latter technique. All six molecules were found to attach electrons dissociatively. The types and relative intensities of the fragment anions depend strongly on the number and relative positions of the F atoms in the molecule and on the presence of O or S atoms in the molecule. The fluorosulphides attach lower energy electrons than do the fluoroethers. The magnitude of the total electron attachment rate constants increases with increasing number of F atoms in the molecule. The observed negative ions (in decreasing order of intensity) and the positions of the peak intensities (given in parentheses in eV) are: F^- (5.3) and CF_3O^- (4.8) from CF_3OCF_3; CF_3O^- (3.7), F^- (5.7), HF_2^- (6.1), CFO^- (5.9), and CF_3^- (6.7) from CF_3OCF_2H; CF_3O^- (3.0), HF_2^- (4.7), F^- (5.0), and CFO^- (4.9) from CF_2HOCF_2H; F^- (6.7) from CF_3OCH_3; CF_3S^- (0.6) and F^- (3.8) from CF_3SCF_3; CF_3S^- (~0.0) from CF_3SCH_3. Energetic considerations were employed to identify possible fragmentation mechanisms of the negative ion states (NISs) leading to the production of the observed fragment negative ions and to deduce values for the electron affinities of the radicals CF_3O and CF_3S. CNDO/2 and MNDO molecular orbital calculations were performed on all six molecules investigated in an effort to rationalize the types, relative intensities, and positions of the maxima in the cross sections of the observed anions.

I. INTRODUCTION

The study of the attachment of low-energy (0–10 eV) electrons to the fluoroethers (CF_3OCF_3, CF_3OCF_2H, CF_2HOCF_2H, and CF_3OCH_3) and fluorosulphides (CF_3SCF_3 and CF_3SCH_3) is of basic and of practical interest. These molecules are an attractive group to study the effect of atomic substitution in the molecule on its electron attaching properties. In addition, since the electron attachment rate constants for these molecules are pressure independent (see Sec. III B), they provide a straightforward comparison of the results obtained by the electron beam and by the electron swarm techniques. From the practical point of view, the magnitude and energy dependence of the attachment rate constants for CF_3OCF_3 and CF_3SCF_3 are such as to make them good gas dielectrics, and also good electronegative gases to be used as additives in gas mixtures for diffuse-discharge switching applications.[1,2]

II. EXPERIMENTAL

Both the TOFMS and the electron swarm techniques employed in the present study have been described previously (e.g., see Refs. 3 and 4). In the TOFMS experiment a heated filament is used to produce an electron beam with full width at half-maximum (FWHM) of ~0.5 eV. With the retarding potential difference technique (RPD)[5] a quasimonoenergetic electron beam is achieved whose FWHM is usually ~0.12–0.15 eV. However, the intensities of the majority of the anions in the present study were too low to allow application of the RPD method. The energy resolution of the electron beam in the present experiment was assumed to be approximately constant over the total range of electron energies (~0–10 eV) employed. The shape of the electron beam energy distribution was monitored by observing the very narrow (FWHM ~ 10 meV[6]) SF_6^-* resonance which peaks at ~0.0 eV.[7] The SF_6 gas was always admixed in the system with the gas under study. To remove the effect of the broad electron energy distribution on the measured relative cross sections an unfolding procedure[3] was employed. It was found earlier[3] that by using this procedure the unfolded cross sections were comparable or narrower than those obtained by application of the RPD technique (see Sec. III; compare data in Figs. 1 and 2, see also Fig. 3).

In the electron swarm experiment the determination of the electron energy distribution function $f(\epsilon, E/N)$ and hence the mean electron energy $\langle\epsilon\rangle$ is more complicated, as it not only depends on E/N, but also on the gas under study. Moreover, the electron energy distribution functions are accurately known for only a few gases. In the present experiments the measurements were performed in both N_2 and Ar buffer gases for which $f(\epsilon, E/N)$ are known over the range of E/N values we used. The elastic and inelastic scattering

[a] Research sponsored by the Office of Health and Environmental Research and the Division of Electric Energy Systems of the U.S. Department of Energy, under contract DE-AC05-84OR21400 with Martin Marietta Energy Systems, Inc., and the Office of Naval Research, under contract DOE No. 40-1246-82.

[b] Also, Department of Physics, The University of Tennessee, Knoxville, Tennessee 37996.

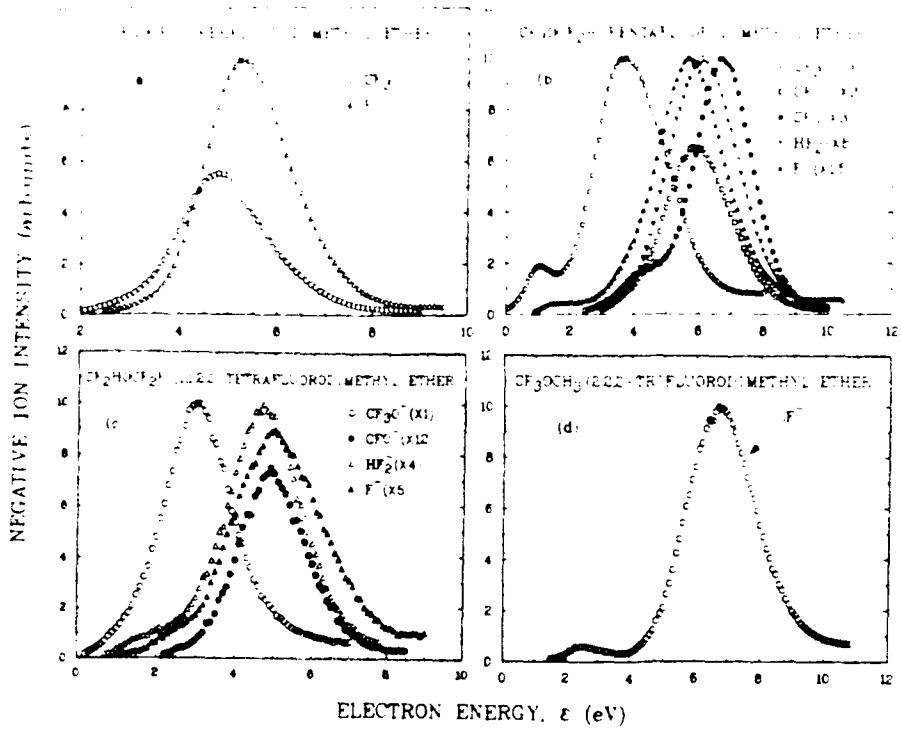

FIG 1. Negative ion intensity as a function of electron energy ϵ (nonunfolded data) for (a) CF_3OCF_3, (b) CF_3OCF_2H, (c) CF_2HOCF_2H, and (d) CF_3OCH_3.

cross sections in Ar and N_2, the numerical solution of the Boltzmann equation used to obtain $f(\epsilon, E/N)$ and the accuracy of the resultant distribution functions used in this study have been previously described.[4] Small quantities of the attaching gas under study are mixed into these buffer gases at such concentrations, that the addition of the attaching gas does not affect the electron energy distribution function of the buffer gas alone. When, however, the attaching gas did not attach electrons efficiently, a high concentration (up to ~ 1 part in 10^4) of the attaching gas was required, and the measurements were performed as a function of the partial attaching gas number density in order to remove the effect of the attaching gas on the electron energy distribution function. This problem is more acute in Ar and can lead to large uncertainties in the measured attachment rate constants when these are small (see Sec. III B).

The present swarm measurements were performed at room temperature (~ 300 K) using high total pressures P_T in the range $0.13 < P_T < 1.0$ MPa and over a mean electron energy $\langle\epsilon\rangle$, which ranges from thermal energy (~ 0.04 eV) to ~ 1.0 eV for N_2 and from 0.3 to 4.8 eV for Ar. The measured electron attachment rate constants $k_a(E/N)$ and the buffer

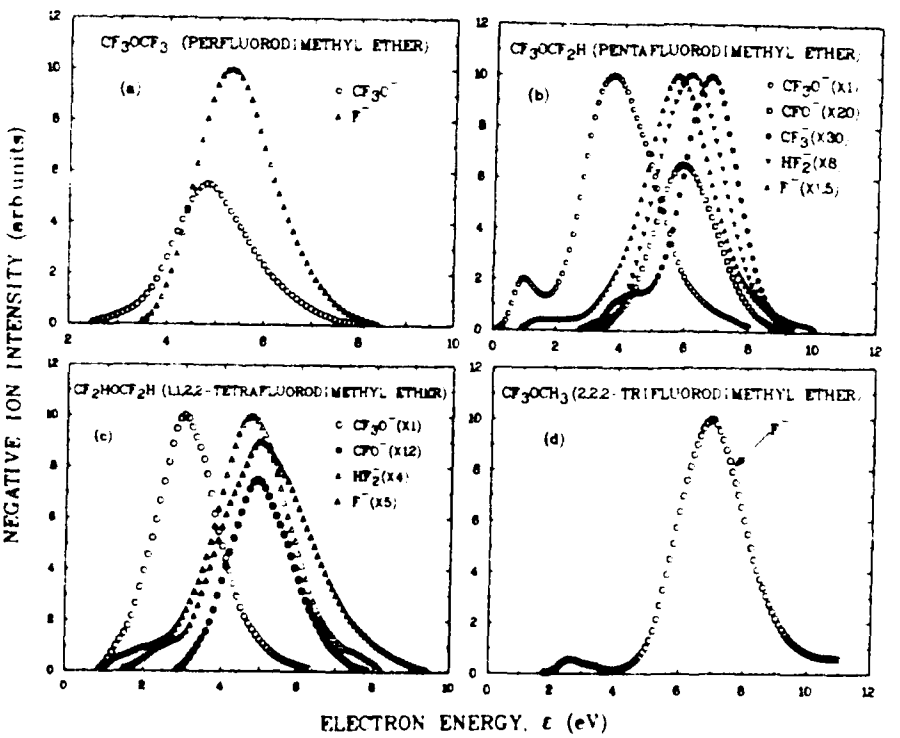

FIG 2. Negative ion intensity as a function of electron energy ϵ (unfolded data) for (a) CF_3OCF_3, (b) CF_3OCF_2H, (c) CF_2HOCF_2H, (d) CF_3OCH_3.

gas electron energy distribution functions ($f_0 \epsilon^{1/2} N$) were used to determine the absolute total attachment cross sections $\sigma_a \epsilon$ for some of the molecules studied using the unfolding procedure developed by Christophorou *et al.*[4] Using N_2 and Ar as buffer gases, $\sigma_a \epsilon$ were obtained within the ranges of ~0.02–1.5 and 0.3–9.0 eV, respectively.[4]

The gases CF_3OCF_3, CF_3OCF_2H, and CF_2HOCF_2H were purchased from PCR Research Chemical Inc., with a quoted minimum purity of 97%–99%. The compounds CF_3OCH_3 and CF_3SCH_3 were synthesized by Dr. J. L. Adcock of the Chemistry Department of the University of Tennessee. For CF_3SCF_3, two samples were used, one was purchased from Armageddon Chemical Company and the other was prepared by Dr. J. L. Adcock. Impurities in these compounds were determined by the electron beam technique, the effect of these impurities on the swarm measured electron attachment rate constants is discussed in Sec. III B.

III. RESULTS

A. Negative ion fragments

The present TOF mass spectrometric study has shown that low-energy electrons attached dissociatively to the fluoroether and the fluorosulphide molecules investigated. No parent anions were observed in any of these molecules.

1. Fluoroethers

The relative cross sections as a function of ϵ for all the fragment anions observed from the four fluoroethers studied are shown in Fig. 1. Each curve represents the average of at least four sets of data. Each set of data was deconvoluted and the averages of the corresponding unfolded functions are shown in Fig. 2. The relative peak intensities, positions of maxima in the ion intensity, full width at half-maximum (FWHM) of the observed maxima in the negative ion intensity vs ϵ plots, and the appearance onsets for the observed fragment anions are listed in Table I. It is evident from these results that the type of anions, their relative intensity, and the number and position of the resonance maxima in the relative cross sections of the various anions depend strongly on the number and relative positions of the F atoms in the molecule. The molecules with one or both of the methyl groups partially fluorinated form multiple fragment ions more readily upon electron impact than those with methyl groups containing atoms of only one type (either H or F). Five anions (CF_3O^-, CFO^-, CF_3^-, HF_2^-, F^-) and four anions (CF_3O^-, CFO^-, HF_2^-, and F^-) have been observed, respectively, for CF_3OCF_2H and CF_2HOCF_2H. The formation of CFO^- and HF_2^- requires multiple molecular fragmentation and the formation of CF_3O^- from CF_2HOCF_2H also requires strong rearrangement of the transient parent anion. For both molecules the predominant ion is CF_3O^-, with the other anions having intensities up to 30 times less than that of CF_3O^-. On the other hand, for CF_3OCF_3 only two ions (CF_3O^- and F^-) and for CF_3OCH_3 only one ion (F^-) have been detected. The ratio of the relative intensity of F^- to CF_3O^- is about 2:1 for CF_3OCF_3. A possible explanation of the absence (or extremely weak intensity) of CF_3O^- from CF_3OCH_3 is discussed in Sec. IV B.

2. Fluorosulphides

The relative cross sections for negative ion formation as a function of ϵ for the fluorosulphides CF_3SCF_3 and

TABLE I. Negative ions due to low-energy electron impact on CF_3OCF_3, CF_3OCF_2H, CF_2HOCF_2H, and CF_3OCH_3.

Molecule	Observed negative ion	Relative peak ion intensity	Energy of maximum ion intensity (eV)[b]	FWHM[a] (eV)[b]	Appearance onset (eV)[b]
CF_3OCF_3	CF_3O^-	550	4.8 ± 0.05	1.85	2.5 ± 0.1
	F^-	1000	5.3 ± 0.05	1.85	3.5 ± 0.2
CF_3OCF_2H	CF_3O^-	200	1.0 ± 0.2	1.0	0.2 ± 0.1
		1000	3.7 ± 0.1	2.5	2.0 ± 0.3
	CFO^-		d		2.8 ± 0.1
		35	5.9 ± 0.05	2.3	4.0 ± 0.2
	CF_3^-		d		3.1 ± 0.1
		35	6.7 ± 0.05	2.0	4.8 ± 0.1
	HF_2^-	125	6.1 ± 0.05	2.4	3.7 ± 0.2
	F^-		d		1.0 ± 0.1
		650	5.7 ± 0.05	2.35	2.8 ± 0.2
CF_2HOCF_2H	CF_3O^-	1000	3.0 ± 0.05	1.8	0.9 ± 0.1
	CFO^-	60	4.9 ± 0.05	1.9	2.9 ± 0.1
	HF_2^-		d		1.0 ± 0.2
		250	4.7 ± 0.05	2.25	2.6 ± 0.3
	F^-		d		1.7 ± 0.2
		200	5.0 ± 0.05	2.75	2.8 ± 0.2
CF_3OCH_3	F^-	50	2.5 ± 0.1	1.0	1.8 ± 0.1
		1000	6.7 ± 0.1	2.5	4.7 ± 0.3

[a] Full width at half-maximum of the respective ion intensity as a function of electron energy.
[b] The energy scale calibration was made using SF_6 and taking for the SF_6^-/SF_6 resonance the value of 0.37 eV (Ref. 7). The ± refers to the standard deviation from the average.
[c] Values listed are from the unfolded data.
[d] Unresolved peak. Only the appearance onset ascribed to these peaks is listed in the table.

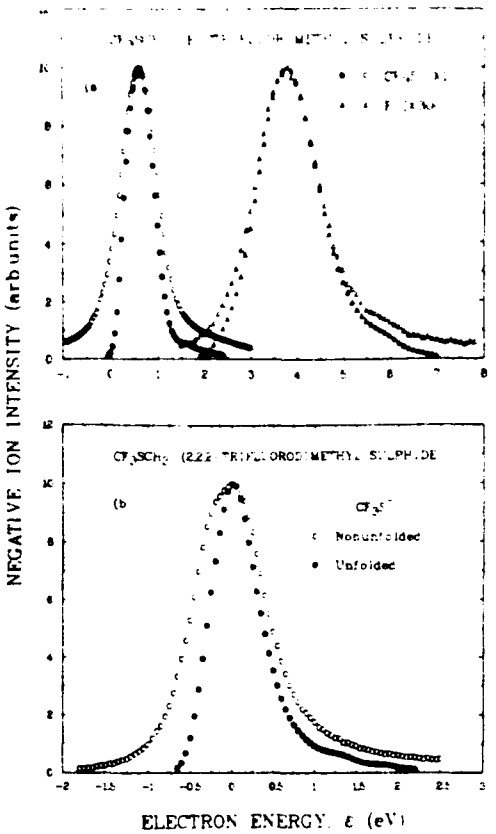

FIG 3. Negative ion intensity as a function of electron energy ϵ (open symbols: nonunfolded, solid symbols: unfolded data) for (a) CF_3SCF_3, (b) CF_3SCH_3.

CF_3SCH_3 are shown in Fig. 3. The relative peak intensities, energy of maximum ion intensity, FWHM of the ion resonances, and the appearance onsets for each observed negative ion are summarized in Table II. The types of anions observed are analogous to the corresponding fluoroethers, i.e., CF_3S^- and F^- from CF_3SCF_3 and CF_3S^- from CF_3SCH_3. There is, however, a rather large difference in the relative intensities of these anions and the positions of the resonance maxima as compared to those for the fluoroethers. For the fluorosulphides the predominant anion is CF_3S^- peaking at 0.6 eV for CF_3SCF_3 and at thermal energies for CF_3SCH_3. In contrast, for the fluoroether CF_3OCF_3, the CF_3O^- ion peaks at 4.8 eV and the F^- ion at 5.3 eV and for CF_3OCH_3, the F^- ion peaks at 6.7 eV. For CF_3SCF_3 the F^- ion current is 300 times less intense than CF_3S^-, while F^- is almost twice as intense as

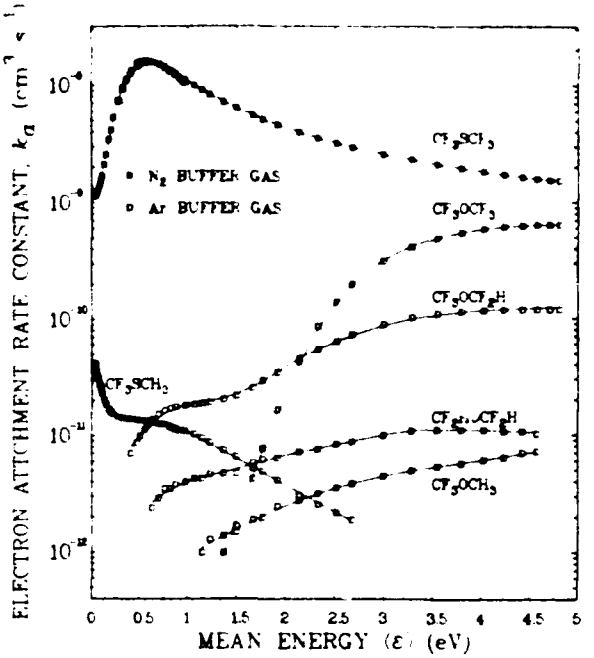

FIG 4. Total electron attachment rate constants k_a for the fluoroethers and fluorosulphides measured as a function of mean electron energy $\langle\epsilon\rangle$ in both Ar and N_2 buffer gases.

CF_3O^- in CF_3OCF_3; also whereas for CF_3OCH_3, F^- is the only anion which has been observed in this study, for CF_3SCH_3, F^- was not observed at all.

B. Total electron attachment rate constants

In Fig. 4 are shown the $k_a(\langle\epsilon\rangle)$ for all the fluoroethers and fluorosulphides measured in the swarm study using Ar as a buffer gas. Also shown in Fig. 4 are the $k_a(\langle\epsilon\rangle)$ for the fluorosulphides using N_2 as a buffer gas. These two sets of measurements are listed, respectively, in Tables III and IV. Between 6 and 12 independent sets of measurements were made for each of the attaching gases in each of the buffer gases. When the $k_a(E/N)$ were found to depend on the partial attaching gas number density N_A [as was the case for all the attaching gas/argon buffer gas mixtures, e.g., see Figs. 5(a) and 5(b) for the dependence of $k_a(E/N)$ on the partial concentration of CF_3SCF_3 and CF_3OCF_3, respectively, in argon] the measured k_a as a function of N_A at a fixed total pressure was extrapolated to zero concentration. The values

TABLE II. Negative ions due to low-energy electron impact on CF_3SCF_3 and CF_3SCH_3.

Molecule	Observed negative ion	Relative peak ion intensity	Energy of maximum ion intensity (eV)[b]	FWHM[a] (eV)[c]	Appearance onset (eV)[c]
CF_3SCF_3	CF_3S^-	1000	0.6 ± 0.05	0.7	~0
	F^-	3	3.8 ± 0.1	1.5	1.9 ± 0.1
CF_3SCH_3	CF_3S^-	1000	~0	0.7	

[a]Full width at half-maximum of the respective ion intensity as a function of electron energy.
[b]The energy scale calibration was made using SF_6 and taking for the SF_5^-/SF_6 resonance the value of 0.37 eV (Ref. 7). The $\pm$ refers to the standard deviation from the average.
[c]Values listed are from the unfolded data.

TABLE III. Electron attachment rate constants for the fluoroethers CF_3SCF_3 and CF_3SCH_3 in a buffer gas of N_2 as a function of E/N and ϵ

E/N (10^{-17} V cm^2)	$\langle\epsilon\rangle$ (eV)	CF_3SCF_3 (10^{-12} cm^3 s^{-1})	CF_3SCH_3 (10^{-12} cm^3 s^{-1})
0.0516	0.0404	0.114	4.2
0.0466	0.0430	0.115	4.1
0.0621	0.0463	0.117	3.8
0.0931	0.0546	0.120	3.5
0.124	0.0646	0.125	3.2
0.155	0.0757	0.130	3.0
0.186	0.0873	0.140	2.7
0.217	0.099	0.153	2.5
0.248	0.111	0.168	2.3
0.310	0.133	0.21	2.03
0.373	0.154	0.26	1.85
0.466	0.184	0.35	1.69
0.528	0.203	0.42	1.60
0.621	0.231	0.53	1.53
0.776	0.279	0.74	1.45
0.931	0.327	0.94	1.41
1.087	0.374	1.12	1.39
1.24	0.417	1.26	1.38
1.55	0.493	1.45	1.36
1.86	0.555	1.54	1.33
2.17	0.601	1.59	1.32
2.48	0.647	1.57	1.29
3.10	0.711	1.52	1.26
3.73	0.759	1.45	1.25
4.66	0.812	1.35	1.21
5.28	0.839	1.31	1.17
6.21	0.872	1.24	1.13
7.76	0.911	1.17	1.11
9.31	0.938	1.11	
10.9	0.957	1.08	
12.4	0.972	1.05	

of $k_a(E/N)$ at $N_A \to 0$ were taken to be those that would be measured had $f(\epsilon,\langle\epsilon\rangle)$ been characteristic of the pure buffer gas.

The sample CF_3SCH_3 was found in the TOFMS study to contain a small amount of a chlorine-containing impurity which produced Cl^- when subjected to low-energy ($\epsilon < 10$ eV) electron impact. The Cl^- signal was $\sim 20\%$ as intense and had approximately the same energy dependence as the CF_3S^- signal produced by dissociative attachment to the CF_3SCH_3 molecule. Attempts to remove this impurity (which was estimated to be $< 1\%$ of sample) by gas chromatography-mass spectrometry methods failed. Consequently, it is estimated that the measured $k_a(E/N)$ in the swarm study may be $\sim 20\%$ too large for this compound due to the presence of the Cl^- impurity ion. The compound CF_3SCF_3 was also found in the TOFMS study to contain small amounts of a chlorine-containing impurity and perhaps also F_2, which produced small Cl^- and F^- signals, respectively, both peaking at ~ 0 eV. The contribution to the total electron attachment from these impurities was estimated to be $< 1\%$ of the total negative ion production and thus their effect on the measured $k_a(E/N)$ values in CF_3SCF_3 is expected to be negligible except at thermal energies. All the negative ions we observed in the electron impact studies of the fluoroethers were identified as fragment ions of the parent molecules and thus impurity problems should not affect the $k_a(E/N)$ measurements in these compounds.

The overall accuracy of the $k_a(E/N)$ measurements in CF_3SCF_3 and CF_3OCF_3 is expected to be $\sim 5\%$–7%. (See Ref. 4 for the sources and estimates of error in this experiment.) For the remaining molecules in this study, the overall accuracy of the measured rate constants decreases as the magnitude of the electron attachment rate constant decreases, such that for CF_3SCH_3 and CF_3OCF_2H, the estimated uncertainty is $\sim 10\%$–15%, and for CF_2HOCF_2H and CF_3OCH_3 $\sim 20\%$. This increased uncertainty is mainly due to an increased statistical inaccuracy in the measurements when the rate constants are small and also possible influences of the attaching gas on the electron energy distribution function in the gas mixtures compared to those in the pure buffer gas, due to the necessity of using relatively high (up to one part in 10^4) concentrations of the attaching gas in the Ar buffer gas. It appears that errors from these sources restrict this technique to the study of electron attachment processes in molecules whose $k_a(E/N)$ have peak values of $> 10^{-12}$ cm^3 s^{-1} using Ar as a buffer gas, and $> 10^{-13}$ cm^3 s^{-1} using N_2 as the buffer gas.

The measured total electron attachment rate constants have been found to be independent of the total gas pressure P_T for all the compounds in the present study, indicating that dissociative electron attachment processes are responsible for the observed electron attachment in these molecules. This is in contrast to our recent measurements in the perfluoroalkanes,[3,4] where the measured $k_a(E/N)$ depended

TABLE IV. Electron attachment rate constants for several fluoroethers and fluoroalkanes in a buffer gas of argon as a function of E/N and ϵ.

E/N (10^{-16} V cm^2)	ϵ (eV)	CF_3OCF_3 (10^{-9} cm^3 s^{-1})	CF_3OCF_2H (10^{-9} cm^3 s^{-1})	CF_3HOCF_2H (10^{-9} cm^3 s^{-1})	CF_3OCH_3 (10^{-9} cm^3 s^{-1})	CF_3SCF_3 (10^{-9} cm^3 s^{-1})	CF_3SCH_3 (10^{-9} cm^3 s^{-1})
0.932	0.308					0.73	
0.124	0.335					0.92	
0.155	0.364					1.09	
0.217	0.412		0.07			1.33	
0.311	0.473		0.09			1.53	
0.373	0.509		0.10			1.58	
0.466	0.559		0.11			1.61	
0.528	0.590		0.12			1.60	
0.621	0.634		0.136	0.24		1.58	
0.777	0.702		0.151	0.29		1.50	
0.932	0.764		0.163	0.35		1.41	
1.09	0.822		0.170	0.35		1.32	1.19
1.24	0.876		0.175	0.38		1.24	1.15
1.55	0.976		0.181	0.40		1.11	1.10
1.86	1.068		0.186	0.43		1.00	1.03
2.17	1.15		0.190	0.43	1.0	0.91	0.96
2.49	1.23		0.194	0.47	1.3	0.84	0.88
3.11	1.37	0.010	0.206	0.48	1.4	0.73	0.76
3.73	1.50	0.017	0.222	0.48	1.5	0.64	0.67
4.66	1.67	0.043	0.26	0.59	1.9	0.55	0.53
5.28	1.77	0.078	0.30	0.63	2.0	0.51	0.50
6.21	1.92	0.168	0.35	0.65	2.5	0.46	0.42
7.77	2.14	0.43	0.46	0.73	2.8	0.40	0.31
9.32	2.33	0.86	0.55	0.77	3.2	0.35	0.26
10.9	2.52	1.38	0.63	0.85	3.6	0.32	0.22
12.4	2.69	1.95	0.72	0.88	3.9	0.295	0.19
15.5	3.00	3.10	0.88	1.00	4.5	0.256	
18.6	3.29	4.09	1.01	1.09	5.0	0.230	
21.7	3.55	4.86	1.09	1.11	5.4	0.210	
24.9	3.80	5.46	1.14	1.10	5.7	0.194	
27.9	4.03	5.87	1.17	1.10	6.1	0.182	
31.1	4.26	6.13	1.18	1.07	6.4	0.172	
34.2	4.43	6.30	1.18	1.07	7.0	0.164	
37.3	4.58	6.38	1.19	1.02	7.2	0.159	
40.4	4.71	6.41	1.19			0.155	
43.5	4.81	6.40	1.19			0.153	
46.6	4.89					0.151	

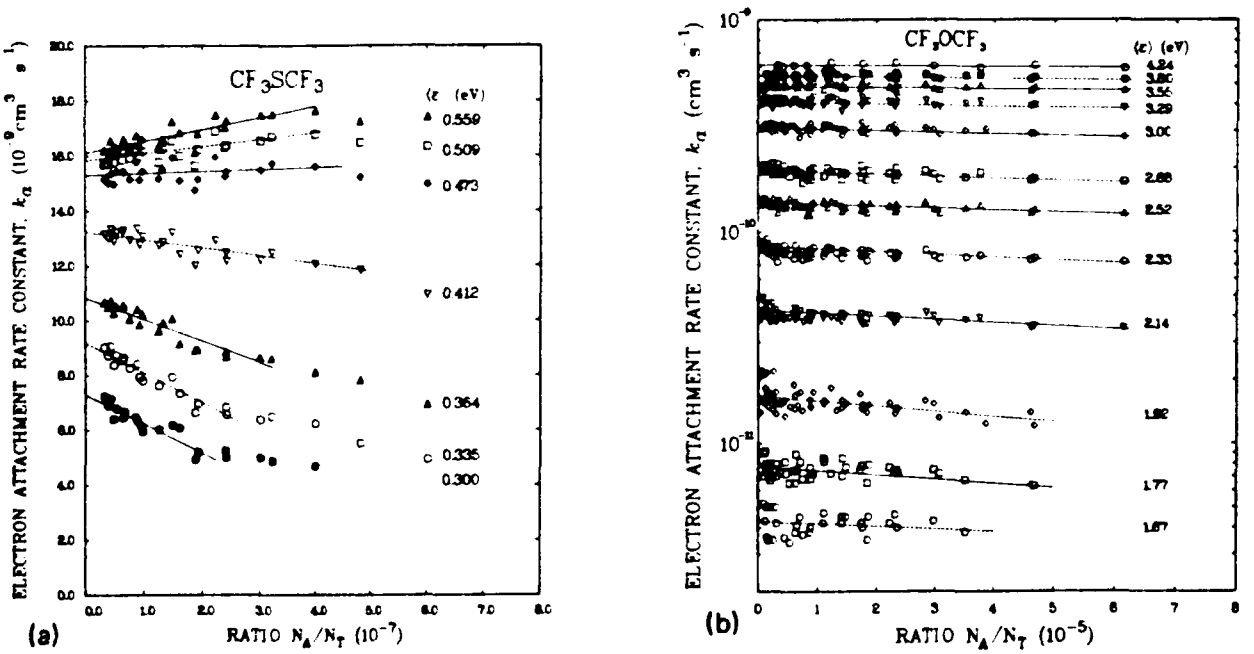

FIG. 5. Total electron attachment rate constants k_a for (a) CF_3SCF_3 and (b) CF_3OCF_3 in argon plotted as a function of the ratio of the attaching gas number density N_A to the total gas number density N_T at several values of the mean electron energy (ϵ).

strongly on pressure for C_2F_5 and n-C_4F_9 and to a lesser extent for n-C_6F_{13}, indicating that electron attachment to those molecules at the pressures used in these experiments was predominantly by parent negative ion stabilization. From the results presented in Fig. 4 it is apparent that increasing the F substitution in both the fluoroethers and the fluorosulphides increases the rate of electron attachment. Furthermore, the fluoroethers predominantly attach electrons at higher energies than do the fluorosulphides. This observation is again in agreement with the measurements of the TOFMS study presented in the previous section.

C. Swarm unfolded total electron attachment cross sections

The measured total electron attachment rate constants $k_a(E/N)$ are related to the total electron attachment cross section $\sigma_a(\epsilon)$ by

$$k_a(E/N) = \frac{\eta(E/N)}{N} \frac{w(E/N)}{N}$$

$$= \left(\frac{2}{m}\right)^{1/2} \int_0^\infty \epsilon^{1/2} \sigma_a(\epsilon) f(\epsilon, E/N)\, d\epsilon, \quad (1)$$

where η/N is the normalized electron attachment coefficient, $w(E/N)$ is the electron drift velocity, m is the electron mass, and $f(\epsilon, E/N)$ is the electron energy distribution at each E/N value normalized by

$$\int_0^\infty f(\epsilon, E/N)\, d\epsilon = 1. \quad (2)$$

If both $k_a(E/N)$ and $f(\epsilon, E/N)$ are known over a wide range of E/N values, then $\sigma_a(\epsilon)$ can be determined over a wide range of electron energies using the swarm unfolding technique.[8] The $k_a(E/N)$ we used in Eq. (1) are those obtained by extrapolating the measured attachment rate constants to zero concentration of the attaching gas, so that it is

TABLE V. Swarm unfolded electron attachment cross sections $\sigma_a(\epsilon)$ for the fluoroethers and the fluorosulphides obtained by unfolding the $k_a(E/N)$ data in N_2 and in Ar.

ϵ (eV)	CF_3OCF_3[a] (10^{-17} cm^2)	CF_3OCF_2H[a] (10^{-18} cm^2)	CF_3SCF_3[a] (10^{-16} cm^2)	CF_3SCH_3[a] (10^{-16} cm^2)	ϵ (eV)	CF_3SCF_3[b] (10^{-16} cm^2)	CF_3SCH_3[b] (10^{-18} cm^2)
0.25		0.07	1.19	0.34	0.03	1.23	5.0
0.3		0.08	1.33	0.29	0.04	1.24	3.9
0.35		0.08	1.78	0.28	0.05	1.05	2.3
0.4		0.09	2.33	0.28	0.06	0.90	1.62
0.5		0.14	4.09	0.29	0.07	0.80	1.22
0.6		0.20	6.30	0.30	0.08	0.73	0.99
0.7		0.28	6.55	0.30	0.09	0.70	0.84
0.8		0.36	4.83	0.28	0.10	0.68	0.76
0.9		0.44	3.10	0.25	0.12	0.68	0.64
1.0		0.51	1.93	0.22	0.14	0.70	0.57
1.1		0.53	1.20	0.19	0.16	0.73	0.51
1.2		0.49	0.75	0.17	0.18	0.78	0.46
1.3		0.41	0.48	0.15	0.20	0.83	0.42
1.4		0.32	0.32	0.10	0.25	1.04	0.35
1.5		0.26	0.22	0.04	0.30	1.32	0.31
1.6		0.21	0.157		0.35	1.83	0.29
1.7		0.19	0.115		0.4	2.66	0.28
1.8		0.18	0.087		0.5	5.21	0.30
1.9		0.17	0.069		0.6	7.46	0.32
2.0		0.18	0.056		0.7	7.25	0.31
2.1		0.19	0.048		0.8	5.30	0.29
2.3		0.21	0.038		0.9	3.18	0.24
2.5	0.002	0.26	0.034		1.0	1.71	0.21
2.7	0.004	0.36	0.032		1.1	0.88	0.17
3.0	0.007	0.62	0.032		1.2	0.37	0.14
3.3	0.018	1.00	0.034		1.3	0.13	0.11
3.6	0.055	1.28	0.035		1.4	0.04	0.08
4.0	0.21	1.41	0.036		1.5	0.01	0.06
4.5	0.64	1.43	0.035				
5.0	1.08	1.47	0.034				
5.5	1.24	1.50	0.034				
6.0	1.14	1.43	0.033				
6.5	0.92	1.20	0.032				
7.0	0.69	0.93	0.030				
7.5	0.51	0.71	0.028				
8.0	0.37	0.55	0.025				
8.5	0.27	0.45	0.022				
9.0	0.20	0.40	0.019				
9.5	0.15	0.37	0.017				
10.0	0.11	0.35	0.014				

[a] Using $k_a(E/N)$ in Ar.
[b] Using $k_a(E/N)$ in N_2.

permissible to use the electron energy distribution functions of the pure buffer gas.

The swarm unfolded $\sigma_a(\epsilon)$ for CF_3OCF_3 and CF_3OCF_2H in Ar are listed in Table V and are plotted in Figs. 6 and 7, respectively. Attachment cross sections for CF_3HOCF_2H and CF_3OCH_3 are not given, as it has been found that the $k_a(E/N)$ values for these two molecules are too small and thus too uncertain to give stable and reproducible unfolded values of $\sigma_a(\epsilon)$. The reasons are that the statistical scatter in the $k_a(E/N)$ values is considerably larger ($\sim 20\%$) than for CF_3OCF_3 (5%–7%) and CF_3OCF_2H (10%–15%), and since it was necessary to use comparatively high concentrations of the attaching gas in the buffer gas (up to one part in 10^4) it is possible that the effect of the attaching gas on the electron energy distribution functions has not been completely removed by extrapolating k_a to $N_A \rightarrow 0$ (see Sec. II).

The total cross sections for negative ion formation for CF_3OCF_3 and CF_3OCF_2H obtained in the TOFMS study are also given in Figs. 6 and 7, respectively, normalized to the peak of the swarm unfolded $\sigma_a(\epsilon)$. It can be seen that there is a fair agreement between the peak positions and the half-widths of the major negative ion resonances for these two molecules, but there are differences in the cross section magnitudes, particularly at the higher energies, where the high energy tail of the swarm unfolded cross sections is considerably larger than those obtained in the TOFMS study. A similar trend has been noted between the swarm unfolded cross sections and the TOFMS results for the perfluoroalkanes.[4] It seems unlikely that errors in the scattering cross sections used to obtain $f(\epsilon, E/N)$ at higher energies (i.e., $\epsilon > 4$ eV) in Ar can account for the difference in the peak positions and the high energy tail of the attachment cross sections obtained by the two methods. A possible explanation of the difference may be ion discrimination effects in our mass spectrometric study since the detection efficiency in the TOFMS study may vary with the mass of the negative ion and more significantly with the translational energy of the fragment anions, and since several of the negative ions produced by dissociative attachment to these molecules possess excess energy (up to several eV; see Table VII), the detection efficiency of the TOFMS apparatus may decline with the amount of translational energy possessed by the negative ion, leading to a reduction in the measured total cross sections.

The unfolded attachment cross section functions $\sigma_a(\epsilon)$ for CF_3SCF_3 obtained from the measurements of $k_a(E/N)$ in Ar and N_2 buffer gases are listed in Table V and are plotted in Fig. 8 along with the normalized total negative ion cross section obtained in the TOFMS study. Considerable effort was expended in the present study to obtain as accurate $k_a(E/N)$ values as possible for CF_3SCF_3 in both the Ar and N_2 buffer gases in order to facilitate a comparison between the two unfolded cross sections obtained using the two buffer gases and that obtained in the TOFMS study. It can be seen in Fig. 8 that there is good general agreement between the swarm unfolded cross sections with regard to the peak position and half-width of the negative ion resonance. While the agreement in the overall magnitude of the cross section derived from the electron attachment measurements in N_2 and Ar is within the combined estimated uncertainty ($\sim 10\%$) of the swarm unfolded cross sections, the difference in the two cross section functions appears to be real, and is thought to be primarily due to differences in the accuracy of the distribution functions used to unfold the $k_a(E/N)$ data in Ar and N_2. It is expected that the distribution functions in Ar are more accurate than those of N_2 in this energy range due to

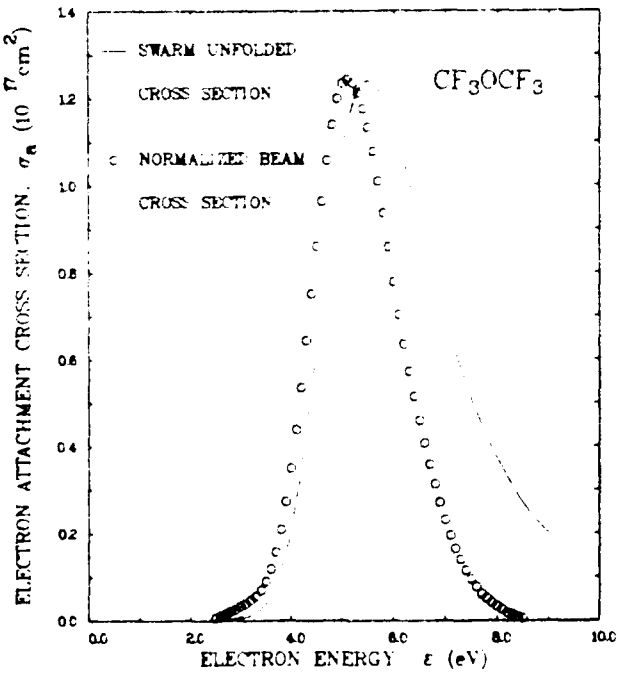

FIG. 6. Swarm unfolded total electron attachment cross section $\sigma_a(\epsilon)$ for CF_3OCF_3 in comparison with the total negative ion cross section obtained in the TOFMS study. The TOFMS study cross section has been normalized to the peak in the unfolded cross section.

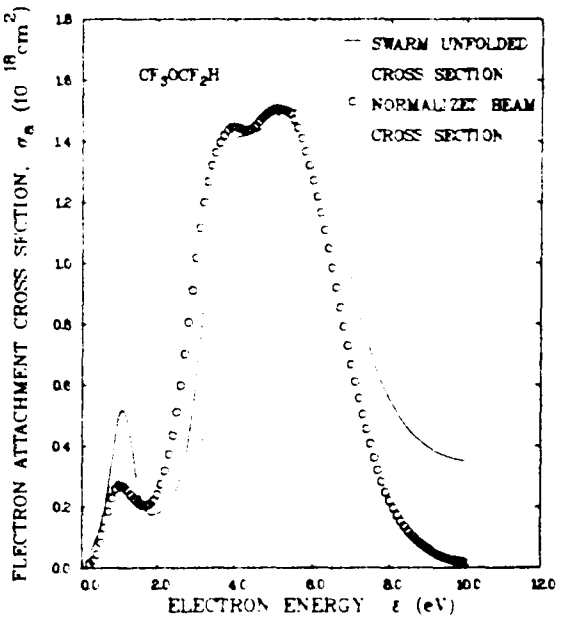

FIG. 7. Swarm unfolded total electron attachment cross section $\sigma_a(\epsilon)$ for CF_3OCF_2H in comparison with the total negative ion cross section obtained in the TOFMS study.

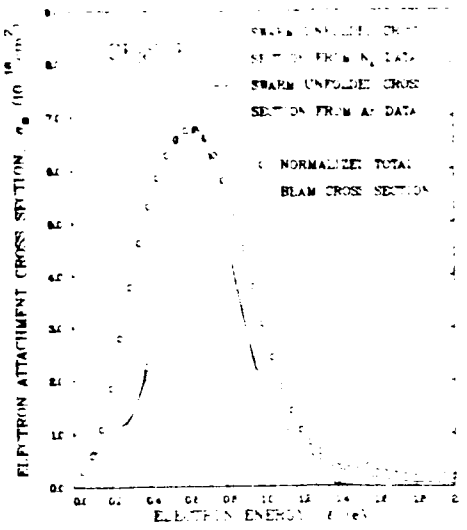

FIG. 8. Swarm unfolded total electron attachment cross section $\sigma_a(\epsilon)$ for CF_3SCF_3 at low electron energies using N_2 and Ar as buffer gases in comparison with the total negative ion cross section obtained in the TOFMS study.

the close agreement between the experimental and calculated transport data in Ar (in general $< 1\%$) than in N_2 ($\sim 5\%$), and uncertainties in the accuracy of the "two term" Boltzmann solution at higher mean energies.[9,10] The agreement between the peak position obtained from the swarm unfolded $\sigma_a(\epsilon)$ cross sections and that obtained by the TOFMS study is good, but the half widths in the resonance of the swarm unfolded $\sigma_a(\epsilon)$ cross sections are smaller than those obtained in the TOFMS study. This difference is possibly due to the fact that the electron energy distribution functions used in the swarm unfolding are known more accurately than the distribution function used in the unfolding of the beam data (see Sec. II).

The present study, along with the previous one on the perfluoroalkanes,[4] enables us to draw the following conclusions regarding the accuracy of the attachment cross sections obtained using the swarm unfolding technique. When the peak values of $k_a(E/N)$ are $> 10^{-10}$ cm^3 s^{-1}, then the peak position, peak value, and half-width of the resultant swarm unfolded attachment cross sections are determined to within an estimated uncertainty of $\sim 10\%$, provided the peak in the attachment cross section lies within the mean energy range covered by the experiment. When the $k_a(E/N)$ values peak at mean energies which lie at the highest or just beyond the highest mean energy values for which the measurements were made (e.g., CF_3OCF_3 and CF_3OCF_2H in the present study and CF_4 in the previous study[4]), the resonance can still be resolved, but with an increased uncertainty ($\sim 20\%$). When the $k_a(E/N)$ peak values are in the range $10^{-11} < k_a(E/N) < 10^{-10}$ cm^3 s^{-1}, the statistical uncertainty in the measurements also leads to an increased overall uncertainty in the unfolded $\sigma_a(\epsilon)$ cross section of $\sim 20\%$. For $k_a(E/N)$ values below 10^{-11} cm^3 s^{-1}, the statistical uncertainty in the data and the unknown influences [since in these cases high concentrations have to be used (up to one part in 10^4)] of the attaching gas on the electron energy distribution functions of the buffer gas do not allow accurate, reproducible swarm unfolded $\sigma_a(\epsilon)$ cross sections to be obtained.

IV. DISCUSSION

A. Energetics of dissociative electron attachment processes and thermochemical data

For a reaction of the form

$$e + RX \rightarrow R + X^-, \tag{3}$$

the energy balance equations of interest are

$$\Delta H_r = \Delta H_f(R) + \Delta H_f(X) - \text{E.A.}(X) - \Delta H_f(RX), \tag{4}$$

$$\text{AO}(X^-) = \Delta H_r + E^*, \tag{5}$$

$$\text{AO}(X^-) = D(R\text{–}X) - \text{E.A.}(X) + E^*, \tag{6}$$

where ΔH_r is the heat of the reaction, $\Delta H_f(R)$, $\Delta H_f(X)$, and $\Delta H_f(RX)$ are the heats of formation of R, X, and RX, respectively, E.A.(X) is the electron affinity of X, AO(X^-) is the appearance onset of X^-, $D(R\text{–}X)$ is the bond dissociation energy of RX, and E^* is the excess energy of the reaction comprised of the internal energy of excitation and the total translational energy of the fragments.

We used Eqs. (4)–(6) and the thermochemical data in Table VI (literature data or data derived in the present study) to identify possible dissociative attachment processes leading to the formation of the observed negative ions. The proposed fragmentation processes along with the respective estimated heats of reaction are summarized in Tables VII and VIII. Several remarks concerning the information in Table VII can be made.

(i) Some of the observed anions (CFO^- and HF_2^-) can only be produced indirectly in multiple-fragment reactions accompanied by intramolecular atomic rearrangement within the transient anion. In many cases, on the basis of energetic considerations, we attribute to multiple-fragment reactions even the formation of the anions F^- and CF_3^-, which can be produced via direct two-fragment reactions.

(ii) In all cases only reactions with ΔH_r lying below the corresponding AO of the negative ion have been listed in Table VII. A comparison of the respective ΔH_r and AO [Eq. (5)] shows that most of the processes describing the formation of the anions from the fluoroethers are characterized by considerable excess energy (see last column of Table VII).

(iii) The energy dependences of the relative cross sections of the various anions produced from the four fluoroethers (Figs. 1 and 2) suggest that there may be two NISs for each molecule—one below and another above 3 eV. For the symmetric molecule CF_3OCF_3 the two states are degenerate, while for the asymmetric molecule CF_3OCF_2H there is an indication of a third low-lying (at ~ 1 eV) NIS. The first NIS leads mostly to the production of CF_3O^- (this anion was not observed for CF_3OCH_3) and its position shifts to higher energies with increasing number of F atoms in the molecule. A similar observation can be made for the two fluorosulphides studied. In Fig. 9 are summarized the energy dependence of the relative cross sections for CF_3O^- and CF_3S^- produced, respectively, from the fluoroether and fluorosulphide molecules in this study. The formation of anions via the high-energy NIS of the fluoroethers studied is generally accompanied by release of excess energy. How-

TABLE VI. Thermochemical data.

Quantity	Value in eV and reference	Quantity	Value in eV and reference
ΔH_fF	0.82[a]	ΔH_fCOF$_2$	−6.62[a]
ΔH_fH	2.26[b]	ΔH_fCF$_4$	−4.94[a]
ΔH_fO	2.58[b]	ΔH_fCHF$_3$	−7.22[a]
ΔH_fCF	2.65[a]	ΔH_fCH$_2$F$_2$	−4.63[a]
ΔH_fCO	−1.15[b]	ΔH_fCF$_4$	−9.58[a]
ΔH_fFO	1.13 ± 0.4[a]	ΔH_fCF$_3$O	[−6.6][c]
ΔH_fHF	−2.82[b]	D(F$_3$C–O)	[3.9 ± 0.4][c]
ΔH_fHF$_2^-$	[−2][c]	ΔH_fCF$_3$OCF$_3$	[−15.4 ± 0.4] [−15.5][d]
ΔH_fCFH	1.3 ± 0.3[b]	ΔH_fCF$_3$OCF$_2$H	[−13.5 ± 0.4] [−13.4][e]
ΔH_fCFO	−1.78 ± 0.65[b]	ΔH_fCF$_2$HOCF$_2$H	[−11.3 ± 0.4] [−11.3][f]
ΔH_fHOF	−1.02[b]	ΔH_fCF$_3$OCH$_3$	[−9.0 ± 0.4] [−9.0][g]
ΔH_fCH$_3$	1.51[b]	E.A.(F)	3.45
ΔH_fCHF$_2$	−3.04[a]	E.A.(CF$_3$)	2.1[h]
ΔH_fCH$_2$F	−0.3[a]	E.A.(HF$_2$)	3.0[i]
ΔH_fCHFO	−3.9[j]	E.A.(CFO	2.7,3.3[k]
		D(F$_3$C–F)	5.3 ± 0.2[m]

[a] Reference 11.
[b] Reference 12.
[c] This and all other values enclosed in brackets have been estimated using the data in this table as described in the footnotes of the table. The ΔH_fHF$_2$, for example, was found using HF$_2^-$→HF + F and Eq. (4) and assuming that $\Delta H_r = D$(HF–F)≃0 eV, since HF$_2$ is an unstable system, being detected only as a negative ion (Ref. 13).
[d] Obtained using CF$_3$OF→CF$_3$O + F and Eq. (4) with $\Delta H_r = D$(CF$_3$O–F) = 1.9 eV (Ref. 14) and ΔH_fCF$_3$OF) = −7.7 eV (Ref. 15).
[e] Obtained using CF$_3$OF→CF$_3$ + OF and Eq. (4) with D(CF$_3$–OF) = ΔH_r.
[f] Obtained using CF$_3$OCF$_3$→CF$_3$ + OCF$_3$ and Eq. (4) with $\Delta H_r = D$(F$_3$C–O) = 3.9 ± 0.4 eV. This and all subsequent values enclosed in parentheses are the results of MNDO calculations (see Sec. IV B).
[g] Obtained using CF$_3$OCF$_2$H→CF$_2$H + OCF$_3$ and Eq. (4) with $\Delta H_r = D$(F$_2$HC–O) = 3.9 ± 0.4 eV.
[h] Obtained using CF$_2$HOCF$_2$H→CF$_2$H + O + CF$_2$H and Eq. (4) with $\Delta H_r = 2D$(F$_2$HC–O) = 7.8 ± 0.4 eV.
[i] Obtained using CF$_3$OCH$_3$→CH$_3$ + OCF$_3$ and Eq. (4) with $\Delta H_r = D$(H$_3$C – O) = 3.9 ± 0.4 eV.
[j] Reference 16.
[k] Reference 17.
[l] References 18(a) and 18(b), respectively.
[m] Reference 3.

ever, when the precursor of those fragment anions is the low-energy NIS, the anions are generally formed with no excess energy.

(iv) The negative ion cross section functions for many of the anions observed from the fluoroethers studied exhibit two (or more) maxima. We were not always able to attribute these maxima to separate NISs with *different* asymptotic limits (see Table VII). Thus the formation of CF_3O^-, CFO^-, and CF_3^- from CF_3OCF_2H, and F^- from CF_2HOCF_2H and CF_3OCH_3 at both of their maxima are interpreted (see footnote d in Table VII) as originating from two separate NISs which, however, converge to the same asymptotic limit. However, we could not explain the low-energy peak of HF_2^- from CF_2HOCF_2H.

(v) From the energetics described in Tables VII and VIII we estimated the E.A. of the radicals CF_3O and CF_3S (see the last column of these tables). The values derived from the various molecules of the present study show good consistency. Also the average (3.6 eV) E.A. value of CF_3O obtained is in good agreement with a MNDO calculated E.A. value (3.86 eV[21]) of this radical.

B. CNDO/2 and MNDO molecular orbital calculations

In addition to the energetic considerations described in Se IV A, in our effort to rationalize our findings on the types, relative intensities, and energy positions of the various anions we observed, we have performed CNDO/2 and MNDO molecular orbital calculations using the codes described, respectively, by Pople and Beveridge[23] and Thiel.[24] Such semiempirical calculations are of limited value, especially when applied to dissociative electron attachment processes. Dissociative attachment to molecules is envisioned (e.g., see Ref. 25) to take place in two steps: a very fast ($\sim 10^{-16}$ s) initial step where the electron is captured by the neutral molecule to form a transient parent negative ion in a vertical transition and a later step where the transient anion either loses the electron by autodetachment or it dissociates moving along a dissociative potential energy curve (surface). Obviously the semiempirical calculations relate only to the first step and can provide information on: (i) the energies of the virtual (empty) molecular orbitals; and (ii) the charge density distributions in the neutral molecules and respective transient parent negative ions. Using Koopmans' theorem[26] we assumed the energies of the first and second negative ion states (NISs) to be given, respectively, by the energies of the first and second virtual orbitals. Both the CNDO/2 and MNDO calculations did show that the orbital energies of the fluorosulphides are much lower than those of the analogous fluoroethers. This is consistent with the experimental finding that the NISs of the fluorosulphides lie lower than those of the corresponding fluoroethers. The relation between the

TABLE VII. Possible dissociative attachment processes leading to the formation of various anions from CF_3OCF_3, CF_3OCF_2H, CF_3OCFH_2, and CF_3OCH_3.

Ion	AO (eV)	Reaction	ΔH_r° (eV)	Thermochemical data deduced (eV)
CF_3O^-	2.5 ± 0.1	$e + CF_3OCF_3 \rightarrow CF_3O^- + CF_3$	$(0.3 \pm 0.5$	$E^{*a} = 2.2 \pm 0.6$
	0.2 ± 0.1	$e + CF_3OCF_2H \rightarrow CF_3O^- + CF_2H$	$(0.3 \pm 0.5$	E.A.$(CF_3O) \geq 3.7 \pm 0.5$ [3.35,][19,3,86]
	2.0 ± 0.3	$\rightarrow CF_3O^- + (CF_2H)^{*c}$	$(0.3 \pm 0.5$	$E^* = 1.7 \pm 0.8^c$
	0.9 ± 0.1	$e + CF_2HOCF_2H \rightarrow CF_3O^- + CH_2F$	$(0.8 \pm 0.4$	E.A.$(CF_3O) \geq 3.5 \pm 0.5^c$
F^-	3.5 ± 0.2	$e + CF_3OCF_3 \rightarrow F^- + CF_3 + OCF_2$	1.2 ± 0.4	$E^* = 2.3 \pm 0.6$
		$\rightarrow F^- + CF_3OCF_2$	$[1.85 \pm 0.1]$	$E^* = 1.65 \pm 0.3$
	1.0 ± 0.1	$e + CF_3OCF_2H \rightarrow F^- + COF_2 + CF_2H$	1.2 ± 0.4	
	2.8 ± 0.2	$\rightarrow F^- + CF_3OCFH$	$[1.85 \pm 0.1]$	$E^* = 0.95 \pm 0.3$
	1.7 ± 0.2	$e + CF_2HOCF_2H \rightarrow F^- + CFHO + CF_2H$	1.7 ± 0.4	
		$\rightarrow F^- + CFHOCF_2H$	$[1.85 \pm 0.1]$	
	2.8 ± 0.2	$\rightarrow F^- + (CFHOCF_2H)^{*c}$		$E^* = 0.95 \pm 0.3$
	1.8 ± 0.1	$e + CF_3OCH_3 \rightarrow F^- + CH_3 + OCF_2$	1.25 ± 0.4	
		$\rightarrow F^- + CF_2OCH$	$[1.85 \pm 0.1]$	
	4.7 ± 0.3	$\rightarrow F^- + (CF_2OCH_3)^{*c}$		$E^* = 2.85 \pm 0.4$
CFO^-	2.8 ± 0.1	$e + CF_3OCF_2H \rightarrow CFO^- + CF_3 + HF$	0.95 ± 1	$E^* = 1.85 \pm 1$
		$\rightarrow CFO^- + CF_4 + H$	1.4 ± 1	$E^* = 1.4 \pm 1$
		$\rightarrow CFO^- + CHF_3 + F$	2.3 ± 1	$E^* = 0.5 \pm 1$
	4.0 ± 0.2	$\rightarrow CFO^- + (CHF_3)^{*c}$		$E^* = 1.7 \pm 1$
	2.9	$e + CF_2HOCF_2H \rightarrow CFO^- + CHF_2 + HF$	0.7 ± 1	$E^* = 2.2 \pm 1$
		$\rightarrow CFO^- + CHF_3 + H$	1.6 ± 1	$E^* = 1.3 \pm 1$
		$\rightarrow CFO^- + CH_2F_2 + F$	2.7 ± 1	
HF_2^-	3.7 ± 0.2	$e + CF_3OCF_2H \rightarrow HF_2^- + CO + CF_3$	2.4 ± 0.4	$E^* = 1.3 \pm 0.6$
	1.0 ± 0.2	$e + CF_2HOCF_2H \rightarrow HF_2^- + ^b$		
	2.6 ± 0.3	$\rightarrow HF_2^- + CO + CF_2H$	2.1 ± 0.4	
CF_3^-	3.1 ± 0.1	$e + CF_3OCF_2H \rightarrow CF_3^- + CF_2HO$	$[1.8 \pm 0.4]$	$E^* = 1.3 \pm 0.5$
		$\rightarrow CF_3^- + CFO + HF$	1.85 ± 1	$E^* = 1.25 \pm 1.1$
	4.8 ± 0.1	$\rightarrow CF_3^- + (CF_2HO)^{*c}$		$E^* = 3$

[a] Heat of reaction determined using Eq. (4) and the data of Table VI. Values in parentheses were obtained using Eq. (4), the data of Table VI, and E.A.$(CF_3O) = 3.6$ eV. Values in brackets were found from Eqs. (5) and (6) and the data in Table VI.

[b] Excess energy determined from Eq. (5).

[c] Electron affinity determined from Eq. (6) using $D(F_3CO\text{–}CF_2H) = 3.9 \pm 0.4$ eV (Table VI). It was assumed that $E^* \geq 0$ eV. The first two numbers in parentheses are values found, respectively, from Refs. 19 and 20. The third number is the result of MNDO calculations (Ref. 21).

[d] Any fragmentation of these radicals (different from those already shown for the lower energy peak) would lead to ΔH_r values higher than the AO. The E^* value listed refers to that proposed reaction for the low-energy peak for which ΔH_r is closest to the AO of the high-energy peak.

[e] Electron affinity determined from Eqs. (4) and (5) using the data in Table VI and assuming that $E^* \geq 0$ eV.

observed positions of the NISs and the calculated orbital energies was better for the fluoroethers than for the fluorosulphides. In Fig. 10 we compare the measured NIS peak positions and the first two MNDO virtual orbital energies for the fluoroethers. A broad correlation between the experimental positions of the NISs and the MNDO orbital energies is evident. The CNDO/2 calculations, however, (the results of which are not shown in the figure) did not clearly show any such correlation.

The charge density distributions for each neutral molecule and its corresponding transient parent negative ion were also calculated by both methods and the differences between these distributions were used to find how the attached electron's charge is distributed in the molecule. The calculations again showed a distinct difference between the fluoroether and fluorosulphide molecules in the way the charge of the attached electron is distributed in the molecule. For the fluorosulphide transient anions $\sim 50\%$ of the electron's charge is localized in the S atom. This suggests that the CF_3S^- formation from either CF_3SCF_3 or CF_3SCH_3 is asso-

TABLE VIII. Possible dissociative attachment processes leading to the formation of CF_3S^- and F^- from CF_3SCF_3, and F^- from CF_3SCH_3.

Ion	AO (eV)	Reaction	ΔH_r (eV)	Thermochemical data deduced (eV)
CF_3S^-	0	$e + CF_3SCF_3 \rightarrow CF_3S^- + CF_3$	a	E.A.$(CF_3S) \geq 3.2^b$ [1.8][c]
	0	$e + CF_3SCH_3 \rightarrow CF_3S^- + CH_3$	a	E.A.$(CF_3S) \geq 3.2^b$
F^-	1.9	$e + CF_3SCF_3 \rightarrow F^- + CF_2SCF_3$	1.85 ± 0.1^d	

[a] A value <0 eV, i.e., equal to or less than the corresponding AO can be assigned to these reactions.

[b] Electron affinity determined from Eq. (6) and assuming that the dissociation energy $D(CF_3S\text{–}CF_3)$ is equal to $D(CH_3S\text{–}CH_3) = 3.17$ eV (Ref. 22).

[c] Reference 19.

[d] Heat of reaction determined from Eq. (6) using $D(F\text{–}CF_2SCF_3) = 5.3 \pm 0$ eV (Ref. 3) and E.A.$(F) = 3.45$ eV (Table VI), and assuming $E^* \geq 0$ eV.

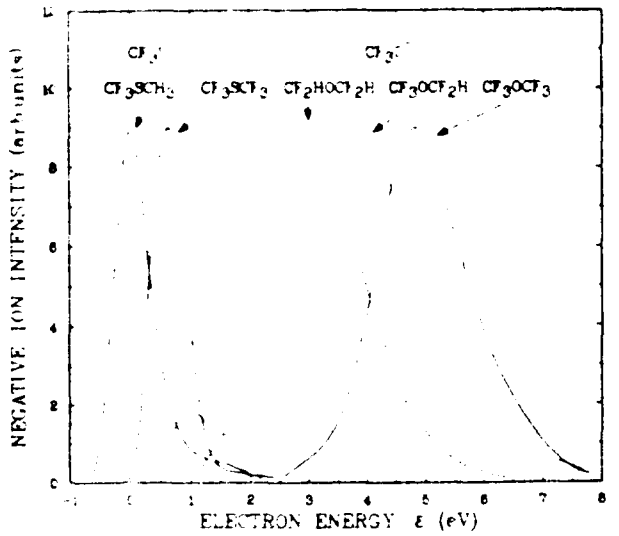

FIG. 9. Negative ion intensity as a function of electron energy ϵ for CF_3O^- from CF_3OCF_3, CF_3OCF_2H, CF_2HOCF_2H and CF_3S^- from CF_3SCF_3, CF_3SCH_3.

ciated preferentially with the S atom and may explain our observation that for CF_3SCF_3 the CF_3S^- ion is ~300 times stronger than F^-, and that for CF_3SCH_3 the F^- was not formed or was so weak as not to be detected. On the other hand, for the fluoroether molecules the attached electron's charge spreads evenly over the entire molecule. This is consistent with the experimental result that for the two molecules CF_3OCF_2H and CF_2HOCF_2H, negative ions have been observed whose formation implies considerable rearrangement of their transient parent negative ions. For the molecules CF_3OCF_3 and CF_3OCH_3 the dissociation is direct and the formation of F^- is favored over the formation of CF_3O^- for the reason that the electron, once captured, has a statistically higher probability of being found on an F atom. This is consistent with the observation that for CF_3OCF_3 the F^- is twice as strong as CF_3O^-, while for CF_3OCH_3, CF_3O^- is so weak or not formed at all that it was not detected.

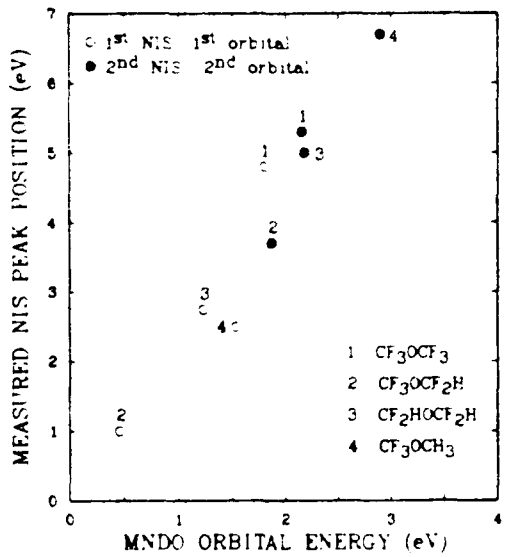

FIG. 10. Measured negative ion resonance state peak positions vs MNDO (virtual) orbital energies for the molecules 1. CF_3OCF_3, 2. CF_3OCF_2H, 3. CF_2HOCF_2H, 4. CF_3OCH_3.

V. CONCLUSIONS

In this study we have measured the total absolute attachment rate constants $k_a(E/N)$ and derived from them the total absolute attachment cross sections $\sigma_a(\epsilon)$, and measured the relative cross sections as a function of incident electron energy for all anions observed in low-energy electron collisions with the fluoroethers CF_3OCF_3, CF_3OCF_2H, CF_2HOCF_2H, and CF_3OCH_3, and the fluorosulphides CF_3SCF_3 and CF_3SCH_3. From these results, we have found that

(i) Substitution of the O atom in the fluoroethers studied by S increases the magnitude of the electron attachment rate constants of these molecules. Furthermore, it significantly lowers the energy positions of the NISs, so that the fluorosulphides attach lower energy electrons than do the corresponding fluoroethers.

(ii) Substitution of H by F atoms in both of the fluoroethers and fluorosulphides substantially increases (by two to three orders of magnitude) the magnitude of the electron attachment rate constant. Also, the number and relative position of the F atoms in the molecule strongly affect the degree of rearrangement and subsequent fragmentation of the transient parent negative ion. The transient parent anions of fluoroethers having one or both partially fluorinated methyl groups, (e.g., CF_3OCF_2H and CF_2HOCF_2H) extensively rearrange themselves and multiply fragment, in contrast to the transient anions of the molecules CF_3OCF_3 and CF_3OCH_3 in which the methyl groups contain either only H or only F atoms.

(iii) Simple molecular orbital calculations have shown that in the case of the fluorosulphides CF_3SCF_3 and CF_3SCH_3 a large fraction of the attached electron's charge becomes localized to the S atom, thus leading predominantly to the formation of negative ion fragments containing S. In the case of the fluoroethers, however, no such localization of the extra electron to any particular atom was indicated.

In addition, the E.A. values for the radicals CF_3O and CF_3S have been determined and energetic considerations were employed to identify possible fragmentation mechanisms of the NISs leading to the production of all observed fragment anions.

From the practical point of view, the energy dependence of $k_a(E/N)$ for CF_3OCF_3 and CF_3SCF_3 is appropriate for gases and gas mixtures for use in diffuse discharge opening switches where it is desirable for the diffuse discharge to have high conductivity, and thus low electron attachment during the conducting state (i.e., low E/N) and low conductivity and high attachment during the opening stage (i.e., high E/N).[27,28] Both CF_3OCF_3 and CF_3SCF_3 have high uniform field breakdown strength equal to 0.9[29] and 1.35[30] times that of SF_6, respectively.

ACKNOWLEDGMENT

We thank Dr. J. L. Adcock for the Chemistry Department of the University of Tennessee for synthesizing and

purifying samples of the compounds CF_3OCH_3, CF_3SCF_3, and CF_3SCH_3.

[1] L. G. Christophorou, S. R. Hunter, J. G. Carter, and S. M. Spyrou, Proceedings of the Workshop on Diffuse Discharge Opening Switches, Tamarron, Colorado, January 13, 1982, pp. 236–251; L. G. Christophorou, S. R. Hunter, J. G. Carter, S. M. Spyrou, and V. K. Lakdawala, Proceedings of the Fourth International Pulsed Power Conference, Albuquerque, New Mexico, June 6–8, 1983, p. 702–708; S. R. Hunter, J. G. Carter, L. G. Christophorou, and V. K. Lakdawala, in *Gaseous Dielectrics IV*, edited by L. G. Christophorou and M. O. Pace (Pergamon, New York, 1984), pp. 224–237.

[2] L. G. Christophorou, S. R. Hunter, J. G. Carter, and R. A. Mathis, Appl. Phys. Lett. **41**, 147 (1982).

[3] S. M. Spyrou, I. Sauers, and L. G. Christophorou, J. Chem. Phys. **78**, 7200 (1983).

[4] S. R. Hunter and L. G. Christophorou, J. Chem. Phys. **80**, 6150 (1984).

[5] W. H. Hickam and R. F. Fox, J. Chem. Phys. **25**, 642 (1956).

[6] A. Chutjian, Phys. Rev. Lett. **46**, 1511 (1981).

[7] L. G. Christophorou, D. L. McCorkle, and J. G. Carter, J. Chem. Phys. **54**, 253 (1971).

[8] L. G. Christophorou, D. L. McCorkle, and V. E. Anderson, J. Phys. B **4**, 1163 (1971).

[9] See, for example, M. Hayashi, Nagoya Institute of Technology, Nagoya, Japan, Report No. IPPJ-AM-19 (1981); S. K. Srivastava, H. Tanaka, A. Chutjian, and S. Trajmar, Phys. Rev. A **23**, 2156 (1981); D. Andrick and A. Bitsch (private communication, 1983) quoted in R. P. McEachran and A. D. Stauffer, J. Phys. B **16**, 4023 (1983).

[10] L. C. Pitchford and A. V. Phelps, Phys. Rev. B **25**, 540 (1982).

[11] J. L. Franklin, J. G. Dillard, H. M. Rosenstock, J. T. Herron, K. Draxl, and F. H. Field, Natl. Stand. Ref. Data Ser. Natl. Bur. Stand. 26 (1969).

[12] *JANAF Thermochemical Tables*, edited by D. R. Stull (Dow Chemical, Midland, Michigan, 1969).

[13] P. N. Noble and R. N. Kortzeborn, J. Chem. Phys. **52**, 5375 (1970).

[14] [illegible] Chem. Commun. **1968**, 1255.

[15] R. D. W. Kemmitt and D. W. Sharp, Adv. Fluorine Chem. **4**, 216 (1965).

[16] R. S. Berry and C. W. Reimann, J. Chem. Phys. **38**, 1540 (1963).

[17] H. M. Rosenstock, D. Draxl, B. W. Steiner, and J. T. Herron, J. Phys. Chem. Ref. Data 6, Suppl. No. 1 (1977).

[18] (a) K. A. G. MacNeil and J. C. J. Thynne, Int. J. Mass Spectrom. Ion Phys. **3**, 35 (1969); (b) P. W. Harland and J. C. Thynne, J. Phys. Chem. **74**, 52 (1970).

[19] F. M. Page and G. C. Goode, *Negative Ions and the Magnetron* (Wiley-Interscience, New York, 1969).

[20] J. C. J. Thynne and K. A. G. MacNeil, Int. J. Mass Spectrom. Ion Phys. **5**, 95 (1970).

[21] M. J. S. Dewar and H. S. Rzepa, J. Am. Chem. Soc. **100**, 784 (1978).

[22] T. L. Cottrell, *The Strength of Chemical Bonds*, 2nd ed. (Butterworths, London, 1958).

[23] J. A. Pople and D. L. Beveridge, *Approximate Molecular Orbital Theory* (McGraw-Hill, New York, 1970).

[24] W. Thiel, Quantum Chemistry Program Exchange, No. 353, Indiana University, Bloomington, Ind.

[25] L. G. Christophorou, D. L. McCorkle, and A. A. Christodoulides, in *Electron–Molecule Interactions and their Applications*, edited by L. G. Christophorou (Academic, New York, 1984), Vol. 1, Chap. 6.

[26] T. Koopmans, Physica **1**, 104 (1933).

[27] R. F. Fernsler, D. Conte, and I. M. Vitkovitsky, IEEE Trans. Plasma Sci. **PS8**, 176 (1980).

[28] K. H. Schoenbach, G. Schaefer, M. Kristiansen, L. L. Hatfield, and A. H. Guenther, IEEE Trans. Plasma Sci. **PS10**, 246 (1982).

[29] R. E. Wootton, S. J. Dale, and N. J. Zimmerman, in *Gaseous Dielectrics II*, edited by L. G. Christophorou (Pergamon, New York, 1980), pp. 137–148.

[30] L. G. Christophorou, D. R. James, R. Y. Pai, R. A. Mathis, I. Sauers, D. H. Smith, L. C. Frees, M. O. Pace, D. W. Bouldin, C. C. Chan, A. Fatheddin, and S. R. Hunter, Oak Ridge National Laboratory Report ORNL-TM-7624 (1981).

APPENDIX D

(Accepted for publication in *Journal of Chemical Physics*)

Effect of temperature on the dissociative electron attachment to $CC\ell F_3$ and C_2F_6[a)]

S. M. Spyrou[b)] and L. G. Christophorou[b)]

Atomic, Molecular and High Voltage Physics Group, Health and Safety Research Division, Oak Ridge National Laboratory, Oak Ridge, Tennessee 37830

ABSTRACT

The total electron attachment rate constant, $k_a(\langle\varepsilon\rangle)$, for $CC\ell F_3$ and C_2F_6 has been measured using an electron swarm technique in the mean electron energy range 0.41 to 4.81 eV and over the range of temperature, T, from 300 to 750 K. At each value of T the total electron attachment cross section $\sigma_a(\varepsilon)$ was determined from the measured $k_a(\langle\varepsilon\rangle)$ using the swarm unfolding technique and was compared with the results of a mass spectrometric study. The $\sigma_a(\varepsilon)$ for C_2F_6 shows a single peak (due to F^- and CF_3^-) which shifts from 3.9 eV at 300 K to ∿3.3 eV at 750 K. (The onset shifts correspondingly from 2.3 to 1.5 eV.) For $CC\ell F_3$ the $\sigma_a(\varepsilon)$ shows two peaks: at ∿1.5 eV (due to $C\ell^-$) and at ∿4.7 eV (due to $C\ell^-$, F^-, $CC\ell F_2^-$, and $C\ell F^-$). The peak at ∿1.5 eV is especially sensitive to changes in T. The peak value of $\sigma_a(\varepsilon)$ increased by a factor of ∿3, and the energy position of the peak and onset shifted to progressively lower energies when T increased from 300 to 700 K. The analysis of these results led us to conclude that the changes in $k_a(\langle\varepsilon\rangle)$ and $\sigma_a(\varepsilon)$ for the dissociative attachment processes of these molecules with increasing T result from

---

a) Research sponsored by the Division of Electric Energy Systems and the Office of Health and Environmental Research, U.S. Department of Energy, under contract DE-AC05-84OR21400 with Martin Marietta Energy Systems, Inc., and the Office of Naval Research under contract DOE No. 40-1246-82.

b) Also Department of Physics, The University of Tennessee, Knoxville, Tennessee 37996.

the increase with T of the total internal (= vibrational) energy of the molecule

I. INTRODUCTION

The study of the effects of temperature on electron attachment to molecules is of intrinsic as well as of practical interest. For example in many cases vibrational and/or rotational excitation of molecules affects the magnitude and the energy dependence of the cross section for dissociative attachment and thus the accurate determination of thermochem data which use appearance onsets for specific dissociative attachment anions. Similarly, such knowledge is valuable for many applied areas which employ temperatures higher than ambient (e.g., combustion, flames, circuit breakers, diffuse discharge switches, etc.). Previous studies on the effects of temperature on electron attachment processes have been reviewed [1]

In this paper we report and discuss the results of a swarm study on the effect of T on dissociative electron attachment to the molecules $CC\ell F_3$ and C_2F_6. The magnitude and the energy dependence of the attachmen rate constants for these molecules are appropriate for diffuse discharge switching applications.

II. EXPERIMENTAL

A. Apparatus

A schematic diagram of the high temperature electron swarm apparatu used in the present study is shown in Fig. 1. The basic principles of operation are as described earlier.[2,3] A number of modifications were m

to the basic design to facilitate the measurements at high gas temperatures. In contrast to our other swarm apparatus, the swarm chamber was made ~100 cm long, and the distances of the two end flanges from the middle of the chamber are ~50 cm. To avoid leaks at the flanges when heating or cooling, the region around the flanges was water cooled and was kept at a much lower temperature than the collision region (the region between the anode and cathode; see Fig. 1). This arrangement also allowed the high voltage and signal feedthroughs to be kept at a low T. Special care was also taken in the construction of the long supporting stands holding the anode and the cathode (the Cf^{252} alpha particle source used to produce the electron swarms by the energy decay of the alpha particles was mounted on a plate supported on the cathode), which consist of a stainless steel rod with insulating rods at its two ends.

A furnace and temperature control system (0-1000°C, resolution 1°C, Applied Test System, Inc.) was used to heat the central region of the chamber. The temperature in the collision region was measured by six thermocouples (chromel-alumel, type KX) located as close to the drift region as possible. With the aid of two independently controlled heating elements embedded in the insulating walls of the furnace, the gas temperature between the electrodes was controlled to within 1-2°C.

B. Experimental and analytical procedures

The experimental procedures for the electron swarm experiment have been described in detail previously.[2-4] In the present study the chamber was heated to the desired temperature prior to the measurements. We used Ar and N_2 as carrier gases, and the mixtures of the attaching gases under study with either Ar or N_2 contained as small a fraction (10^{-4} to 10^{-6}) of the attaching gas as possible. This was necessary in

order to alleviate or reduce the influence of the attaching gas on the electron energy distribution function $f(\varepsilon,E/N)$ of the pure buffer gas used in the subsequent analysis. To observe and to correct for any such influence, the measurements were performed as a function of the attaching gas number density N_a at each total gas number density N_t. When k_a depended on N_a/N_t (see Section III), the pressure-independent k_a was determined from an extrapolation of k_a to $N_a/N_t \rightarrow 0$. Such data were taken at each temperature at which measurements were made.

The buffer gas (quoted purity 99.999% for N_2 and 99.9995% for Ar) was further purified by fractional distillation in the liquid nitrogen traps (Fig. 1). The attaching gas samples were deoxygenated by repeated freeze-pump-thaw cycles. For measurements at $T > 300$ K, the attaching/buffer gas mixture was prepared in a separate premixing container at room temperature, and this premixture was used for the measurements. This procedure was adopted for three main reasons: (1) to eliminate problems which might arise from a nonuniform T over the large volume of the swarm chamber, (2) to reduce outgassing problems which, especially at high T, could interfere with the measurements at low attaching gas number densities, and (3) to avoid the problems connected with the reduction in the attaching gas pressure observed (Section IIIA) to occur at elevated T.

The possible sources of error in the measurement of k_a with the present technique have been discussed in Ref. 3. The total uncertainty in the present k_a measurements is estimated to be 6-8% except for the measurements of k_a in $CC\ell F_3$ at the lowest $\langle\varepsilon\rangle$ which were more uncertain (Section IIIA), and the measurements of k_a in $CC\ell F_3$ at $T > 600$ K which were also characterized by larger uncertainty (Section IIIA).

The measured $k_a(E/N,T)$ [or $k_a(\langle\varepsilon\rangle,T)$] were used to determine $\sigma_a(\varepsilon,T)$ by the swarm unfolding procedure[5] using the relation

$$k_a(\langle\varepsilon\rangle,T) = \left(\frac{2}{m}\right)^{\frac{1}{2}} \int_0^{\infty} \varepsilon^{\frac{1}{2}}\, \sigma_a(\varepsilon,T)\, f(\varepsilon,\langle\varepsilon\rangle,T)\, d\varepsilon \,, \qquad (1)$$

where ε and m are the electron energy and mass, respectively. The electron energy distribution functions $f(\varepsilon,\langle\varepsilon\rangle)$, the mean electron energies $\langle\varepsilon\rangle$, and the electron drift velocities w in Ar at the higher temperatures were assumed to be those at room temperature.[3] For N_2, however, this assumption is not valid. In this case, we used $\langle\varepsilon\rangle$ and w values obtained[6] at 400 K.

III. RESULTS

A. Electron attachment rate constants

In Figs. 2 and 3 are shown the $k_a(\langle\varepsilon\rangle,T)$ for $CC\ell F_3$ and C_2F_6, respectively. For both molecules, the measurements at the highest T were limited to $\langle\varepsilon\rangle < \sim 3.5$ eV due to corona problems. For $CC\ell F_3$ additional difficulties arose from substantial rapid disappearance of $CC\ell F_3$ at high T (see later in this section) which did not allow measurements above 700 K. All measurements were performed in a buffer gas of Ar except for the measurements at 300 and 400 K for $CC\ell F_3$ which were also made in N_2 (Fig. 2).

At each value of T, four or more independent sets of measurements were made over a range of N_t from 2.25 to 9.66×10^{19} cm^{-3} and over a range of N_a from 0.7 to 7×10^{14} cm^{-3}. In Figs. 4 and 5 are shown typical examples of the dependence of $k_a(\langle\varepsilon\rangle)$ on the ratio N_a/N_t and T

for $CC\ell F_3$ and C_2F_6, respectively. For all $\langle\varepsilon\rangle$ and T values studied the k_a was obtained for $N_a/N_t \to 0$, and these values were plotted in Figs. 2 and 3 and are listed in Tables I and II.

The effect of the attaching gas on $f(\varepsilon,\langle\varepsilon\rangle)$ was particularly significant for Ar at $\langle\varepsilon\rangle < 1$ eV and resulted in a greater uncertainty (>10%) of k_a in this energy region. To completely remove this effect, the ratio N_a/N_t must be $<10^{-6}$; this, however, was not possible for $CC\ell F_3$ because of the low magnitude of its k_a at low $\langle\varepsilon\rangle$. This is the reason why our measurements of k_a in Ar for $CC\ell F_3$ at 300 and 400 K do not extend to as low values of $\langle\varepsilon\rangle$ as at the higher T. The fact that the measured $k_a(\langle\varepsilon\rangle)$ in Ar are lower than those in N_2 (see Fig. 2) may be attributed to the effect of the attaching gas on the $f(\varepsilon,\langle\varepsilon\rangle)$ of pure Ar, although uncertainties in the determination of $\langle\varepsilon\rangle$ in N_2 could also contribute to this discrepancy.[6] For $CC\ell F_3$ the $k_a(\langle\varepsilon\rangle)$ were independent of time (following the introduction of the mixture into the swarm chamber) for $T \leq 500$ K but decreased progressively with time at $T > 500$ K. This may be attributed to the disappearance of $CC\ell F_3$ via reactions with the stainless steel walls of the hot chamber and/or via thermal decomposition into nonelectron attaching species. Due to the rapid decrease with time of the k_a for $CC\ell F_3$ at $T \geq 600$ K, the following procedure was adopted for the measurement of k_a for this molecule. A premixture of $CC\ell F_3$ with Ar was prepared in a container at room temperature and was introduced into the hot chamber; a series of k_a measurements as a function of time for a number of E/N values were then conducted. From a plot of k_a versus time for each E/N, the value of k_a for that E/N was obtained for t = 0 (i.e., the time the premixture was introduced into the chamber). The chamber was subsequently evacuated, a new quantity of the premixture was introduced into the

chamber, and the measurements were repeated for another range of E/N values. This method gave reliable data (uncertainty <10%) for T ≤ 600 K but less reliable data (uncertainty 10-20%) for 700 K because of the more rapid decrease of k_a at the latter temperature.

B. Swarm unfolded cross sections

The $k_a(\langle\varepsilon\rangle)$ measurements presented in the previous section were unfolded to obtain the total electron attachment cross sections $\sigma_a(\varepsilon)$. These are plotted in Figs. 6 and 7 for $CC\ell F_3$ and C_2F_6, respectively.

The magnitude of the cross section for C_2F_6 does not change appreciably by increasing T. However, the peak position of the resonance and the appearance onset shift to lower energies by more than 0.6 eV when T is raised from 300 to 750 K. The full width at half maximum (FWHM) of the resonance also increases from 1.6 eV at T = 300 K to 2.0 eV at T = 750 K. The present room temperature $\sigma_a(\varepsilon)$ [and $k_a(\langle\varepsilon\rangle)$] data compare well with those of Ref. 3.

The effect of T on the electron attachment to $CC\ell F_3$ is more profound. The magnitude of the low-energy peak in $\sigma_a(\varepsilon)$ [or $k_a(\langle\varepsilon\rangle)$] increases by a factor of ~3, and its position shifts from 1.55 to 1.1 eV when T is increased from 300 to 700 K. The appearance onset shifts to 0 eV when T is raised from 300 to 400 K. On the other hand the magnitude and position of the high energy peak are not noticeably affected by the changes in T in the range studied.

C. Electron beam studies; comparison of electron swarm and electron beam data

The $CC\ell F_3$ and C_2F_6 molecules were also studied in a time-of-flight mass spectrometer (TOFMS). For C_2F_6 two main negative ions, F^- and

CF_2^- were observed, with attachment cross sections having relative peak intensities 3:1 and peaks, respectively, at 3.9 and 4 eV. These results have been reported earlier.[7] In Fig. 8 the present room temperature swarm unfolded $\sigma_a(\varepsilon)$ is compared with the normalized total attachment cross section of the TOF study.[7] The agreement of the peak position, the FWHM, and the onset of the resonance as obtained in the two experiments is satisfactory considering the overall uncertainty in the two experiments.

The nonunfolded and unfolded (see Ref. 7) relative cross sections as a function of ε for the four anions Cl^-, F^-, ClF^-, and ClF_2^- observed for ClF_3 are shown in Figs. 9(a) and 9(b), respectively. The relative peak intensities, energy of maximum ion intensity, FWHM, and appearance onset of these anions are listed in Table III, where a comparison is made with the literature data. With a few exceptions, the agreement between the present beam results and those of Illenberger et al.[8] is good. Illenberger et al. reported the magnitude of the second peak in the Cl^- cross section to be ~10 times larger than that of the first peak. The present beam and swarm results, as well as the beam results of Verhaart et al.,[9] indicate that the first Cl^- resonance process has a higher cross section than the second. The 0.7 ± 0.3 eV onset leading to Cl^- formation measured by Illenberger et al. is higher than the ~0.3 eV onset we determined. However, the 0.3 eV value was not reproducible as it depended on the electron source condition and filament temperature and most likely corresponds to a T higher than ambient (see below). Finally, the 3.9 eV peak for ClF^- measured by Illenberger et al.[8] is lower by ~0.8 eV compared with the 4.7 eV value of the present work (the appearance onset for this anion was found by both studies to be the same). The 4.7 eV value seems to be more consistent with the grouping

of the resonance maxima of all anions observed for $CC\ell F_3$ at 4.5 ± 0.2 eV [see Fig. 9(b)].

In Fig. 10 we compare the room temperature total swarm unfolded $\sigma_a(\varepsilon)$ and the beam total relative electron attachment cross section for $CC\ell F_3$, the latter has been normalized to the high-energy peak (at ~5 eV) of the swarm unfolded $\sigma_a(\varepsilon)$. The beam cross section (at the low-energy peak) is broader and its onset lies at lower energies compared with the swarm data; actually, it is in better agreement with the 400 K swarm unfolded cross section (Fig. 6), which may indicate that the temperature in the collision region of the TOFMS is higher than ambient due to heating caused by the filament. The difference in the relative magnitude of the two peaks as determined from the beam and the swarm experiment may result from mass discrimination or discrimination due to excess kinetic energy of the dissociative attachment fragments in the beam experiment.

IV. DISCUSSION

A. Energetics of dissociative electron attachment processes

Before discussing the effect of T on the electron attachment processes for $CC\ell F_3$ and C_2F_6, it is worth considering the energetics of these processes. In Table IV are summarized possible fragmentation processes along with their heats of reaction leading to the formation of the four fragment anions we observed in low-energy electron impact with $CC\ell F_3$. In the last column of the same table are listed the excess energies, E^*, of some of the proposed reactions and the electron affinities, EA, of the radicals $C\ell F$ and $CC\ell F_2$. These are compared with the literature data whenever available. All quantities were determined as described in the

footnotes of Table IV using appropriate energy balance equations. For a reaction of the form

$$e + RX \longrightarrow R + X^- \tag{2}$$

these energy balance equations, if we neglect any initial internal excitation of RX, are

$$\Delta H_r = \Delta H_f(R) + \Delta H_f(X) - EA(X) - \Delta H_f(RX) , \tag{3}$$

$$AO(X^-) = \Delta H_r + E^* , \tag{4}$$

$$AO(X^-) = D(R\text{-}X) - E(AX) + E^* , \tag{5}$$

where ΔH_r is the heat of the reaction, $\Delta H_f(R)$, $\Delta H_f(X)$, and $\Delta H_f(RX)$ are the heats of formation of R, X, and RX, respectively, EA(X) is the electron affinity of X, $AO(X^-)$ is the appearance onset of X^-, D(R-X) is the bond dissociation energy of RX, and E^* is the excess energy of the reaction comprised of the internal energy of excitation and the total translational energy of the fragments. A similar analysis for C_2F_6 can be found in Ref. 7.

B. Temperature dependence of electron attachment

From the results presented in Section III it is clear that for both $CCl F_3$ and C_2F_6 the temperature affects considerably both $k_a(\langle\varepsilon\rangle)$ and $\sigma_a(\varepsilon)$. As T increases, $k_a(\langle\varepsilon\rangle)$ increases, and this increase is progressively larger at lower energies (Figs. 2 and 3). For $\sigma_a(\varepsilon)$ the effect of T can be summarized as follows: As T increases, the energy position of the resonance maximum (for $CCl F_3$ we refer to the low-energy peak) and the appearance onset decrease (see Fig. 11), while the resonance width

(Fig. 11) and the magnitude of the cross section (Figs. 6 and 7) increase. This behavior is analogous to the one observed for anions produced from dissociative attachment to diatomic molecules.[1] In the case of O^- from O_2 the effects of increasing T on $\sigma_a(\varepsilon)$ were attributed[1,18] to the population of higher vibrational levels and the high sensitivity of $\sigma_a(\varepsilon)$ to the range of nuclear motion. Thus, it can be shown that dissociative attachment to vibrationally excited O_2 molecules results in a broadening of the Franck-Condon region [which increases the FWHM of $\sigma_a(\varepsilon)$], a decrease in ε_{max} [the energy at which $\sigma_a(\varepsilon)$ peaks] and AO, and an increase in the magnitude of $\sigma_a(\varepsilon)$ resulting from the increase in the survival probability of O_2^{-*} with increasing vibrational quantum number. Subsequent studies[1,19,20] on O_2 and other diatomic molecules (e.g., H_2, HCℓ, HF) confirmed the dominant effect of vibrational excitation on $\sigma_a(\varepsilon)$ and the relatively small effect of rotational excitation.

Similar arguments can be advanced concerning the effect of increased internal energy of a polyatomic molecule with increasing T on its electron attachment properties, although the situation for polyatomic molecules may be more complex because of their large number of vibrational degrees of freedom. Nevertheless, the present study on polyatomic molecules shows that--consistent with the findings on the diatomic molecules[18-20]--the effects of T on $k_a(\langle\varepsilon\rangle)$ and $\sigma_a(\varepsilon)$ can be understood in terms of the increase in the total vibrational energy of the molecule with increasing T.

In Fig. 11 are plotted the energy, ε_{max}, at which $\sigma_a(\varepsilon)$ peaks, the appearance onset, AO, of $\sigma_a(\varepsilon)$, and the FWHM of $\sigma_a(\varepsilon)$ for C_2F_6 as a function of T. These quantities are listed in Table V. If we assume that the linear dependence of ε_{max} and AO on T seen in Fig. 11 continues

to T = 0 K, a linear least square fit to the data in Fig. 11 gives a value of 4.3 eV for ε_{max} and a value of 2.81 eV for AO at T = 0 K. Similarly, by a linear least square extrapolation, AO → 0 eV when T → ∼1600 K and ε_{max} → 0 eV when T → ∼3200 K (see Table V). The value ε_{max} = 4.3 eV at T = 0 K gives the energy difference between the negative ion state from the ground, v = 0, vibrational level of the neutral state at the equilibrium distance of the latter. This is the energy close to which $\sigma_a(\varepsilon)$ would peak if all the C_2F_6 molecules were in the v = 0 level. In this case the value AO would be 2.81 eV instead of 2.3 eV as observed at room temperature. The finding that AO = 0 eV at T ≃ 1600 K would imply that at this value of T the internal energy of the molecule is such that even zero-energy electrons can be attached to C_2F_6 and thus reach the negative ion state. For this to be so, large amounts (∼2 eV, since F^- and CF_3^- from C_2F_6 cannot be produced at energies < ∼1.8 eV[7]) of energy are required.

These findings can be rationalized in a way similar to that adopted for electron attachment to hot diatomic molecules, namely, as attachment of thermal energy electrons to C_2F_6 molecules in vibrational levels v lying at ∼1.8 eV. Although the fraction, N_v, of C_2F_6 molecules excited to these high-lying vibrational levels is very small ($\sim 10^{-6}$) compared to that N_0, of C_2F_6 molecules in the v = 0 level, the cross section, σ_v, for thermal electron attachment to C_2F_6 (v = 1.8 eV) can be much larger than that, σ_0, for attachment of an electron of energy ∼1.8 eV to the C_2F_6 (v = 0) molecule, such that $N_v\sigma_v \geq N_0\sigma_0$. Alternatively, since C_2F_6 is a polyatomic molecule, let us consider the total average internal energy of the molecule which we assume to be principally the vibrational energy of the molecule. Let us further assume that as T increases each

normal vibrational mode is excited by an equal probability and that the total internal energy $\langle\varepsilon\rangle_{int}$ of the molecule is the sum of the energy in the various normal modes x, viz.,

$$\langle\varepsilon\rangle_{int} = \sum_{x=1}^{N} \sum_{v=0}^{\infty} B_v \, \varepsilon_{v,x} \qquad (6)$$

In Eq. (6) N are the normal modes (3n-6 for a nonlinear molecule with n atoms, including degenerate modes), $\varepsilon_{v,x} = (v + 1/2)\, h\nu_x$ are the vibrational energies of the normal mode x in the v = 0,1,2...levels, and B_v are the corresponding Boltzmann factors defined for each x by

$$B_v = \frac{e^{-\varepsilon_v/kT}}{\sum_{v=0}^{\infty} e^{-\varepsilon_v/kT}} \qquad (7)$$

We used expressions (6) and (7) and determined $\langle\varepsilon\rangle_{int}$ (T) for C_2F_6 using the values of ν_x reported in Ref. 21. These are listed in Table V. The $\langle\varepsilon\rangle_{int}$ at T = 0 K is

$$\langle\varepsilon\rangle_z = \sum_{x=1}^{N} \frac{1}{2} h\nu_x = 0.790 \text{ eV} \qquad (8)$$

i.e., is equal to the sum of the zero-point energies of all N normal modes. At T = 1610 K (i.e., at the temperature for which AC → 0 eV) $\langle\varepsilon\rangle_{int}$ is equal to ~2.6 eV (when including $\langle\varepsilon\rangle_z$) or ~1.8 eV (when $\langle\varepsilon\rangle_z$ is excluded). The agreement between the two values [i.e., the value (= ~1.8 eV) of $\langle\varepsilon\rangle_{int}$ when AP → 0 eV, and the minimum (~1.8 eV) energy required for dissociative attachment] is most interesting. It indicates

that the internal vibrational energy of the molecule can be transferred from one mode to another very efficiently and that it can be initiated in a particular (critical) mode leading to the reaction. Just as unimolecular reaction theory asserts,[22] it also indicates that the molecule's internal energy is predominantly vibrational and that all the vibrational energy can be used in the dissociation process.

Finally, in Figs. 12(a) and 12(b) are shown examples of the traditional plots of log k_a versus T^{-1} for a number of $\langle\varepsilon\rangle$ for CCl_2F_2 and C_2F_6 respectively. It is seen that these can be fitted to a straight line only for a portion ($T \geq 500$ K) of the T range investigated. The $k_a(\langle\varepsilon\rangle,T)$ data at $T \geq 500$ K have been fitted with the expression

$$k_a(\langle\varepsilon\rangle,T) = C(\langle\varepsilon\rangle)\, e^{-D(\langle\varepsilon\rangle)/kT} , \qquad (9)$$

and values of $D(\langle\varepsilon\rangle)$ were obtained. In Fig. 13 are shown $D(\langle\varepsilon\rangle)$ for C_2F_6. Two observations are pertinent: (1) the low values of D and (2) the convergence of D to kT_{300} as $\langle\varepsilon\rangle \rightarrow AO_{300}$ (=2.3 eV). Both are consistent with the dominant effect of vibrational excitation on dissociative attachment which is further demonstrated by the similarity of the k_a versus T^{-1} and $(\langle\varepsilon\rangle_{int} - \langle\varepsilon\rangle_z)$ versus T^{-1} functions shown in Fig. 14.

VI. SUMMARY AND CONCLUSIONS

The effect of temperature on dissociative electron attachment to the molecules CCl_2F_2 and C_2F_6 was studied using a high temperature swarm apparatus. This effect was found to be more profound for CCl_2F_2 than for C_2F_6. The $k_a(\langle\varepsilon\rangle)$ and $\sigma_a(\varepsilon)$ for CCl_2F_2 are smaller than those of C_2F_6

and also lie at lower energies. This study confirms previous findings that the enhancement of dissociative electron attachment with increasing T is more significant when the room temperature $\sigma_a(\varepsilon)$ is small, and when the result of the heating of the molecule shifts the dissociative attachment resonance to an energy range close to 0 eV.

The enhancement of dissociative attachment by increasing T was understood as the result of vibrational excitation of the molecule. Evidence was presented that the excitation energy from the various modes of the molecule can be transferred from one mode to the rest and be utilized for the energetics of the dissociative attachment.

ACKNOWLEDGMENTS

We are grateful to Mr. J. G. Carter for valuable technical assistance in the design and construction of the present high temperature swarm apparatus, to Dr.S. R. Hunter for useful suggestions, and to Mr. P. Datskos for assistance with some of the experiments.

[1]L. G. Christophorou, Environ. Health Perspect. 36, 3 (1980); L. G. Christophorou, D. L. McCorkle, and A. A. Christodoulides in *Electron-Molecule Interactions and Their Applications*, edited by L. G. Christophorou (Academic Press, New York, 1984), Vol. 1, Chapt. 6.

[2]L. G. Christophorou, *Atomic and Molecular Radiation Physics* (Wiley-Interscience, New York, 1971).

[3]S. R. Hunter and L. G. Christophorou, J. Chem. Phys. 80, 6150 (1984).

[4]S. M. Spyrou, Ph.D. Thesis, The University of Tennessee, 1983.

[5]L. G. Christophorou, D. L. McCorkle, and V. E. Anderson, J. Phys. B 4, 1163 (1971).

[6]S. R. Hunter and J. G. Carter, private communication (1984).

[7]S. M. Spyrou, I. Sauers, and L. G. Christophorou, J. Chem. Phys. 78, 7200 (1983).

[8]E. Illenberger, H. U. Scheunemann, and H. Baumgartel, Chem. Phys. 37, 21 (1979).

[9]G. J. Verhaart, W. J. Van der Hart, and H. H. Brongersma, Chem. Phys. 34, 161 (1978).

[10]R. S. Berry and C. W. Reimann, J. Chem. Phys. 38, 1540 (1963).

[11]S. S. Chen, R. C. Wilhoit, and B. J. Zwolinski, J. Phys. Chem. Ref. Data 5, 571 (1976).

[12](a) J. L. Franklin, J. G. Dillard, H. M. Rosenstock, J. T. Herron, K. Draxl, and F. H. Field, NSRDS-NBS26 (1969); (b) S. W. Benson and H. E. O'Neal, NSRDSNBS21 (1970).

[13]L. M. Leyland, J. R. Majer, and J. C. Robb, Trans. Faraday Soc. 66, 898 (1970).

[14]A. G. Gaydon, *Dissociation Energies and Spectra of Diatomic Molecules* (Chapman and Hall, London, 1968).

[15]H. Dispert and K. Lacmann, Int. J. Mass Spectrom. Ion Phys. 28, 49 (1978).

[16]J.C.J. Thynne, Dyn. Mass Spectrom. 3, 67 (1972).

[17]A. V. Dudin, L. N. Gorokhov, and A. V. Baluev, Bull. Acad. Sci. USSR Div. Chem. Sci., English Transl. 28, 2227 (1979).

[18]T. F. O'Malley, Phys. Rev. 155, 59 (1967); W. R. Henderson, W. L. Fi and R. T. Brockmann, Phys. Rev. 183, 157 (1969).

[19]J. N. Bardsley and J. M. Wadehra, Phys. Rev. A 20, 1398 (1979).

[20]J. M. Wadehra, Phys. Rev. A 29, 106 (1984).

[21]T. Shimanouchi, Natl. Stand. Ref. Data Ser., National Bureau of Standards 39 (1972), Vol. I.

[22]W. Forst, *Theory of Unimolecular Reactions* (Academic Press, New York, 1973); R. J. Robinson and K. A. Holbrook, *Unimolecular Reactions* (Wiley-Interscience, New York, 1972).

TABLE I. Electron attachment rate constants k_a for CCl_3F in a buffer gas of argon as a function of E/N, $\langle\varepsilon\rangle$, and T.

			k_a (10^{-11} cm^3 s^{-1}) T(K)					
E/N (10^{-18} V cm^2)	$\langle\varepsilon\rangle$ T = 300 K (eV)	w T = 300 K (10^5 cm s^{-1})	300	400	500	550	600	700
0.217	0.412	1.097						4.20
0.311	0.473	1.200						5.80
0.373	0.509	1.258					3.60	7.00
0.466	0.559	1.335				3.40	4.50	8.20
0.528	0.590	1.38			2.80	3.80	5.00	9.10
0.621	0.634	1.44			3.30	4.60	5.80	10.03
0.777	0.702	1.53			4.20	5.50	7.00	11.80
0.932	0.764	1.61		3.20	5.00	6.60	8.20	12.70
1.09	0.822	1.68		3.76	5.60	7.50	9.20	13.10
1.24	0.876	1.75		4.20	6.30	8.10	9.84	13.30
1.55	0.976	1.87	3.43	5.04	7.05	9.15	10.64	13.44
1.86	1.068	1.95	3.88	5.52	7.50	9.55	10.76	13.44
2.17	1.15	2.03	4.07	5.76	7.60	9.60	10.76	13.30
2.49	1.23	2.10	4.16	5.85	7.60	9.58	10.70	13.00
3.11	1.37	2.22	4.22	5.81	7.46	9.30	10.30	12.20
3.73	1.50	2.33	4.20	5.62	7.08	8.75	9.80	11.60
4.66	1.67	2.46	4.04	5.31	6.60	8.05	9.10	10.90
5.28	1.77	2.54	3.95	5.12	6.38	7.75	8.76	10.50
6.21	1.92	2.64	3.89	5.00	6.15	7.40	8.30	10.00

TABLE I. (Continued)

E/N (10^{-18} V cm^2)	$\langle\varepsilon\rangle$ T = 300 K (eV)	w T = 300 K (10^5 cm s^{-1})	k_a (10^{-11} cm^3 s^{-1}) T(K) 300	400	500	550	600	700
7.77	2.14	2.79	3.97	4.97	6.10	7.15	8.00	9.40
9.32	2.33	2.92	4.25	5.15	6.15	7.20	8.05	9.20
10.97	2.52	3.04	4.55	5.45	6.40	7.40	8.10	9.26
12.4	2.69	3.14	4.82	5.70	6.58	7.56	8.20	9.36
15.5	3.00	3.33	5.30	6.06	6.92	7.78	8.40	9.40
18.6	3.29	3.49	5.60	6.22	7.02	7.80	8.48	9.36
21.7	3.55	3.63	5.71	6.25	7.00	7.74	8.40	
24.9	3.80	3.76	5.73	6.15	6.88	7.55	8.30	
27.9	4.03	3.88	5.67	6.05	6.68	7.28	7.96	
31.1	4.26	3.99	5.60	5.94	6.50	7.10	7.70	
34.2	4.43	4.18	5.51	5.80	6.37	6.95	7.50	
37.3	4.58	4.38	5.43	5.70	6.24	6.80		
40.4	4.71	4.62	5.34	5.64	6.14	6.71		
43.5	4.81	4.90	5.30	5.55	6.07			

TABLE II. Electron attachment rate constants k_a for C_2F_6 in a buffer gas of argon as a function of E/N, $\langle\varepsilon\rangle$, and T.

			k_a (10^{-10} cm^3 s^{-1}) T(K)					
E/N (10^{-16} V cm^2)	$\langle\varepsilon\rangle$ T = 300 K (eV)	w T = 300 K (10^5 cm s^{-1})	300	400	500	570	650	750
1.55	0.976	1.87						0.16
1.86	1.068	1.95					0.15	0.24
2.17	1.15	2.03			0.04	0.11	0.22	0.35
2.49	1.23	2.10		0.06	0.14	0.27	0.37	0.60
3.11	1.37	2.22	0.17	0.29	0.39	0.61	0.80	1.10
3.73	1.50	2.33	0.40	0.59	0.76	1.10	1.35	1.80
4.66	1.67	2.46	0.92	1.23	1.47	1.97	2.30	2.84
5.28	1.77	2.54	1.32	1.73	2.00	2.57	2.90	3.50
6.21	1.92	2.64	1.99	2.44	2.80	3.42	3.80	4.40
7.77	2.14	2.79	3.08	3.57	3.90	4.56	4.95	5.60
9.32	2.33	2.92	4.01	4.48	4.75	5.40	5.80	6.40
10.97	2.52	3.04	4.71	5.10	5.40	5.98	6.35	7.00
12.4	2.69	3.14	5.20	5.54	5.80	6.38	6.70	7.35
15.5	3.00	3.33	5.75	6.01	6.24	6.72	6.97	7.65
18.6	3.29	3.49	5.94	6.13	6.32	6.73	6.95	7.60
21.7	3.55	3.63	5.95	6.10	6.20	6.56	6.82	7.40
24.9	3.80	3.76	5.84	5.94	6.06	6.34	6.56	
27.9	4.03	3.88	5.69	5.76	5.88	6.14	6.35	

TABLE II. (Continued)

E/N (10^{-18} V cm^2)	$\langle\varepsilon\rangle$ T = 300 K (eV)	w T = 300 K (10^5 cm s^{-1})	k_a (10^{-10} cm^3 s^{-1}) T(K) 300	400	500	570	650	750
31.1	4.26	3.99	5.52	5.58	5.66	5.92	6.12	
34.2	4.43	4.18	5.38	5.44	5.5	5.74	5.94	
37.3	4.58	4.38	5.23	5.30	5.35	5.56	5.77	
40.4	4.71	4.62	5.10	5.16	5.24	5.40	5.62	
43.5	4.81	4.90	5.01	5.06	5.10	5.29	5.53	

TABLE III. Negative ions due to low-energy electron impact on $CC\ell F_3$.

Negative ion	Relative peak ion intensity	Energy of maximum ion intensity (eV)[b]	FWHM[a] (eV)[c]	Appearance onset (eV)[c]
$CC\ell F_2^-$	75	4.4 ± 0.1 (4.2)[d]	0.9	3.5 ± 0.15 (3.5 ± 0.3)[d]
$C\ell F^-$	10	4.7 ± 0.1 (3.9)[d]	1.55	3.0 ± 0.15 (3.0 ± 0.3)[d]
F^-	500 (500)[e]	4.3 ± 0.05 (4.1)[d] (4.3)[e]	1.4	2.8 ± 0.2 (3.0 ± 0.2)[d]
$C\ell^-$	1000 (1000)[e]	1.4 ± 0.1 (1.3)[d] (1.4)[e]	1.1	0.3 ± 0.3 (0.7 ± 0.3)[d]
	550 (730)[e]	5.0 ± 0.1 (4.8)[d] (5.0)[e]	1.45	3.8 ± 0.2 (3.4 ± 0.3)[d]

[a]Full width at half maximum of the respective ion intensity as a function of electron energy.

[b]Energy scale calibration determined using for the SF_5^-/SF_6 resonance the value of 0.37 eV. The ± refers to the standard deviation from the average value.

[c]Values listed are from the present unfolded beam data.

[d]Reference 8. For these measurements a trochoidal monochromator electron source was used. The relative anion intensities reported are the energy integrated intensities.

[e]Reference 9. For these measurements an electron transmission experiment was used.

TABLE IV. Possible dissociative attachment processes leading to the formation of the various anions observed for $CC\ell F_3$ and deduced thermochemical data

Ion	AO (eV)	Reaction	ΔH_r[a] (eV)	Thermochemical data deduced (eV)
$C\ell^-$	0.3 ± 0.3	$e + CC\ell F_3 \rightarrow C\ell^- + CF_3$	0.05	$E^* \sim 0.3 \pm 0.3$[b] (~0.57)
	3.8 ± 0.2	$\rightarrow C\ell^- + F + CF_2$	4.1	
		$\rightarrow C\ell^- + CF_3{}^*$[c]	0.05	$E^* = 3.75 \pm 0.2$
F^-	2.8 ± 0.2	$e + CC\ell F_3 \rightarrow F^- + CC\ell F_2$	1.9 ± 0.1	$E^* = 0.9 \pm 0.3$ (~1.28)
$C\ell F^-$	3.0 ± 0.15	$e + CC\ell F_3 \rightarrow C\ell F^- + CF_2$	(3.0 ± 0.15)[d]	$EA(C\ell F) > 2.1 \pm 0.15$[d] (1.5 ± 0.3, 1.5 ± 0.4, 2.37 ± 0.21)[e]
$CC\ell F_2^-$	3.5 ± 0.15	$e + CC\ell F_3 \rightarrow CC\ell F_2^- + F$	(3.6 ± 0.25)[f]	$EA(CC\ell F_2) > 1.8 \pm 0.35$[g] (1.6 ± 0.3)

[a]Heat of reaction determined from Eq. (3) using EA(Cℓ) = 3.61 eV,[10] EA(F) = 3.45 eV,[10] and the following values (in eV) for the ΔH_f of $CC\ell F_3$ (-7.33),[11] Cℓ (1.26),[12a] F (0.82),[12a] CF_2 (-1.72)[12b], CF_3 (-4.94)[12a], $CC\ell F_2$ (-2.79 ± 0.1),[13] $C\ell F$ (-0.52).[14] Numbers in parentheses were obtained as described in the corresponding footnotes of this table.

[b]Excess energy determined from Eq. (4); the value in parentheses is from Ref. 8.

[c]Asterisk indicates internal excitation of the CF_3 radical.

[d]Electron affinity determined from Eq. (3) by assuming $\Delta H_r = AO(C\ell F^-) = 3.0 \pm 0.15$ eV and using the ΔH_f values given in footnote a of this table.

TABLE IV. (Continued).

[e] Numbers in parentheses are, respectively, the values of EA(CℓF) of Refs. 15-17.

[f] Heat of reaction determined as described in footnote a of this table using $EA(CC\ell F_2) = 1.8$ eV.

[g] Electron affinity determined from Eq. (5) using for the dissociation energy $D(F - CC\ell F_2)$ the value of 5.3 ± 0.2 eV.[7] The number in parentheses is the value of $EA(CC\ell F_2)$ given in Ref. 15.

TABLE V. Values of ε_{max}, AO, and FWHM for the $\sigma_a(\varepsilon)$ of C_2F_6 and $\langle\varepsilon\rangle_{int}$ for C_2F_6 as a function of T.

T (K)	ε_{max}[a] (eV)	AO[a] (eV)	FWHM[a] (eV)	$\langle\varepsilon\rangle_{int}$[b] (eV)
0	4.3[c]	2.81[c]		0.790[d]
300	3.9	2.3	1.6	0.897
400	3.75	2.1	1.65	0.982
500	3.6	1.95	1.7	1.084
570	3.5	1.8	1.75	1.162
650	3.4	1.7	1.82	1.258
750	3.3	1.5	2.0	1.385
1610		0.0[c]		2.607
3170	0.0[c]			4.972

[a] ε_{max}, AO, and FWHM are, respectively, the energy position of the resonance maximum, the appearance onset, and the full width at half maximum of the $\sigma_a(\varepsilon)$ for C_2F_6 at the respective T.

[b] $\langle\varepsilon\rangle_{int}$ is the total average vibrational energy of the molecule calculated as described in the text.

[c] Extrapolated values assuming that the behavior in Fig. 11 holds in the entire T range 0 to ~3200 K.

[d] Zero-point energy determined from Eq. (8) (see text).

FIGURE CAPTIONS

FIG. 1. Schematic diagram of the high temperature electron swarm apparatus employed in the present study.

FIG. 2. Total electron attachment rate constant k_a as a function of the mean electron energy $\langle\varepsilon\rangle$ for $CC\ell F_3$ at temperatures 300, 400, 500, 550, 600, and 700 K.

FIG. 3. Total electron attachment rate constant k_a as a function of the mean electron energy $\langle\varepsilon\rangle$ for C_2F_6 at temperatures 300, 400, 500, 570, 650, and 750 K.

FIG. 4. The electron attachment rate constant k_a for $CC\ell F_3$ as a function of the ratio N_a/N_t of the attaching gas number density N_a to the total gas number density N_t for a number of $\langle\varepsilon\rangle$, T, and N_t.

FIG. 5. The electron attachment rate constant k_a for C_2F_6 as a function of the rato N_a/N_t of the attaching gas number density N_a to the total gas number density N_t for a number of $\langle\varepsilon\rangle$, T, and N_t.

FIG. 6. Swarm unfolded total electron attachment cross section $\sigma_a(\varepsilon)$ as a function of ε for $CC\ell F_3$ at 300, 400, 500, 550, 600, and 700 K obtained from measurements of $k_a(\langle\varepsilon\rangle)$ in Ar.

FIG. 7. Swarm unfolded total electron attachment cross section $\sigma_a(\varepsilon)$ as a function of ε for C_2F_6 at 300, 400, 500, 570, 650, and 750 K obtained from measurements of $k_a(\langle\varepsilon\rangle)$ in Ar.

FIG. 8. Comparison of the swarm unfolded total attachment cross section $\sigma_a(\varepsilon)$ for C_2F_6 at T = 300 K with the total relative cross section for negative ion production obtained in the electron beam study.[7]

FIG. 9. Negative ion intensity as a function of ε for $CC\ell F_3$ measured in a time-of-flight mass spectrometric study. (a) Nonunfolded data, (b) unfolded data (note the multiplication factors).

FIG. 10. Swarm unfolded total attachment cross section $\sigma_a(\varepsilon)$ for $CC\ell F_3$ at T = 300 K in comparison with the relative total negative ion cross section measured in a beam study (Fig. 9). The beam relative cross section was normalized to the high-energy peak (at ~5 eV) of the swarm unfolded $\sigma_a(\varepsilon)$.

FIG. 11. Energy position of the resonance maximum ε_{max}, the appearance onset AO, and the full width of half maximum FWHM, of the $\sigma_a(\varepsilon)$, as a function of T for C_2F_6.

FIG. 12. Electron attachment rate constant k_a versus 1/T for a number of mean electron energies $\langle\varepsilon\rangle$. (a) $CC\ell F_3$ and (b) C_2F_6.

FIG. 13. Plot of the activation energy D versus $\langle\varepsilon\rangle$ in dissociative electron attachment to C_2F_6. The broken line designated by kT_{300} is the value of kT at T = 300 K.

FIG. 14. Total attachment rate constant, k_a, at the mean electron energy $\langle\varepsilon\rangle$ = 1.5 eV and the average internal energy $\langle\varepsilon\rangle_{int}$ (excluding the zero-point energy $\langle\varepsilon\rangle_z$) versus T^{-1} for C_2F_6 (see text for discussion).

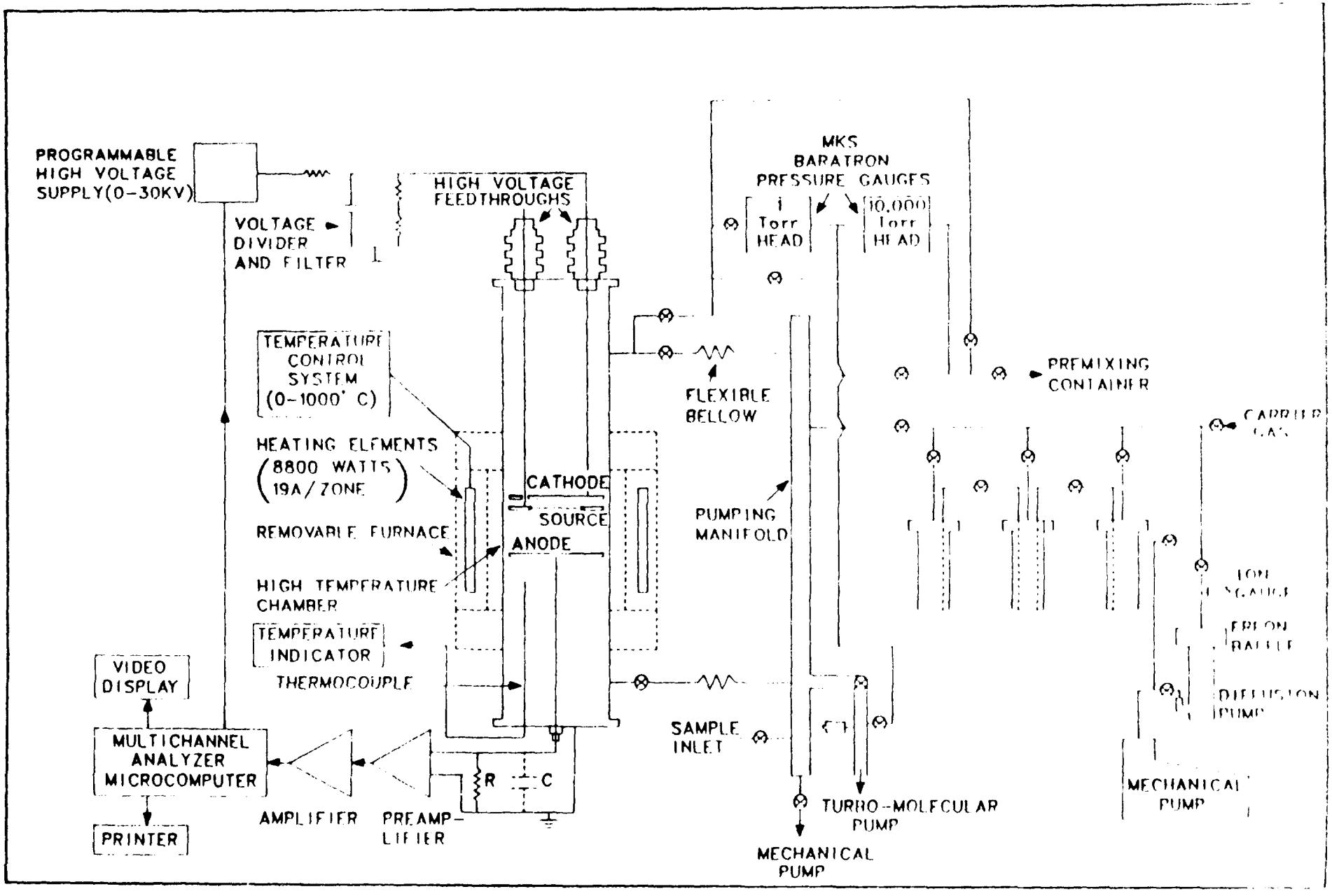
PROGRAMMABLE HIGH VOLTAGE SUPPLY(0-30KV)
VOLTAGE DIVIDER AND FILTER
HIGH VOLTAGE FEEDTHROUGHS
MKS BARATRON PRESSURE GAUGES
1 Torr HEAD
10,000 Torr HEAD
TEMPERATURE CONTROL SYSTEM (0-1000° C)
FLEXIBLE BELLOW
PREMIXING CONTAINER
HEATING ELEMENTS (8800 WATTS 19A/ZONE)
CATHODE
SOURCE
ANODE
PUMPING MANIFOLD
REMOVABLE FURNACE
HIGH TEMPERATURE CHAMBER
TEMPERATURE INDICATOR
THERMOCOUPLE
VIDEO DISPLAY
MULTICHANNEL ANALYZER MICROCOMPUTER
PRINTER
AMPLIFIER
PREAMP-LIFIER
R
C
SAMPLE INLET
TURBO-MOLECULAR PUMP
MECHANICAL PUMP
MECHANICAL PUMP

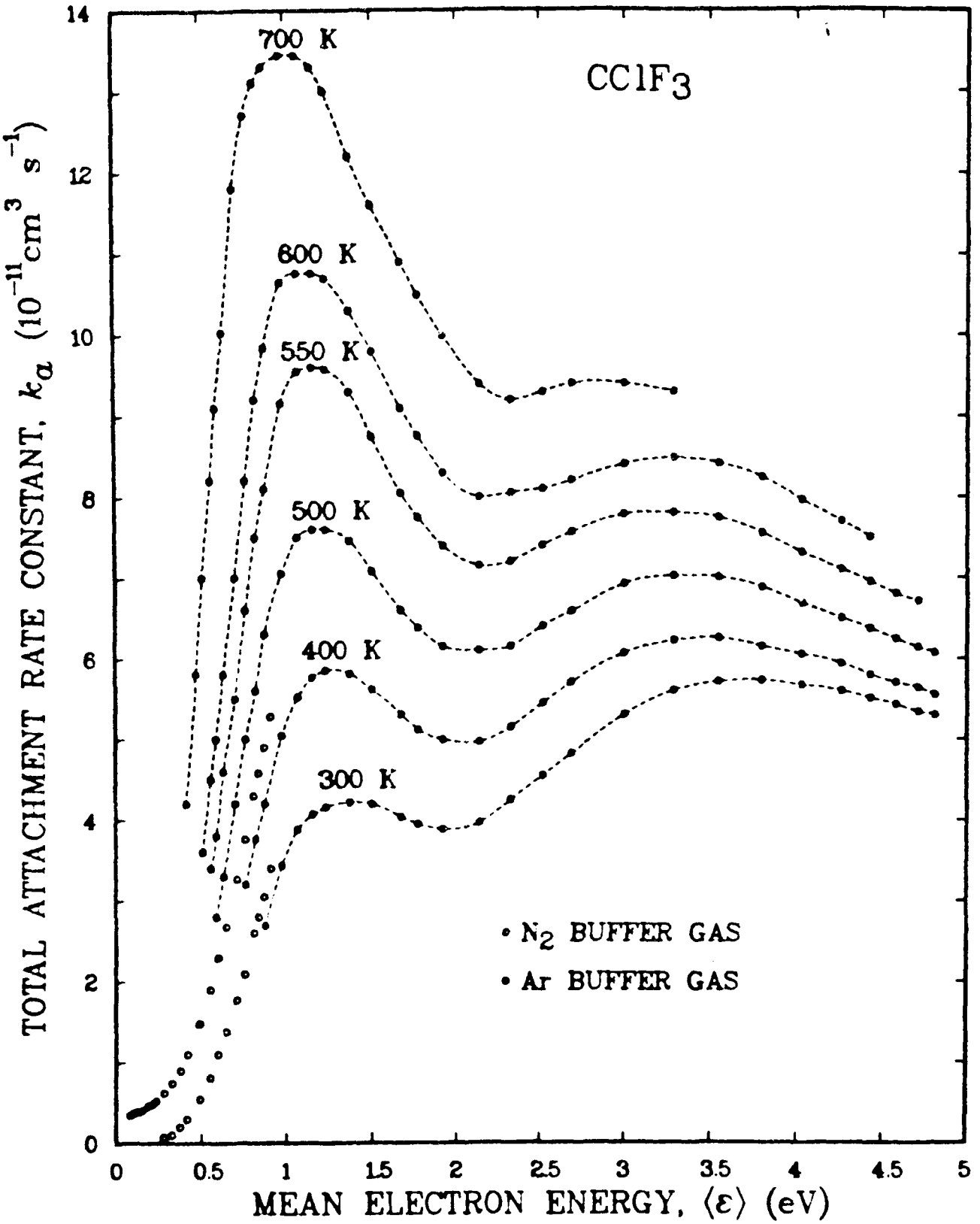
CClF_3
700 K
600 K
550 K
500 K
400 K
300 K
• N_2 BUFFER GAS
• Ar BUFFER GAS
TOTAL ATTACHMENT RATE CONSTANT, k_a (10^{-11}cm^3 s^{-1})
MEAN ELECTRON ENERGY, ⟨ε⟩ (eV)
0
2
4
6
8
10
12
14
0
0.5
1
1.5
2
2.5
3
3.5
4
4.5
5

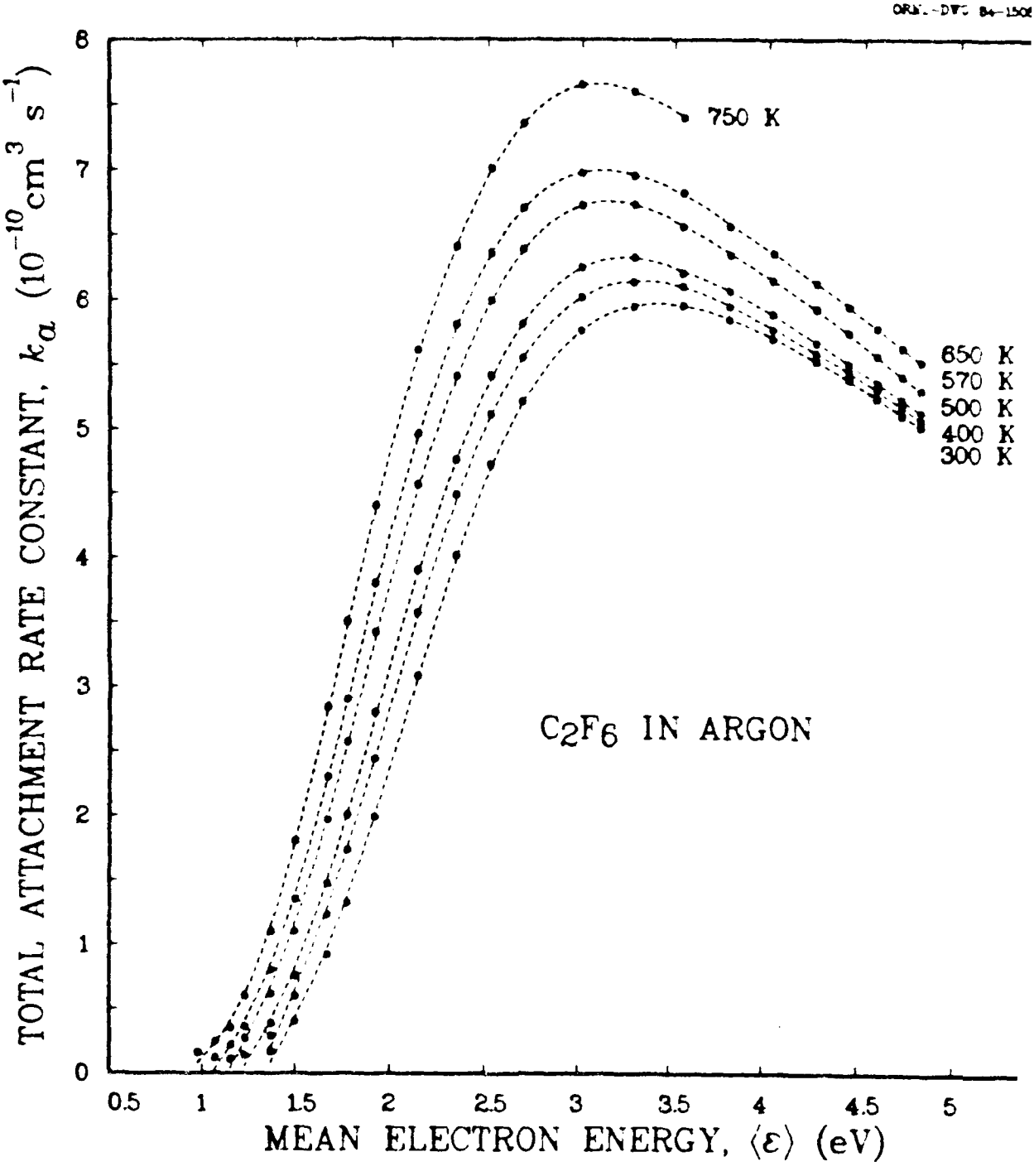
ORNL-DWG 84-1502
TOTAL ATTACHMENT RATE CONSTANT, k_a (10^{-10}cm^3 s^{-1})
MEAN ELECTRON ENERGY, $\langle\varepsilon\rangle$ (eV)
750 K
650 K
570 K
500 K
400 K
300 K
C_2F_6 IN ARGON
0
1
2
3
4
5
6
7
8
0.5
1
1.5
2
2.5
3
3.5
4
4.5
5

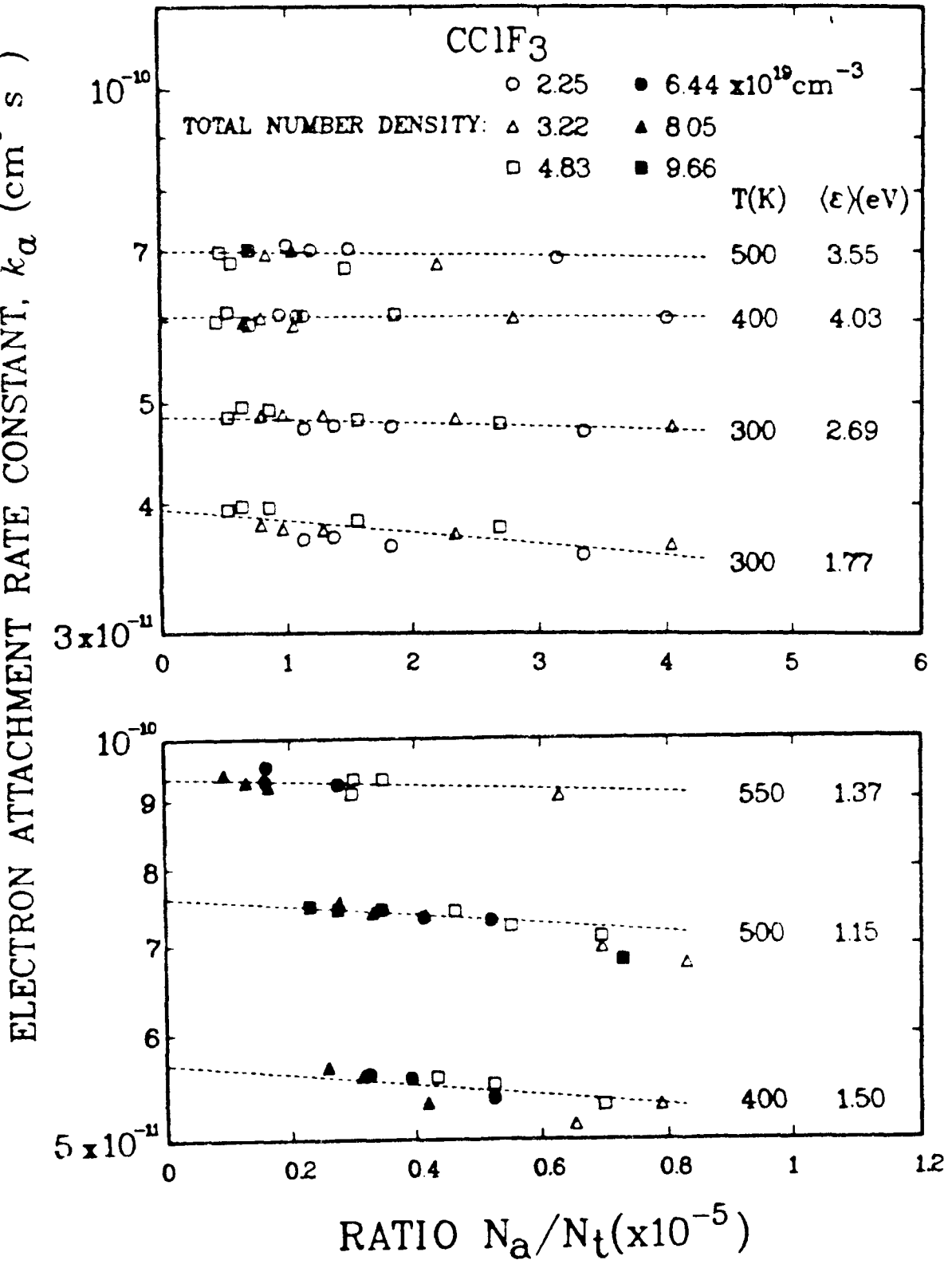

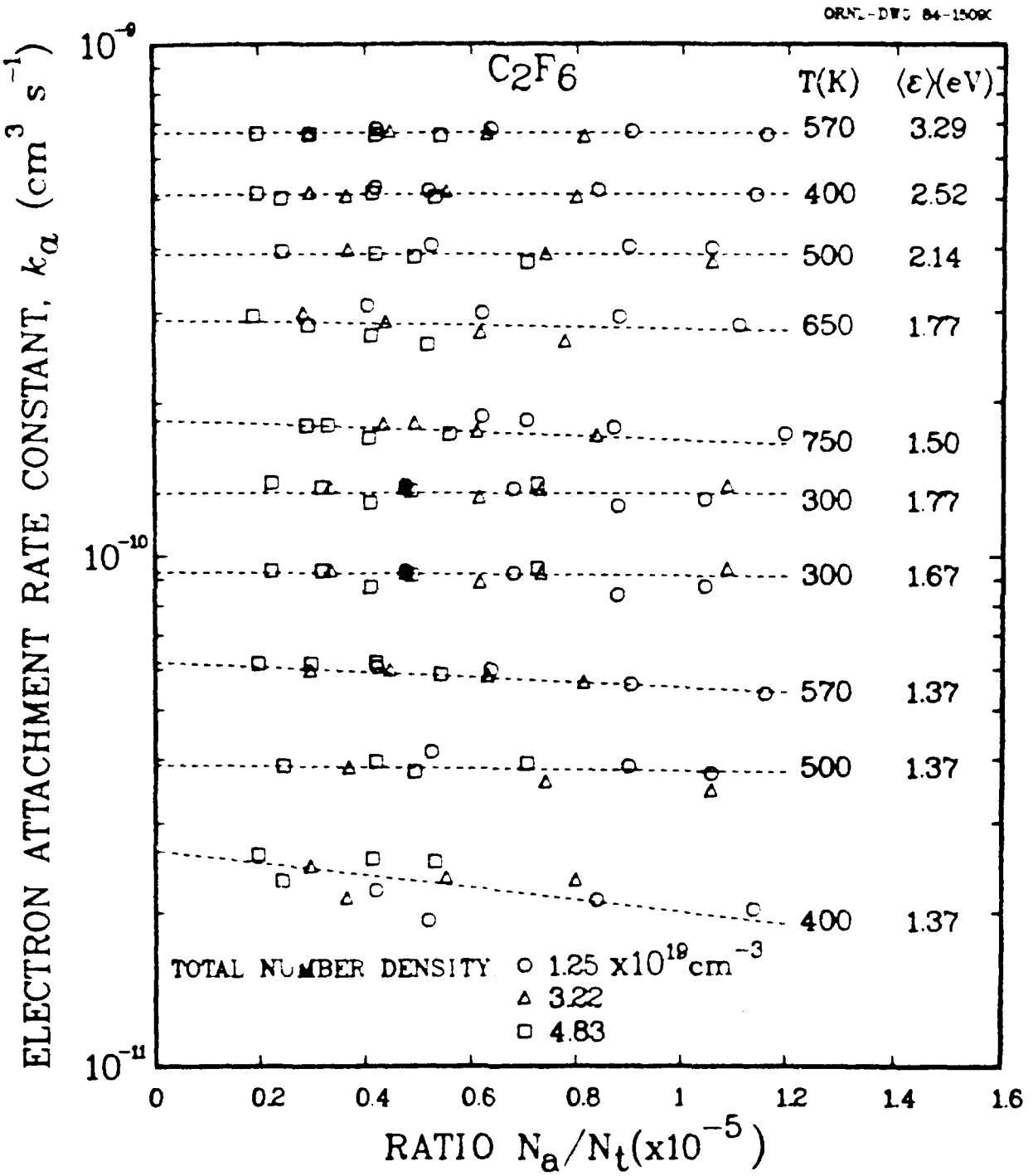
ORNL-DWG 84-15096
C_2F_6
T(K)
⟨ε⟩(eV)
570 3.29
400 2.52
500 2.14
650 1.77
750 1.50
300 1.77
300 1.67
570 1.37
500 1.37
400 1.37
TOTAL NUMBER DENSITY
○ 1.25 x10^19 cm^-3
△ 3.22
□ 4.83
ELECTRON ATTACHMENT RATE CONSTANT, k_a ($cm^3\ s^{-1}$)
10^{-9}
10^{-10}
10^{-11}
0
0.2
0.4
0.6
0.8
1
1.2
1.4
1.6
RATIO $N_a/N_t(x10^{-5})$

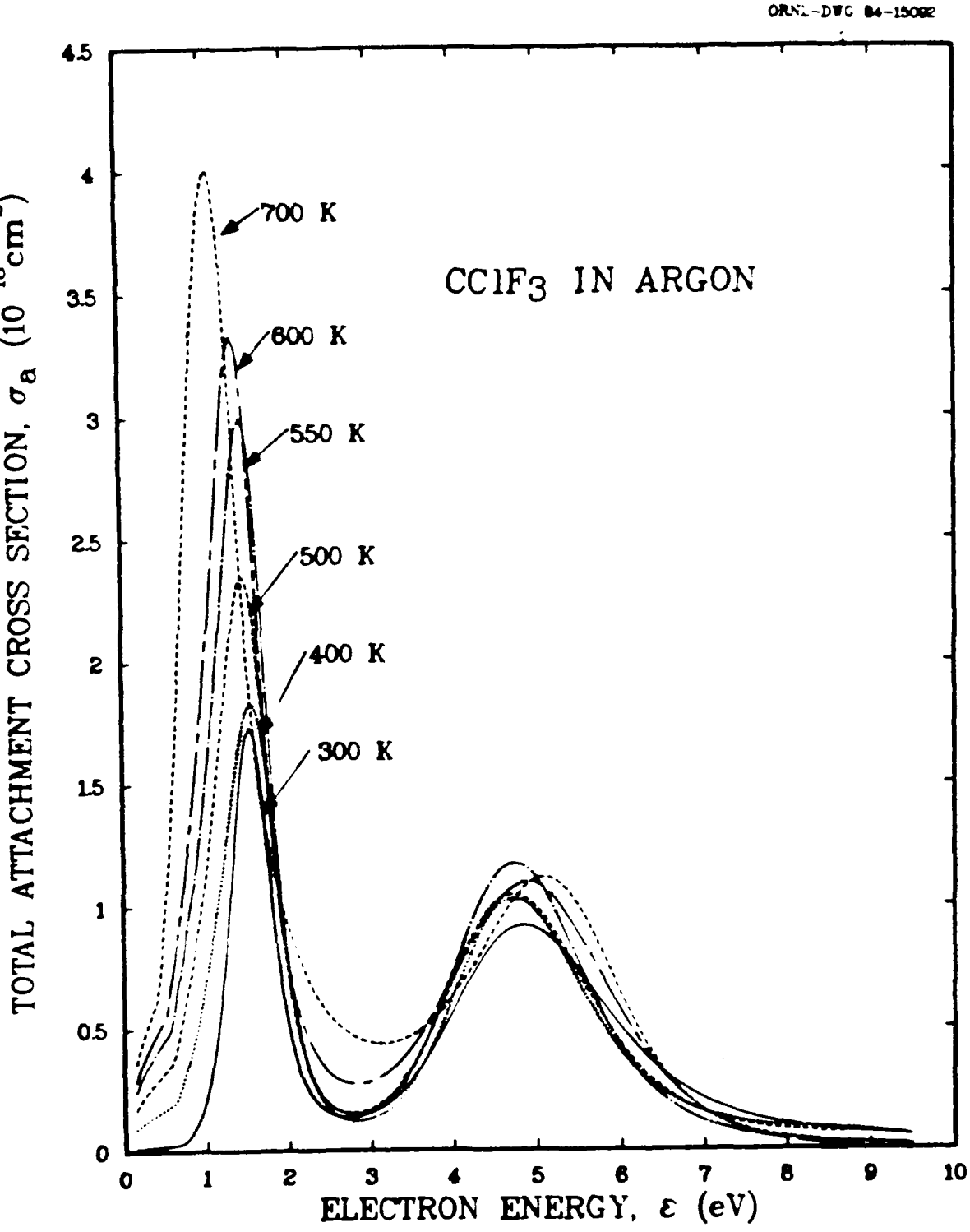
ORNL-DWG 84-15082
CC1F3 IN ARGON
700 K
600 K
550 K
500 K
400 K
300 K
TOTAL ATTACHMENT CROSS SECTION, σa (10^-16 cm^2)
ELECTRON ENERGY, ε (eV)
0
0.5
1
1.5
2
2.5
3
3.5
4
4.5
0
1
2
3
4
5
6
7
8
9
10

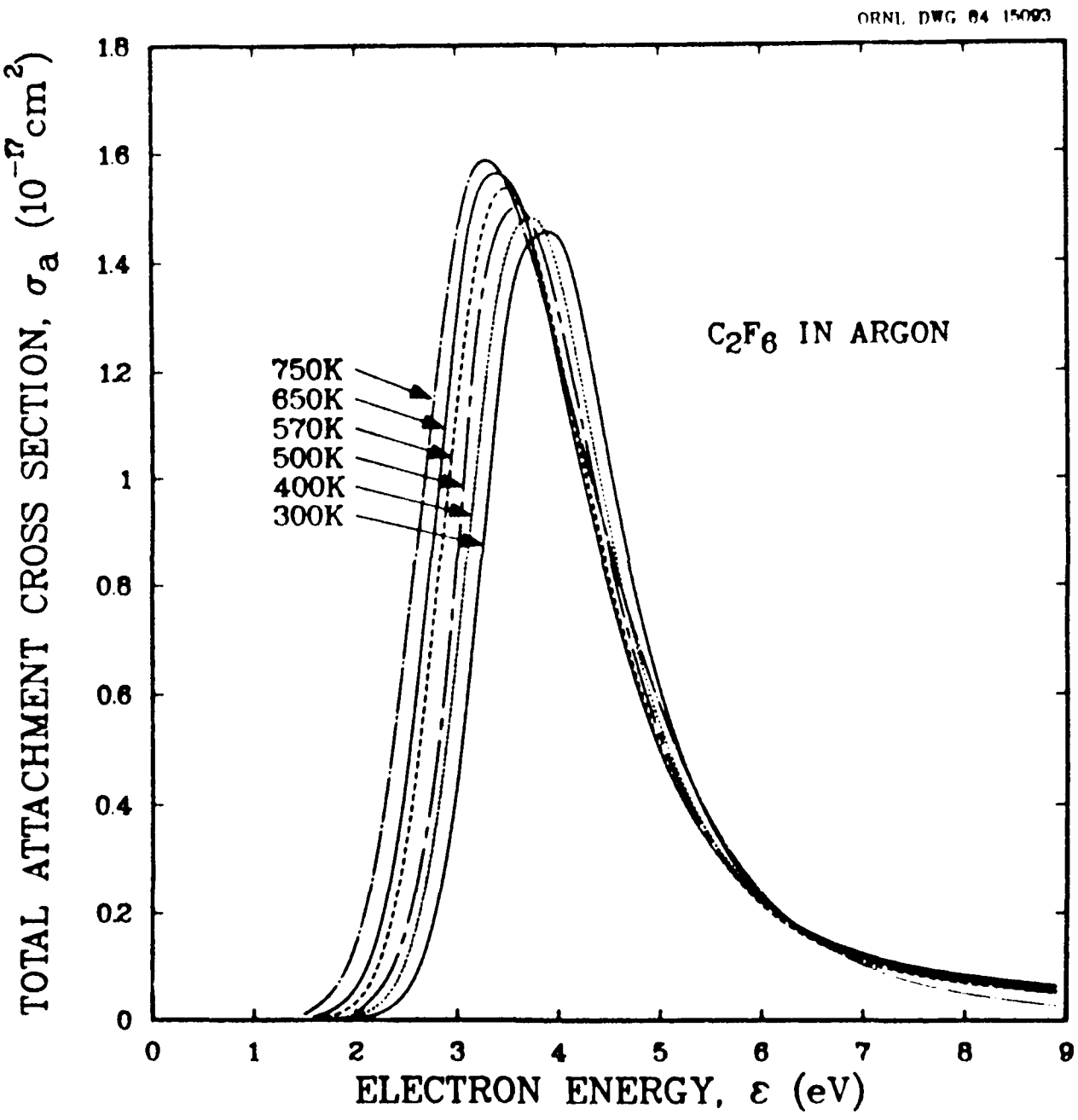
ORNL DWG 84 15093
TOTAL ATTACHMENT CROSS SECTION, σ_a (10^{-17}cm^2)
ELECTRON ENERGY, ε (eV)
C_2F_6 IN ARGON
750K
650K
570K
500K
400K
300K
0
0.2
0.4
0.6
0.8
1
1.2
1.4
1.6
1.8
0
1
2
3
4
5
6
7
8
9

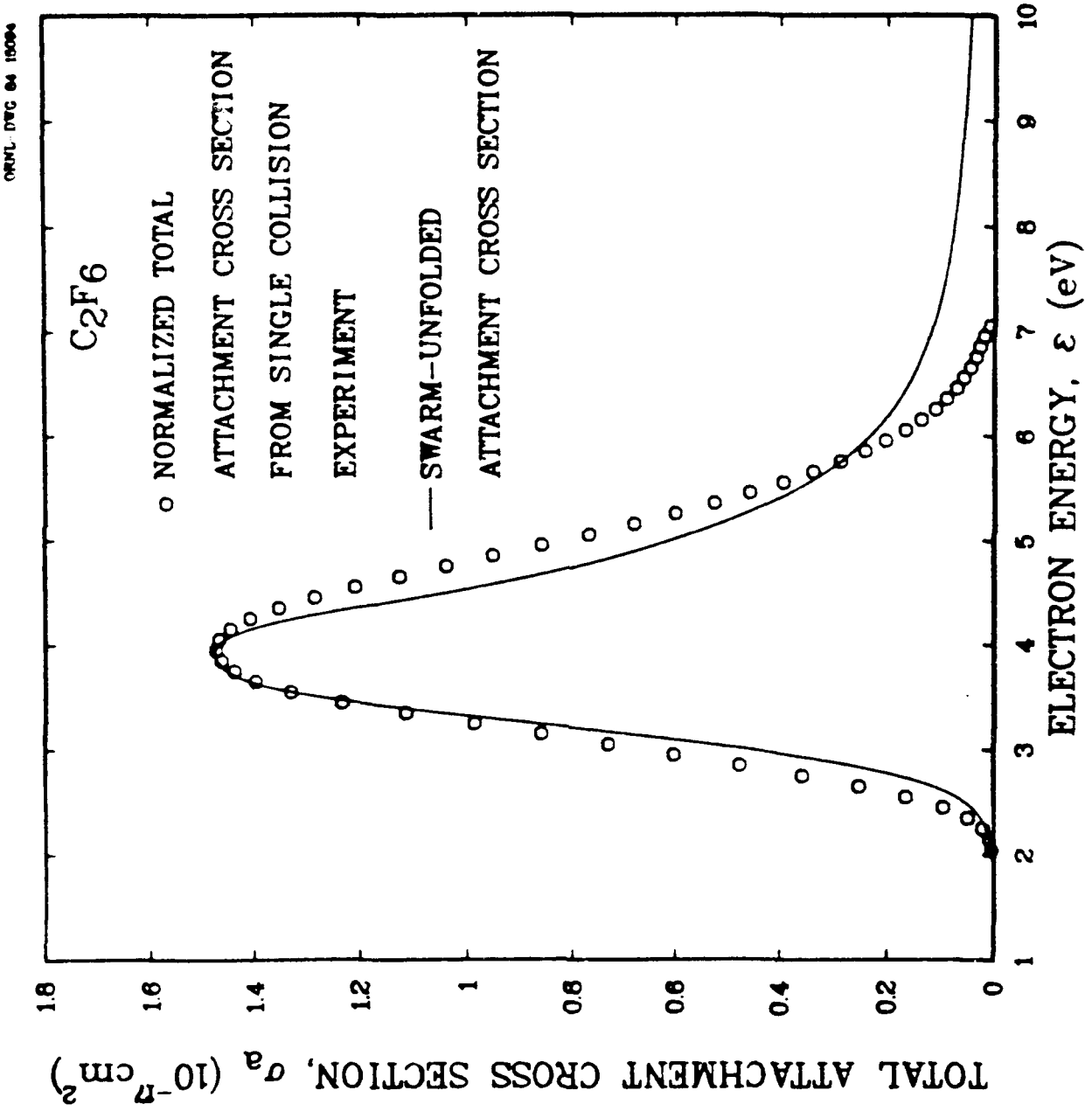
ORNL DWG 84 15084
C_2F_6
o NORMALIZED TOTAL ATTACHMENT CROSS SECTION FROM SINGLE COLLISION EXPERIMENT
— SWARM-UNFOLDED ATTACHMENT CROSS SECTION
TOTAL ATTACHMENT CROSS SECTION, σ_a (10^{-17} cm^2)
ELECTRON ENERGY, ε (eV)
0
0.2
0.4
0.6
0.8
1
1.2
1.4
1.6
1.8
1
2
3
4
5
6
7
8
9
10

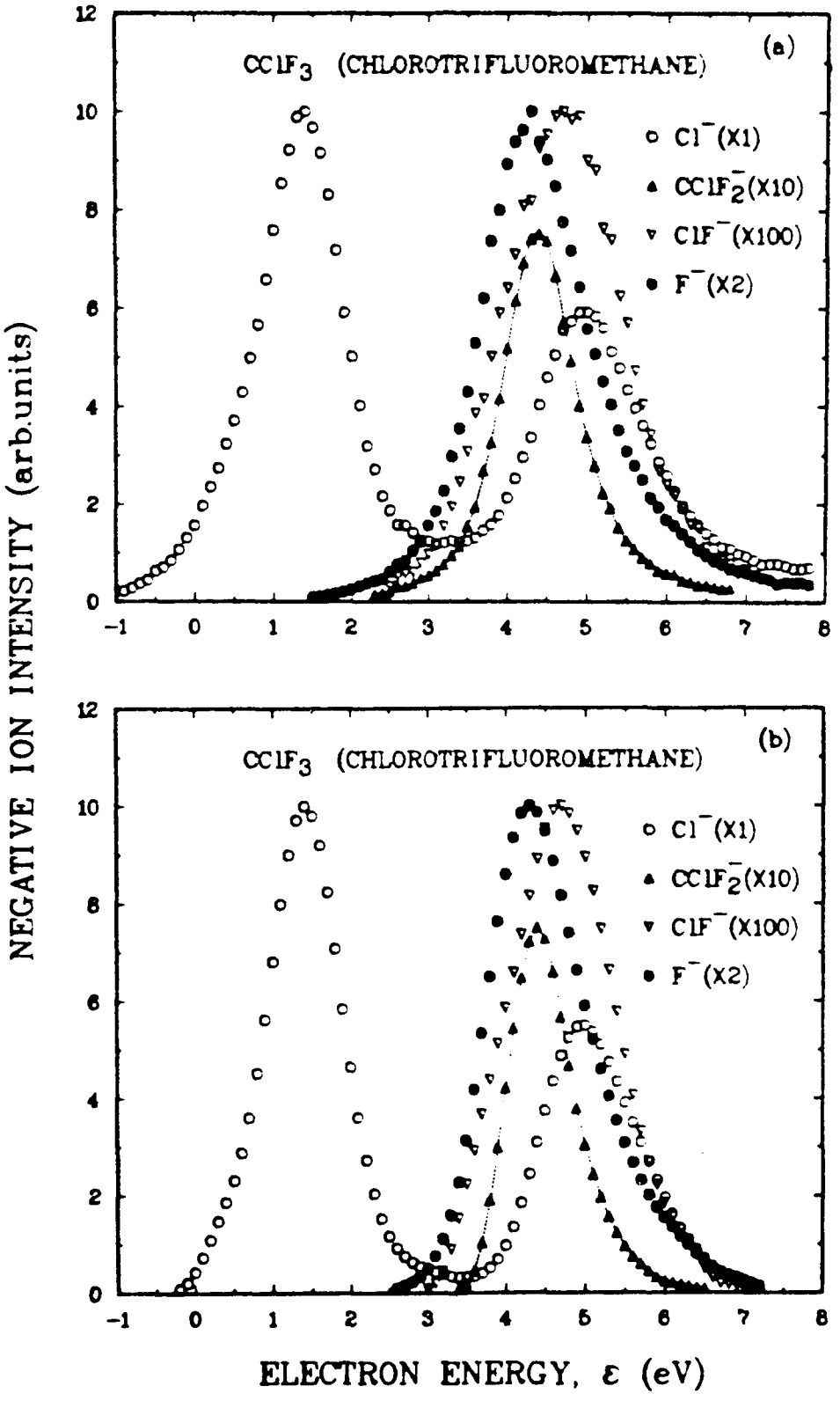
CClF_3 (CHLOROTRIFLUOROMETHANE)
(a)
Cl^-(X1)
$CClF_2^-$(X10)
ClF^-(X100)
F^-(X2)
CClF_3 (CHLOROTRIFLUOROMETHANE)
(b)
Cl^-(X1)
$CClF_2^-$(X10)
ClF^-(X100)
F^-(X2)
NEGATIVE ION INTENSITY (arb.units)
ELECTRON ENERGY, ε (eV)

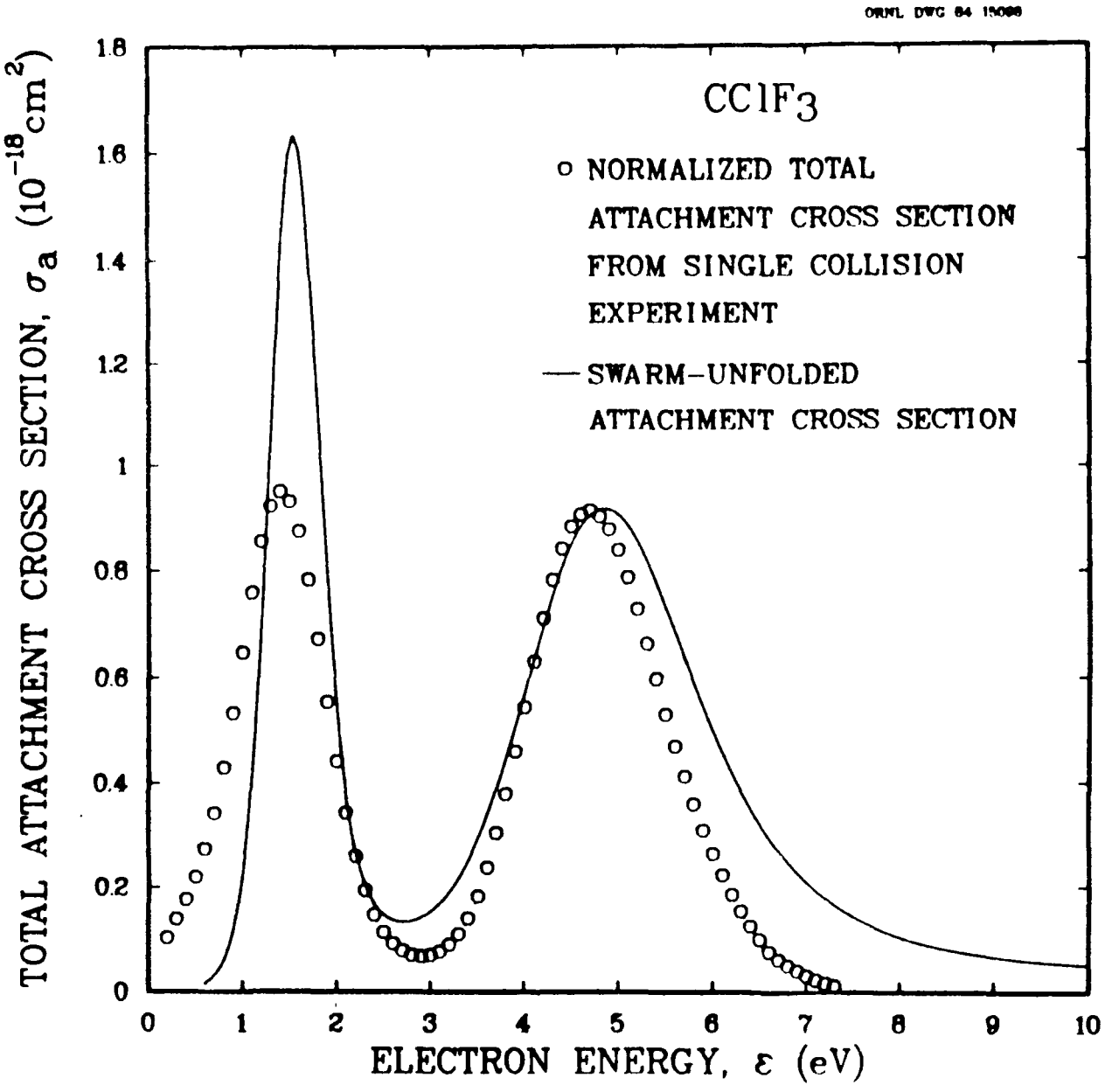
ORNL DWG 84 15088
CC1F3
o NORMALIZED TOTAL ATTACHMENT CROSS SECTION FROM SINGLE COLLISION EXPERIMENT
— SWARM-UNFOLDED ATTACHMENT CROSS SECTION
TOTAL ATTACHMENT CROSS SECTION, σa (10^-18 cm^2)
ELECTRON ENERGY, ε (eV)
0
0.2
0.4
0.6
0.8
1
1.2
1.4
1.6
1.8
0
1
2
3
4
5
6
7
8
9
10

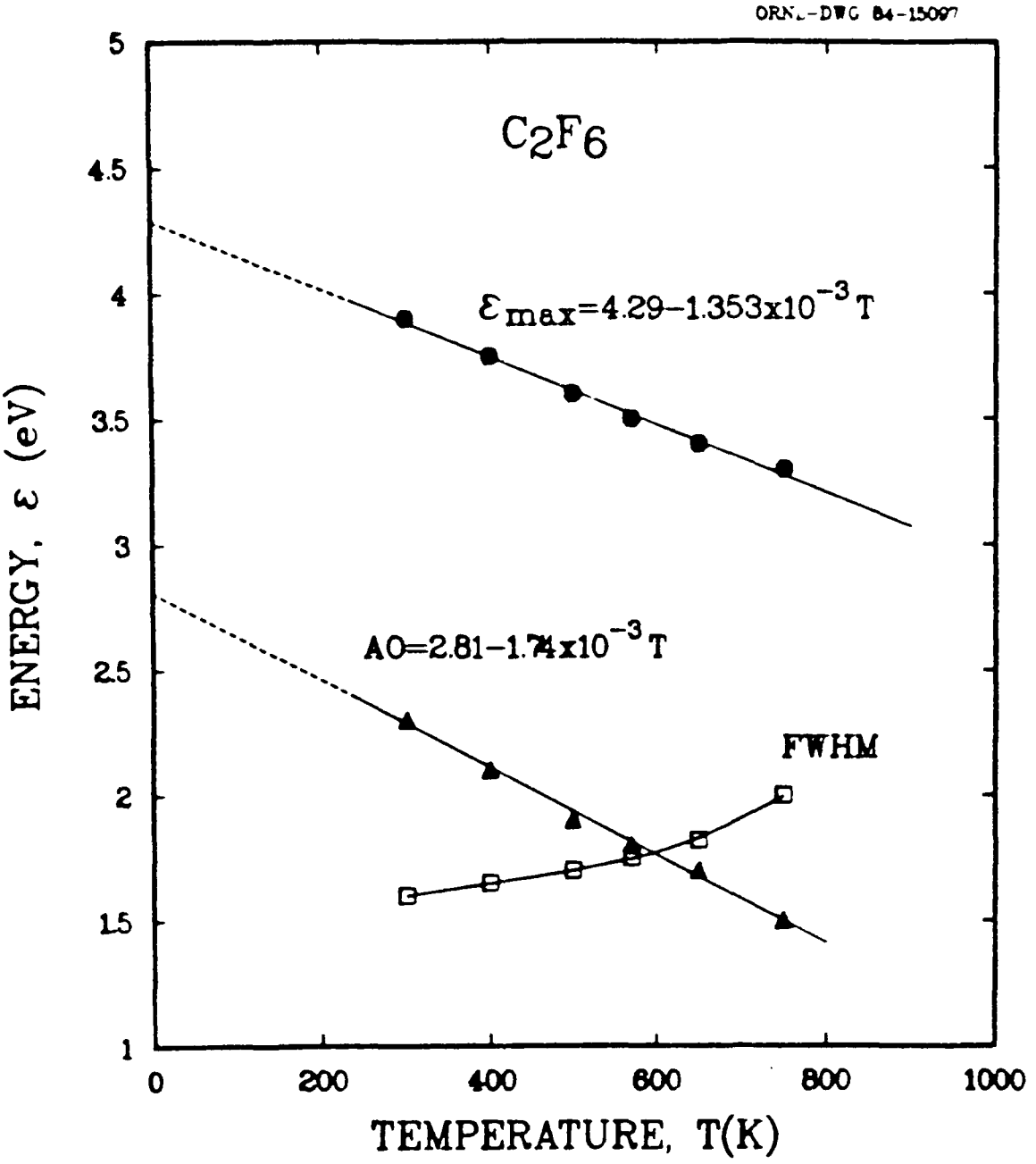
ORNL-DWG 84-15097
C_2F_6
$\varepsilon_{max}=4.29-1.353x10^{-3}T$
$A0=2.81-1.74x10^{-3}T$
FWHM
ENERGY, ε (eV)
TEMPERATURE, T(K)
5
4.5
4
3.5
3
2.5
2
1.5
1
0
200
400
600
800
1000

ORNL-DWG 84-15098

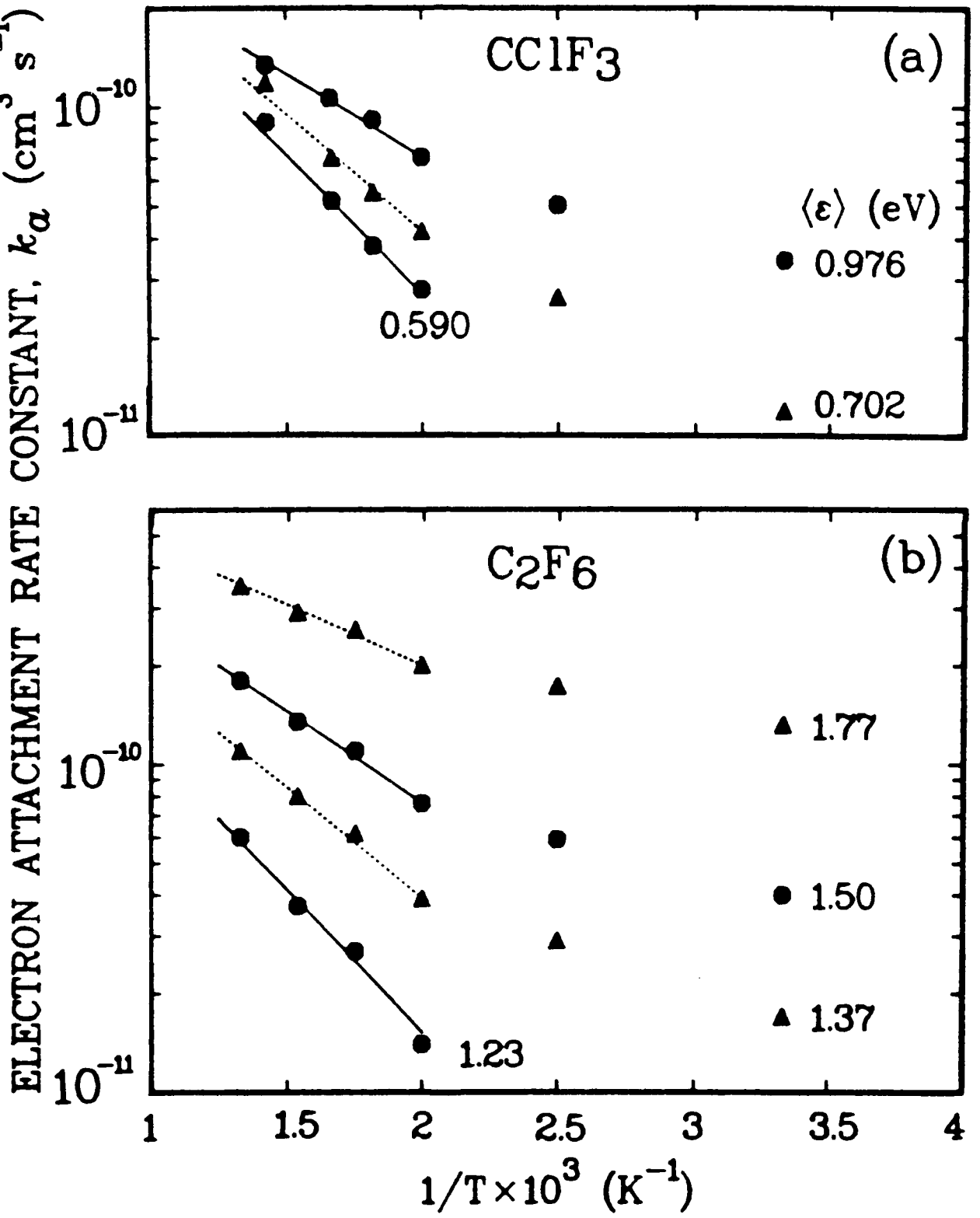

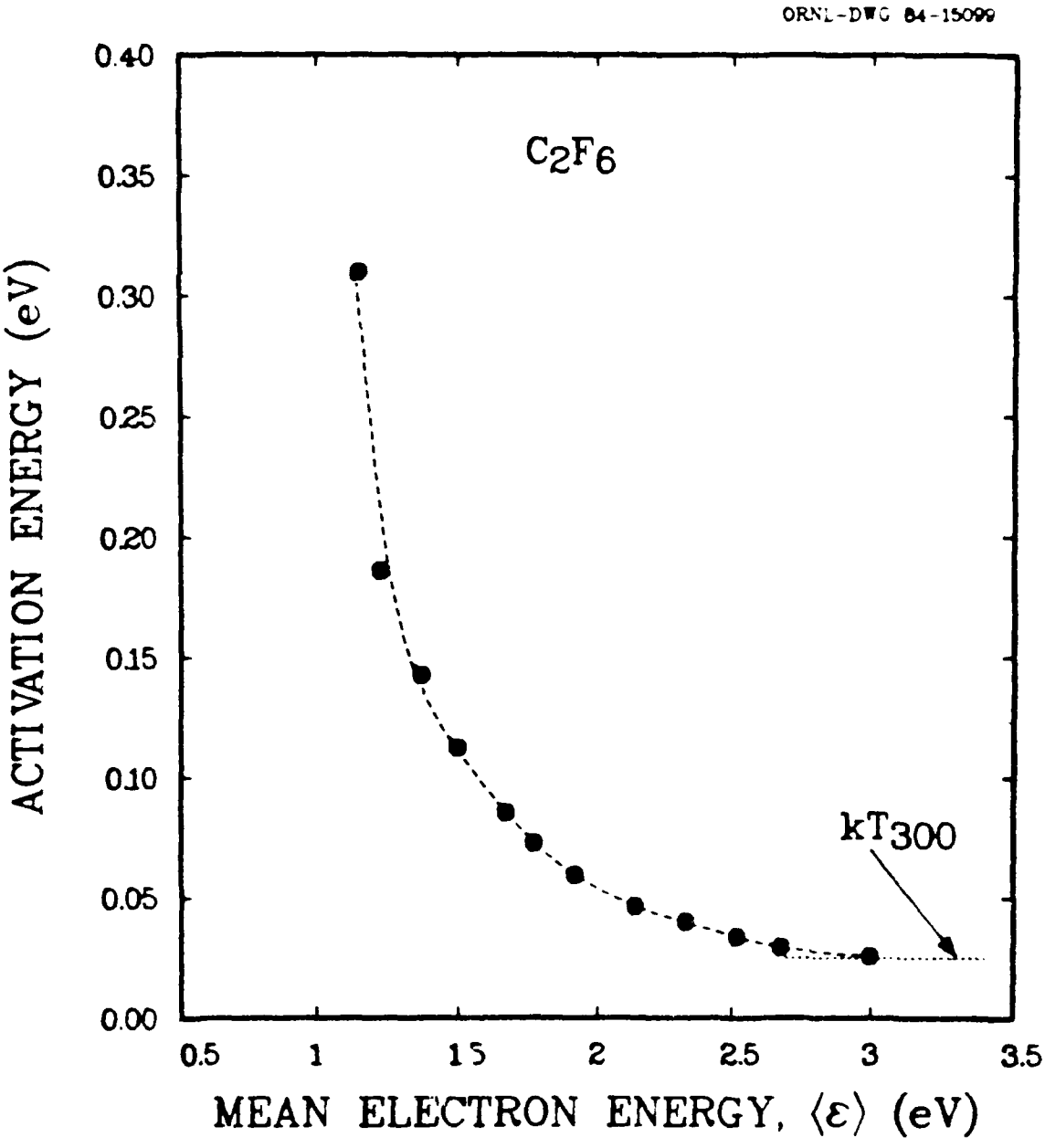
ORNL-DWG 84-15099
C_2F_6
kT_{300}
ACTIVATION ENERGY (eV)
0.40
0.35
0.30
0.25
0.20
0.15
0.10
0.05
0.00
0.5
1
1.5
2
2.5
3
3.5
MEAN ELECTRON ENERGY, ⟨ε⟩ (eV)

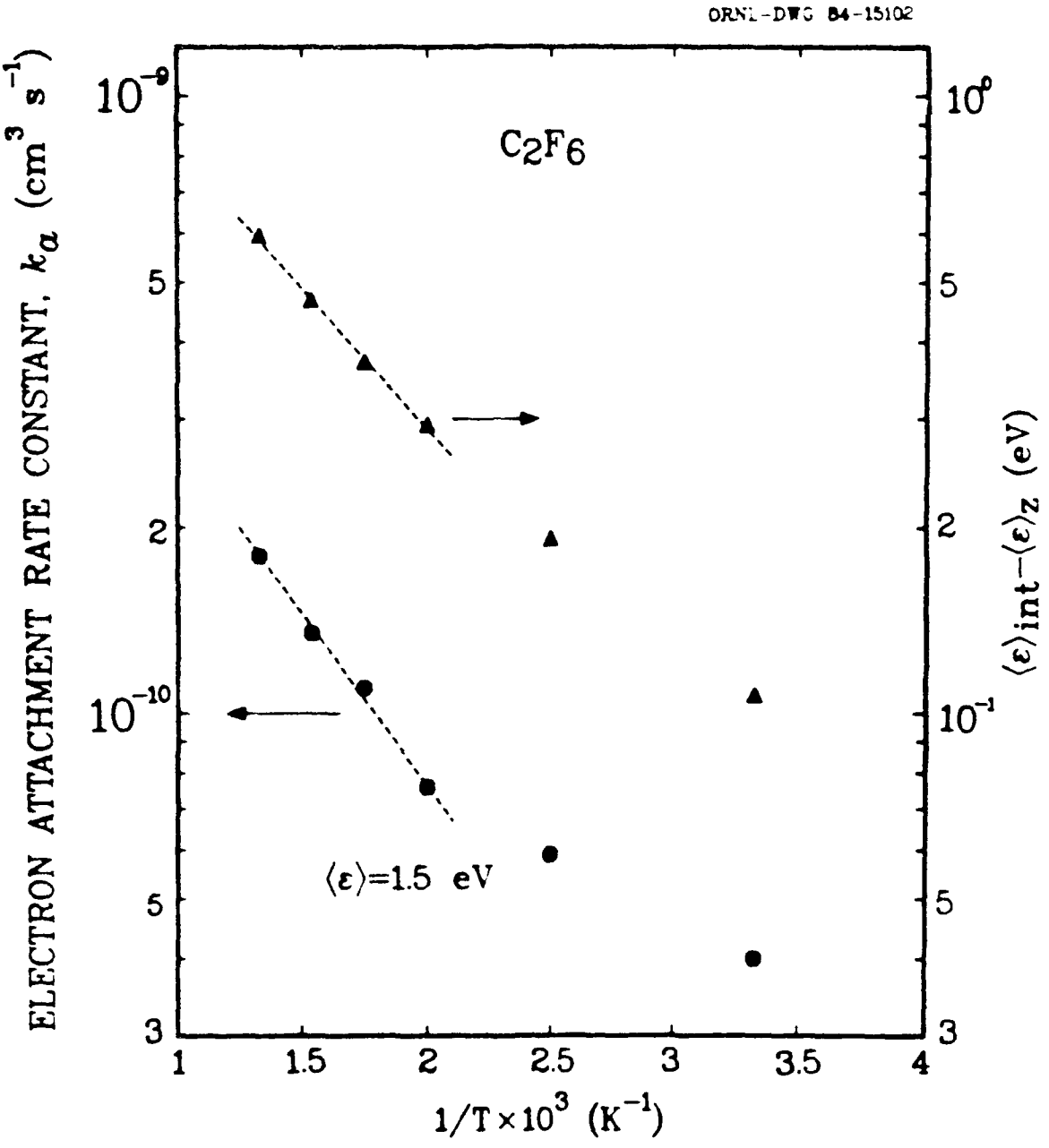
ORNL-DWG 84-15102
C_2F_6
ELECTRON ATTACHMENT RATE CONSTANT, k_a ($cm^3\ s^{-1}$)
$\langle\varepsilon\rangle_{int}-\langle\varepsilon\rangle_z$ (eV)
$\langle\varepsilon\rangle$=1.5 eV
$1/T\times10^3$ (K^{-1})
10^{-9}
10^{-10}
10^0
10^{-1}
5
2
3
1
1.5
2
2.5
3
3.5
4

END

FILMED

3-85

DTIC